CHAPTER 3-4

Solution-Gas-Drive Reservoirs

CONTENTS

I. INTRODUCTION

The oil in virtually all reservoirs contains dissolved gas which contributes energy toward the production of oil. The drive resulting from this energy is known variously as solution-gas drive, dissolved-gas drive, internal-gas drive, or depletion drive. The terms solution-gas drive and dissolved-gas drive are most common and are used interchangeably. When the reservoir pressure falls below the bubble point of the fluid, gas begins to evolve and continues to evolve as long as the pressure declines. In a closed reservoir, where nothing enters the original oil volume during depletion, expansion of the evolved gas may become the sole source of producing energy. Most of this gas is produced, but the portion that remains in the reservoir causes the reservoir pressure to decline less rapidly than it would for a liquid system with no gas in solution. Thus, oil recovery is aided because oil flows toward the wells in proportion to the difference between the average reservoir pressure and the wellbore pressure.

Except for the oil-expansion mechanism, solution-gas drive is generally considered to be the least efficient of all natural producing mechanisms. Ordinarily less than one-fourth the oil in place is ultimately produced by solution-gas drive. By contrast, gas-cap drive or water-drive fields will generally recover at least one-half the oil in place. Moreover, allowing a field to produce by solution-gas drive may reduce the success of a subsequent waterflood. Pressure depletion causes the reservoir oil to shrink and become more viscous. This causes the waterflood residual oil content to be high compared with the original oil content and the displacement to be less efficient. The reservoir engineer should analyze a solution-gas-drive field as early in the field life as possible. If the analysis shows waterflooding to be economically attractive, it probably should be started while the reservoir is at a fairly high pressure level.

An understanding of the solution-gas-drive mechnism is necessary to determine the fluid saturations at the start of a secondary recovery process, and to predict gas-oil ratio behavior under gas or water injection. Moreover, a prediction of the solution-gas-drive performance of a reservoir serves as a base case for economic comparison with secondary recovery or pressure maintenance operations.

This chapter discusses the characteristics of solution-gas-drive fields, ways to analyze the producing history, and methods of predicting reservoir performance. The methods considered in detail include those based on material-balance and relative-permeability concepts. The short-cut procedures are based on generalized correlations. Rigorous analysis by the two-dimensional (2-D) calculation procedure is mentioned briefly. The prediction of oil-production rates during depletion is also covered.

Although the solution-gas-drive mechanism is basically insensitive to producing rate, gravity may influence dipping reservoirs to make their recovery sensitive to rate. In many cases, however, the ultimate recovery is almost insensitive to practical producing rates. Methods for analyzing the effect of gravity and for determining the best means of developing and producing gravity-sensitive reservoirs are discussed in this chapter.

II. CHARACTERISTICS OF SOLUTION-GAS-DRIVE FIELDS

A. Performance Characteristics

Solution-gas-drive fields are characterized by rapidly increasing gas-oil ratios and decreasing oil-production rates. Generally, little or no water is produced. The production performance of a typical solution-gas-drive field on a fractional oil recovery basis is illustrated in Fig. 1. The producing gas-oil ratio remains constant until pressure declines to the bubble point, then declines slowly as the gas saturation builds up to the equilibrium value. This small decline will probably not be noticed on a field basis because wells are at different stages of depletion. At the equilibrium value, the gas becomes mobile, and the GOR increases rapidly until the field nears pressure depletion. The GOR increases because the increasing gas saturation results in higher relative permeability to gas and lower permeability to oil. In the final production

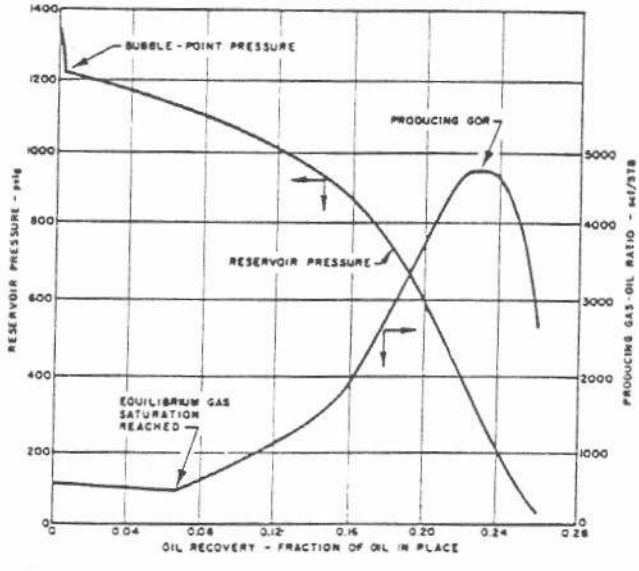

FIG. 1. Performance of typical solution-gas-drive field.

stages the GOR goes down, because at low pressure the reservoir contains comparatively little gas, although its saturation is high. The reservoir pressure decline below the bubble point is related to the producing GOR. As the GOR increases, the rate of pressure decline increases.

At any time, the pressure in the reservoir decreases from the well drainage radius to the wellbore. This pressure profile results in a corresponding gas-saturation profile that increases in the direction of production. Gas saturation increases in the direction of pressure decrease because of increased evolution of dissolved gas. A schematic representation of a typical pressure and saturation profile in a well's drainage area is shown in Fig. 2. Most of the changes in pressure and saturation in Fig. 2 occur within 200 feet of the wellbore. The associated reservoir volume represents only 4 percent of the total reservoir drained by the well. For this reason, the prediction techniques which imply that average pressure and saturation values exist throughout the drainage area (see Fig. 2) are sufficiently accurate for most engineering purposes. The accuracy of these techniques has been proved by comparison with linear predictions[2] that account for the changes in pressure and saturation that exist in the well drainage area.

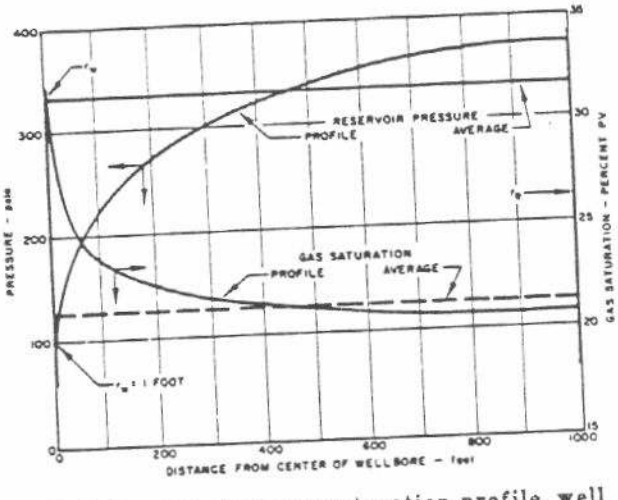

FIG. 2. Pressure and gas-saturation profile, well drainage area.

B. Effect of Rock and Fluid Properties on Recovery

1. ROCK PROPERTIES

a. *Relative Permeability*

Relative permeability is the most important rock property in terms of influence on solution-gas-drive recovery. A relative-permeability curve for a reservoir can be characterized by the equilibrium gas saturation which is the end opint of the curve ($k_g/k_o = 0$). A high value of equilibrium gas saturation means favorable relative permeability and comparatively high oil recovery. Gas-oil relative-permeability curves are plotted on semilog paper so the equilibrium gas saturation cannot be plotted. However, as shown in Fig. 3, the curve is nearly vertical at low values of k_g/k_o,

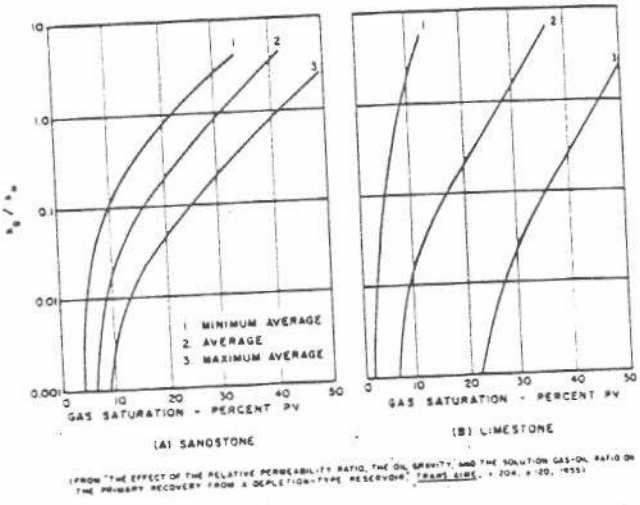

FIG. 3. Relative permeability data used by Arps and Roberts.

so that the gas saturation at $k_g/k_o = 0.001$ is roughly the equilibrium saturation (also see Chapter 1-2, Rock Properties).

Generally speaking, the greater the variation in pore size within a reservoir, the worse the relative-permeability characteristics, and the lower the solution-gas-drive recovery. Gas, being nonwetting in the presence of liquid, will seek the large pores. If the largest pores represent a large fraction of the total permeability but a small fraction of the porosity, the flowing gas-oil ratio will be high for a low gas saturation. This, in effect, allows the energy in the gas to be used up without moving much oil. Vuggy limestones or fractured reservoirs are extreme examples of unfavorable relative permeability.

The theoretical effect of relative permeability on solution-gas-drive recovery has been adequately covered in the literature. A study by Arps and Roberts[1] covered six different types of reservoir rock consisting of minimum average, average, and maximum average relative-permeability characteristics for sandstones and for limestones. The relative-permeability ratio curves used are shown in Figs. 3A and 3B. The following tabulation of predicted recoveries for a representative oil (30°API oil with a solution gas-oil ratio of 600 scf/STB) exemplifies the influence of relative permeability:

Relative Permeability Classification (Fig. 3)	Theoretical Ultimate Recovery, STB/acre-ft (φ = 20%)
Sandstone – Minimum Average	72
– Average	130
– Maximum Average	210
Limestone – Minimum Average	25
– Average	94
– Maximum Average	293

As shown above, the relative-permeability characteristics may cause ultimate recovery to vary threefold for sandstones and more than tenfold for limestones. The extremely low recovery for the minimum average limestone case is probably due to vugs or fractures in the rock.

b. Other Rock Properties

Other commonly measured rock properties such as permeability, porosity, and connate water influence solution-gas-drive recovery to a lesser extent. In general, recovery increases as permeability increases. High-permeability rock usually has better relative-permeability characteristics than tight rock. High permeability also allows the initial producing rates to be high and the reservoir pressure to be low at economic depletion. Porosity has no effect on recovery efficiency except that high porosity usually implies good relative permeability. Obviously, recovery in barrels per acre-foot will tend to increase as porosity increases. Connate water influences recovery in that as connate water increases, recovery usually increases (as a percent of oil in place). One reason for this (neglecting relative-permeability effects) is that as connate water saturation increases, the oil in place decreases. Therefore, a given amount of oil recovery represents a higher percentage of the oil in place.

2. FLUID PROPERTIES

Although rock properties have the most important influence on recovery, fluid properties are also important. Specifically, the formation volume factor, the bubble-point pressure, the solution gas-oil ratio, and the oil viscosity have a significant effect. The first three factors are interrelated; a high solution gas-oil ratio results in a high formation volume factor and a high bubble-point pressure. Thus, the effect of all three factors can be implied from the effect of solution gas-oil ratio. The general effect of solution gas-oil ratio on recovery is illustrated in the following table. Recovery figures apply to a 50° API oil in a sandstone reservoir with 20 percent porosity and average relative-permeability characteristics. The figures are from Arps and Roberts.[1]

Solution GOR, scf/STB	Theoretical Recovery, STB/acre-ft
60	278
200	275
600	195
1000	143
2000	129

The foregoing tabulation shows that oil recovery decreases as the solution gas-oil ratio increases. One obvious reason for this is that the oil formation volume factor increases with the solution gas-oil ratio, thereby reducing the stock-tank oil in place for a given hydrocarbon volume. For lower API gravity oils, the effects are less pronounced because the possible GOR range is less.

An important factor not shown by the foregoing recovery figures is the oil-recovery rate. Since the bubble-point pressure increases as the solution GOR increases, higher producing rates are possible with high solution GOR's. Thus, in estimating the actual worth of a field, the prediction must be put on a time basis. The procedure for doing this is covered in a later section of this chapter.

Arps and Roberts[1] also show that oil viscosity, which can be characterized by the API gravity, significantly affects the solution-gas-drive recovery, as summarized in the following table:

Oil Gravity, °API	Approximate STO Viscosity, cp	Recovery, STB/acre-ft
15	18	95
30	9	130
50	2.5	195

All cases assume a 20 percent porosity sand with average relative-permeability characteristics and a solution gas-oil ratio of 600 scf/STB. As shown in the foregoing table, the recovery for an 18-cp oil is only one-half that for a 2.5-cp oil. The above three recovery points will lie in a straight line if the logarithm of viscosity is plotted against recovery.

C. Typical Performance of a Solution-Gas-Drive Field

The pressure and production history of the Horsehead pool, Arkansas, is shown in Fig. 4. This field produced solely by solution-gas drive until a waterflood was started in 1957. Peak producing rate was not achieved until three years after discovery because of a slow development rate. However, once the field was developed, the oil-production rate and reservoir pres-

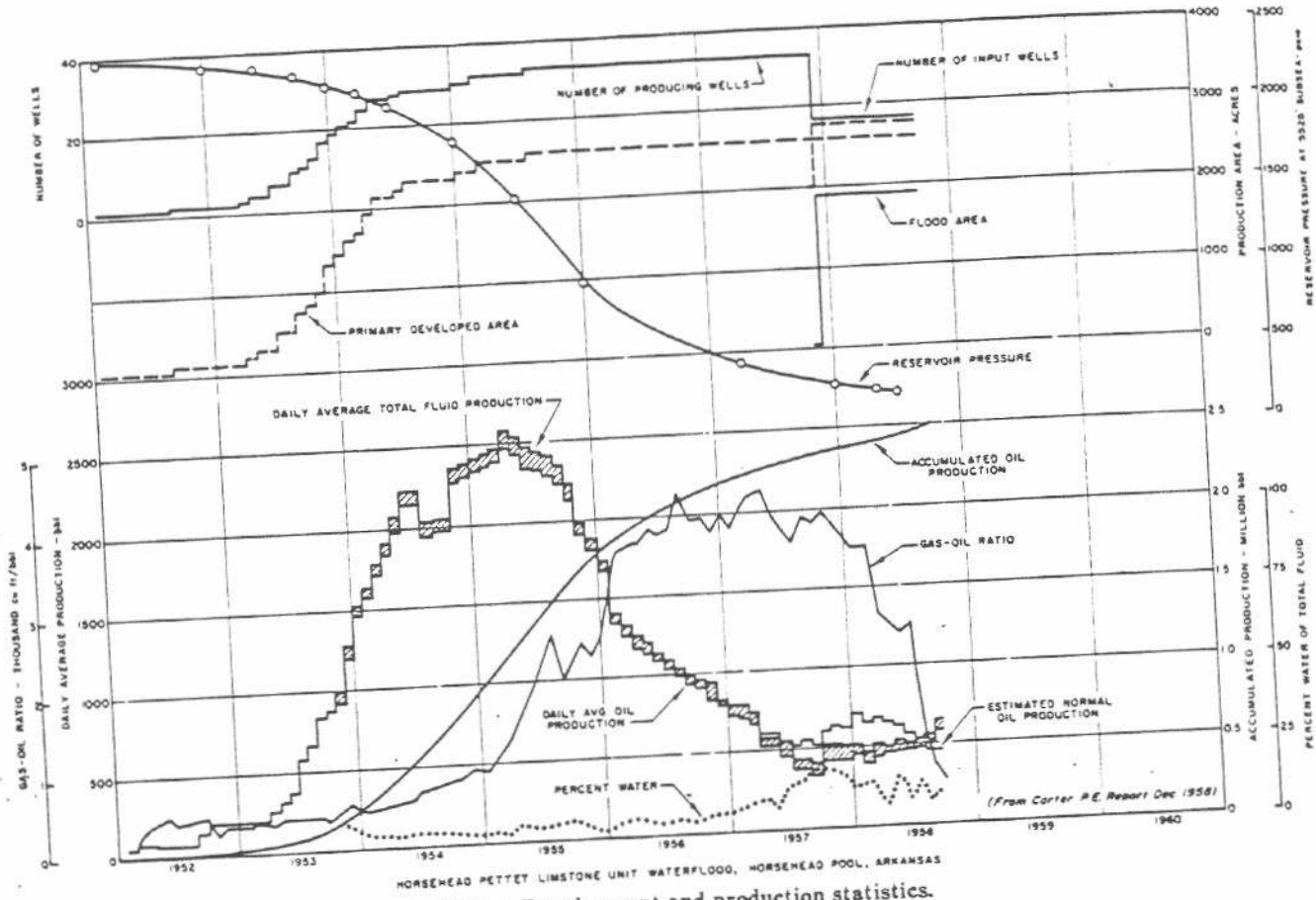

FIG. 4. Development and production statistics.

sure declined very rapidly. The producing gas-oil ratio rose rapidly to a peak and then declined slightly before the field was put under flood.

III. RESERVOIR ANALYSIS

A. Calculation of Oil in Place by Material Balance

The original oil in place for a solution-gas-drive reservoir may be calculated from the pressure-production history when the reservoir fluid characteristics are known. Chapter 5-4, Material Balance, presents an equation for the original oil in place in terms of cumulative oil and gas produced at a known pressure level. For a dissolved-gas-drive field, no gas cap is present and no water influx takes place, so the equation simplifies to the following form:

$$N = \frac{N_p B_o - N_p R_s B_g + G_p B_g}{B_o - B_{oi} + (R_{si} - R_s) B_g}, \qquad (1)$$

where

N = original oil in place, STB,
N_p = cumulative oil produced, STB,
B_o = oil formation volume factor, res B/STB,
B_g = gas formation volume factor, res bbl/scf,
B_{oi} = initial oil formation volume factor, res B/STB,
R_s = solution gas-oil ratio, scf/STB,
R_{si} = initial solution gas-oil ratio, scf/STB, and
G_p = cumulative gas produced, scf.

The following example illustrates the use of equation (1):

Example 1 Calculation of Oil in Place from Fi... Performance Data

Problem: Assuming solution-gas drive as the s... producing mechanism, determine the original oil c... tent of a reservoir that has produced 127,600 STB... oil at an average GOR of 670 scf/STB. Reserv... pressure declined from the bubble point of 1225 ... to 1000 psig. The reservoir fluid characteristics ... shown in Fig. 5.

Solution: The fluid parameters needed for equa... (1) are determined in Fig. 5.

Pressure, psig	B_o, res B/STB	R_s, scf/STB	B_g, res bbl/...
1225	1.18*	550**	—
1000	1.1655	455	0.0026

*Initial oil formation volume factor.

**Initial solution gas-oil ratio.

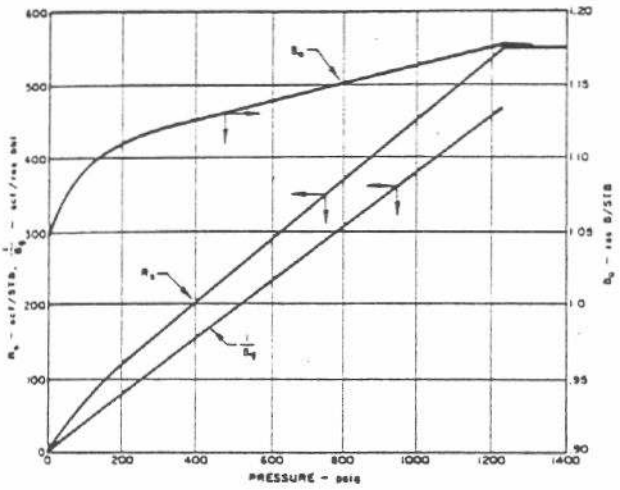

FIG. 5. B_o, R. and $\frac{1}{B_g}$ vs pressure — Example 1.

Substituting the production and fluid characteristics data into equation (1):

$$N = \frac{(127{,}600)(1.1655) - (127{,}600)(455)(0.00261)}{1.1655 - 1.18 + (550 - 455)\,0.00261} + \frac{[(127{,}600)(670)]\,(0.00261)}{1.1655 - 1.18 + (550 - 455)\,0.00261},$$

$N = 943{,}500$ STB.

In practice, N should be calculated for several pressure points to eliminate possible errors in reservoir pressure measurements. If the N values fluctuate but do not increase with time, an average value can be used, but one should give greater weight to the later values. On the other hand, if the calculated N values continually increase as reservoir pressure declines, water is probably entering the reservoir from an adjoining aquifer. In this case, all of the calculated values of N are too large, and the volumetric approach should be used.

The most common sources of error in determining N by equation (1) are:

1. Faulty field-pressure data.
2. Faulty production data.
3. Nonrepresentative fluid data.

The cumulative gas production is often the least accurate of the field data. Unless the produced gas is processed or sold, gas production must be estimated from infrequent tests of the gas-oil ratio. A serious error may result from assuming that fluid properties are constant throughout a reservoir. Large variations in original fluid properties are sometimes observed within a reservoir. These differences are usually associated with changes in subsea depth or with barrier faults within the reservoir. Fluid samples should be taken from various parts of a new reservoir to determine any existing variations in fluid properties. Chapter 1-7, Fluid Properties, presents information that shows the ranges of variation in these properties for some reservoir fluids.

Application of the material-balance equation for determining oil in place for reservoirs covering a large area or having a high closure may require special consideration. Portions of a large reservoir may be at different stages of depletion because of variations in permeability or development time. In such cases, it is more accurate to divide the field into areas and calculate separate N values based on each area's pressure-production history. In a high-closure reservoir, the pressure at the top may be below the saturation pressure while the pressure at the bottom is above saturation. Material-balance calculations should be made separately for the saturated and undersaturated portions of the reservoir. The details of this technique are also given in Chapter 5-4.

B. Calculation of Oil in Place by Volumetric Analysis

The original oil content of a reservoir should always be calculated on a volumetric basis, provided the reservoir volume is known and porosity and connate water values are available. The following equation is used:

$$N = \frac{7758\,A h_n \varphi\,(1 - S_{wi})}{B_{oi}}, \qquad (2)$$

where

A = reservoir area, acres,
h_n = net reservoir thickness, ft,
φ = porosity, fraction of bulk volume, and
S_{wi} = connate water saturation, fraction of pore volume.

The N value calculated by material balance [equation (1)] and the volumetric N value [equation (2)] should agree within 10 percent, provided natural water influx is not important. Of course, the accuracy of either method depends on the quality of the data used. When the two methods give vastly different N values, one must critically analyze the data to select the better value. Unless water influx is suspected or the fluid characteristics data are questionable, the material balance value of N is ordinarily preferred to the volumetric value because it is based on direct measurement of reservoir performance.

C. Relative Permeability from Field Performance

The relative-permeability characteristics of a solution-gas-drive field can be determined from the pressure-production history for the field. Basically, this is done by calculating the relative-permeability ratio

from the instantaneous producing gas-oil ratio, R, and then determining from production information the average gas saturation that corresponds to the calculated value of k_g/k_o.

The relative-permeability ratio is described as:

$$\frac{k_g}{k_o} = \frac{R - R_s}{\left(\frac{\mu_g}{\mu_o}\right)\left(\frac{B_o}{B_g}\right)} \quad (3)^*$$

where

k_g/k_o = gas-oil relative-permeability ratio,

R = instantaneous producing gas-oil ratio, scf/STB,

R_s = solution gas-oil ratio at the existing pressure, scf/STB,

μ_o, μ_g = viscosities of oil and gas at the prevailing pressure, cp, and

B_o, B_g = formation volume factors for oil and gas at the prevailing pressure.

To evaluate the solution gas-oil ratio in equation (3), as well as the oil and gas viscosities and volume factors, we must determine the average reservoir pressure from field data or by material balance.

The calculated k_g/k_o exists at the average pore volume gas saturation, S_g, determined from:

$$S_g = \left[1 - \left(1 - \frac{N_p}{N}\right)\left(\frac{B_o}{B_{oi}}\right)\right](1 - S_{wi}) . \quad (4)^{**}$$

In addition to fluid property and connate water information, the cumulative oil recovery, N_p, must be known to solve equation (4) for the gas saturation. The following example shows the procedure for calculating k_g/k_o versus S_g from field history.

Example 2 Calculation of Gas-Oil Relative-Permeability Ratio Data from Field Performance

Problem: Determine k_g/k_o and S_g at two pressure levels for the reservoir in Example 1. Fluid volume factors and solution GOR's are shown in Fig. 5, and fluid viscosities in Fig. 6. Pertinent data for the pressure-production history are:

	$\bar{p}_R$, Avg. Reservoir Pressure, psig	
	1133	1000
N_p, cumulative oil produced, STB	75,500	127,600
R, producing gas-oil ratio, scf/STB	650	1,500

Connate water saturation is 30 percent.

Solution: Fluid parameters determined at 1133 and 1000 psig from Figs. 5 and 6 are tabulated below:

	p_r psig	
	1133	1000
B_o, res B/STB	1.174	1.1655
R_s, scf/STB	510	455
B_g, res bbl/scf	0.0023	0.00261
μ_o, cp	1.835	1.868
μ_g, cp	0.01622	0.01567

Calculate k_g/k_o by substitution into equation (3):

1. @ 1133 psig,

$$\frac{k_g}{k_o} = \frac{650 - 510}{\left(\frac{1.835}{0.01622}\right)\left(\frac{1.174}{0.0023}\right)} = 0.00242.$$

2. @ 1000 psig,

$$\frac{k_g}{k_o} = \frac{1500 - 455}{\left(\frac{1.868}{0.01567}\right)\left(\frac{1.1655}{0.00261}\right)} = 0.0196.$$

Calculate S_g by substitution into equation (4):

1. @ 1133 psig,

$$S_g = \left[1 - \left(1 - \frac{75{,}500}{943{,}500}\right)\frac{1.174}{1.18}\right](1 - 0.30) = 0.0593.$$

2. @ 1000 psig,

$$S_g = \left[1 - \left(1 - \frac{127{,}600}{943{,}500}\right)\frac{1.1655}{1.18}\right](1 - 0.30) = 0.1021$$

Grouping the above calculations gives two relative-permeability points:

S_g	k_g/k_o
0.0593	0.00242
0.1021	0.0196

Relative-permeability ratios determined from field

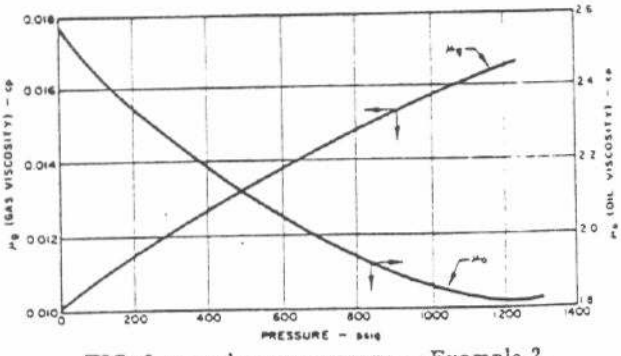

FIG. 6. μ_o and μ_g vs pressure — Example 2.

*See Chapter 5-5, Fluid Flow, for the derivation of this equation.

**See Chapter 5-4, Material Balance, for the basis for this equation.

performance tend to be higher at a given gas saturation than laboratory data on cores from the same reservoir. The field results are influenced by stratification and by the fact that gas saturation at the producing well is higher than the field average. This applies to cases where solution-gas drive is the sole recovery mechanism. If fluid expansion or gravity are important, field performance may show lower relative-permeability ratios as compared with laboratory data. In any case, to use field-derived k_g/k_o data for predicting future performance, plot the field points and extrapolate the curve parallel to the laboratory k_g/k_o curve. Fig. 7 illustrates this for data calculated above.

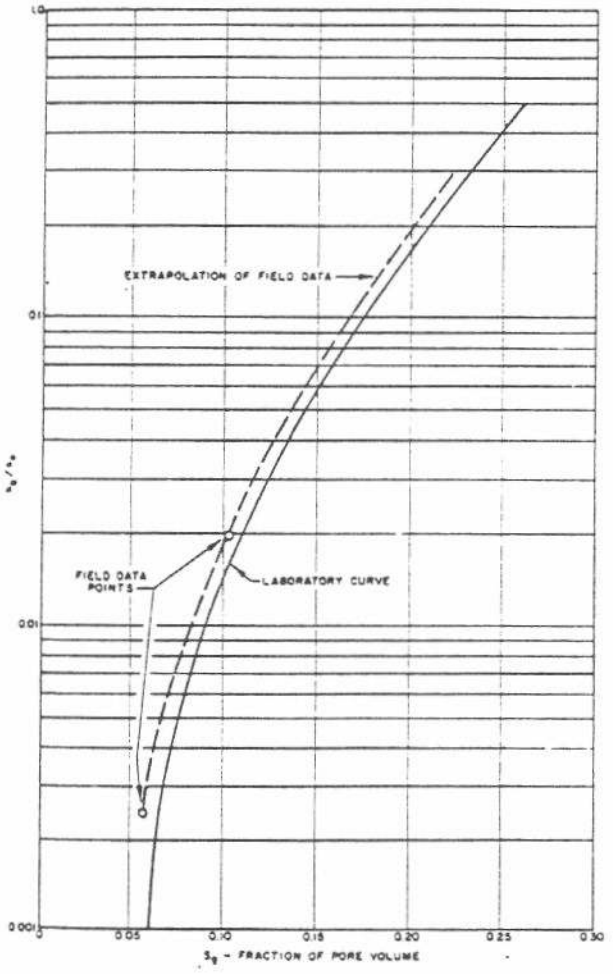

FIG. 7. Extrapolation of field k_g/k_o data.

IV. CALCULATION OF SOLUTION-GAS-DRIVE RECOVERY

The most commonly used approach for calculating the pressure-recovery performance of solution-gas-drive reservoirs is through material-balance concepts. Part A below summarizes five methods that employ these concepts for predicting fluid depletion below the bubble point. Part B discusses fluid expansion between the original and bubble-point pressures. In this range there are almost no complications involved in material-balance concepts. Part C presents the details of predicting fluid production below the bubble-point pressure by the Pirson Method, and includes pertinent remarks about the Muskat Method. Part D briefly describes numerical methods that have been developed for the digital computer, while Part E presents some short-cut methods for use where data are sparse or a recovery estimate is needed in a hurry.

A. Material-Balance Prediction Methods

Five published material-balance equations useful in predicting solution-gas-drive performance are: (1) Pirson's Finite Difference Method, (2) Muskat's Equation in Differential Form, (3) the Humble Method (Schilthuis), (4) the Tracy or Tarner Method, and (5) the Imperial Gas and Oil Phase Material Balances. All of these methods are based on material-balance concepts and give comparable answers.

1. *The Pirson Method*[7] is recommended for hand calculation because of the converging nature of the trial-and-error solution. Recovery for each pressure increment can usually be evaluated in two or three trials. (This is illustrated in Part B, Example 4.)

2. *The Muskat Method*[6] involves a material-balance equation written in differential form and is used in combination with the instantaneous gas-oil ratio equation based on gas-oil relative permeability. This method lends itself to use with high-speed computers and will be discussed in some detail in Part C.2.

3. *The Humble (Schilthuis) Method*[11] is based on the Schilthuis material-balance equation (see Chapter 5-4, Material Balance). The Pirson Method is based on the same equation but is written in finite difference form. The transition from the Schilthuis equation to the Pirson equation is also described in Chapter 5-4.

4. *The Tracy*[13] *or Tarner Method* is based on the same material-balance equation as the other methods but involves the use of pressure-dependent variables. Tracy developed this equation and Tarner extended the method by incorporating the gas-oil ratio equation into it much like Pirson and Muskat. This technique is also described in Chapter 5-4.

5. *The Imperial Gas and Oil Phase Material Balances*[8] provide another method for predicting the solution-gas-drive performance of a reservoir. This method involves the use of two gas-saturation equations: One is based on a gas balance, the other on a liquid balance. Using each equation the basic procedure involves calculating pressure as a function of saturation for a given amount of gas and oil produc-

tion. These data are then plotted and the intersection of the two curves gives the correct pressure for a given saturation value. The method is best handled by a digital computer.

The compositional material-balance technique should be used for a volatile-oil reservoir. This technique, which is covered in detail in Chapter 3-3, Gas-Condensate and Volatile-Oil Reservoirs, provides the best accuracy for reservoirs containing fluid rich in intermediates (C_2 through C_7). Reservoirs requiring this technique will have high formation volume factors (generally greater than 2.0).

B. Material Balance for Fluid Expansion Above the Bubble Point

The previously mentioned material-balance methods for predicting solution-gas-drive recovery are applicable from the bubble-point pressure downward. Oil recovery by oil, rock, and connate water expansion at pressures above the bubble point must be calculated separately. As a rule, recovery above the bubble point is comparatively small; however, in some cases, it can amount to 5 percent or more of the original oil in place. In reservoirs with extremely low saturation pressures, it is possible for the recovery by fluid expansion to be several times the solution-gas-drive recovery.

Oil recovery resulting from the expansion of oil, rock, and connate water above the bubble point can be calculated from the following material-balance equation. A similar equation is presented in Chapter 5-4:

$$NB_{oi}[1 - \bar{c}_{f+w}(p_i - p_b)] = (N - N_p)\,B_{ob}, \quad (5)$$

where

subscript i refers to initial pressure,

subscript b refers to the bubble-point pressure, and

$\bar{c}_{f+w} = \dfrac{c_f + S_{wi}\,c_w}{1 - S_{wi}}$ = reservoir compressibility of porosity and connate water,* bbl per initial hydrocarbon bbl per psi.

Solving equation (5) for N_p, the oil production above the bubble point, we get

$$N_p = N\left\{1 - \frac{B_{oi}}{B_{ob}}[1 - \bar{c}_{f+w}(p_i - p_b)]\right\}. \quad (5a)$$

The following example demonstrates the procedure for calculating oil recovery above the bubble point. In this example, the initial pressure is only 75 psi above the bubble point and the corresponding oil recovery is very slight. Also, the recovery is roughly proportional to the difference between initial and bubble-point pressure.

Example 3 Prediction of Oil Recovery Above the Bubble Point

Problem: Predict the oil recovery during the pressure decline to the bubble point for the reservoir described in Examples 1 and 2 if initial reservoir pressure, p_i = 1300 psig and $\bar{c}_{f+w} = 14.3 \times 10^{-6}$ psi^{-1}. Fig. 5 gives B_o versus pressure; see Example 1 for N.

Solution: Evaluate the factors needed in equation (5a). From Fig. 5, B_{oi} (1300 psig) = 1.1795 and B_{ob} (1225 psig) = 1.18. From Example 1, N = 943,500 STB. Therefore:

$$N = 943{,}500\left\{1 - \frac{1.1795}{1.18}[1 - (14.3\times10^{-6})(1300 - 1225)]\right\}$$

N_p = 1406 STB.

The recovery of 1406 STB from initial to bubble-point pressure represents only 0.15 percent of the original oil in place. In this case, the recovery is insignificant since the oil in place cannot be calculated to this degree of accuracy. However, the recovery above the bubble point should always be calculated to check its significance.

C. Material Balance for Production Below the Bubble Point

1. PIRSON FINITE DIFFERENCE METHOD

The Pirson finite difference equation for a solution-gas-drive reservoir expresses the oil recovery for a decrement in pressure below the bubble point. Derived in Chapter 5-4, this equation is:

$$\Delta\left(\frac{N_p}{N}\right) = \frac{\left[1 - \left(\frac{N_p}{N}\right)_n\right]\Delta\left(\frac{B_o}{B_g} - R_s\right) - B_{ob}^{\dagger}\,\Delta\left(\frac{1}{B_g}\right)}{\left(\frac{B_o}{B_g} - R_s\right)_{n+1} + \frac{R_n + R_{n+1}}{2}} \quad (6)$$

The left-hand side of equation (6) gives the amount of oil recovered (as a fraction of the oil in place at the bubble point) when the reservoir pressure declines from the pressure at n to the pressure at $n + 1$

The factors B_o, B_g, and R_s are strictly functions of pressure for a given reservoir fluid. However, the producing gas-oil ratio (R_n or R_{n+1}) is a function of gas saturation and pressure.

*The calculation of $\bar{c}_{f+w}$ is presented in Chapter 5-4. Sources of data for rock compressibility (c_f) are given in Chapter 1-2, Rock Properties. Water compressibility values can be found in Chapter 1-7, Fluid Properties.

†B_{ob} is used in place of B_o, because recovery above the bubble point has already been accounted for.

The gas-oil ratio, R, can be calculated from equation (3):

$$R = \frac{k_g \mu_o B_o}{k_o \mu_g B_g} + R_s . \qquad (3a)$$

The gas-oil relative-permeability ratio (k_g/k_o) is a function of gas saturation. The gas saturation at the end of a pressure decrement can be determined by modifying equation (4):

$$S_g = \left\{1 - \left[1 - \left(\frac{N_p}{N}\right)_{n+1}\right]\frac{B_o}{B_{ob}}\right\}(1 - S_{wi}) . \qquad (4a)$$

In summary, the steps to follow to predict the pressure-recovery performance of a field by using equations (6), (3a), and (4a) are:

1. Select a pressure decrement to a pressure level, p.
2. Assume a value of $\Delta(N_p/N)$ for the pressure drop to p. This does not have to be a particularly good assumption because the solution generally converges rapidly.
3. Add the assumed $\Delta\ (N_p/N)$ to the N_p/N at the start of the period. This will provide $(N_p/N)_{n+1}$ for use in equation (4a) to calculate S_g.
4. With S_g from step 3, read the corresponding k_g/k_o from the relative-permeability curve.
5. Calculate R_{n+1} by equation (3a).
6. Calculate $\Delta(N_p/N)$ by equation (6).
7. Compare the $\Delta(N_p/N)$ calculated in step 6 to that assumed in step 2. If agreement is not within the desired limits (usually $\pm$ 0.5%), repeat steps 3 through 6 with the value of $\Delta(N_p/N)$ just calculated in step 6. Because of rapid convergence of the solution, usually no more than three trials are needed.
8. After a satisfactory match is obtained between $\Delta(N_p/N)$ calculated and $\Delta(N_p/N)$ assumed, repeat the entire procedure after selecting another pressure level.

Example 4 Prediction of Solution-Gas-Drive Recovery by the Pirson Method

Problem: For the solution-gas-drive reservoir considered in previous examples, calculate the oil recovery and gas-oil ratio performance as a function of pressure below the bubble point. The data given are: B_o, $1/B_g$, and R_s versus pressure (Fig. 5), μ_o and μ_g versus pressure (Fig. 6), and the gas-oil relative-permeability ratio versus pore-volume gas saturation (Fig. 8). Assume that S_{wi} equals 30 percent.

Solution: The first step is to read and list the pressure-dependent variables used in equation (6). Pressure decrements of approximately 100 psi are generally used, although the increments can be varied depending on the degree of accuracy required. The variables as read from Figs. 5 and 6 are listed as functions of pressure in Table I-A, Columns 1 through 5. Columns 6 through 11 are the combinations of variables that enter into equation (6). Table I-B shows the actual calculation of oil recovery from the bubble point to 40 psig for the selected pressure decrements. The reservoir pressure and producing gas-oil ratio are plotted against recovery in Fig. 1. The significance of each column in Table I-B is described below. The subscript n refers to the start of a pressure decrement, while the subscript $(n + 1)$ refers to the end of the decrement.

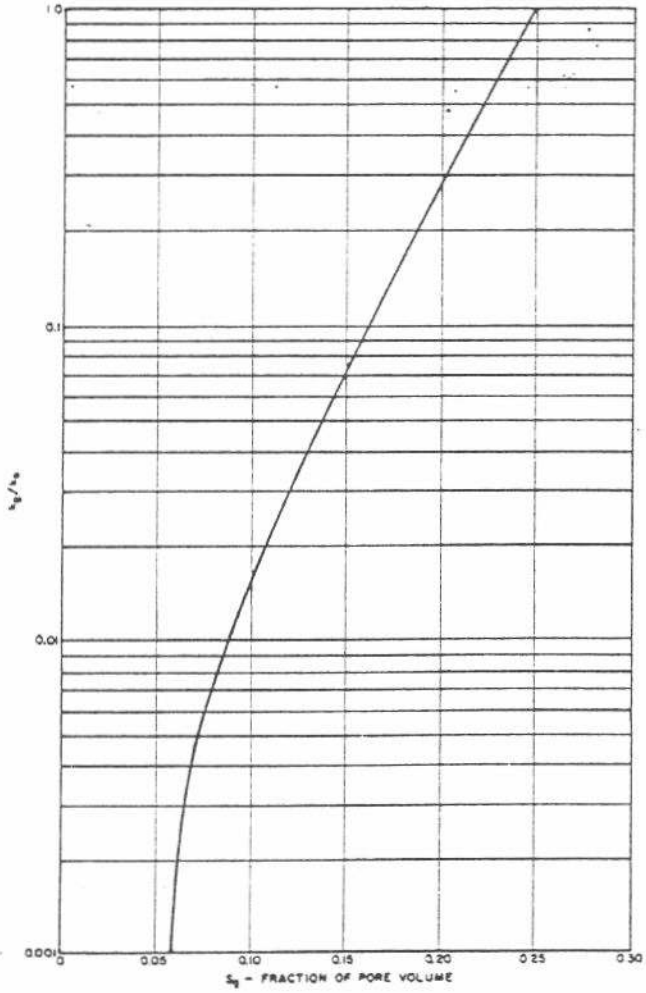

FIG. 8. Relative-permeability ratio vs pore-volume gas saturation — Example 4.

TABLE I-A. Pressure-Dependent Variables for Example 4

pressure, psig	(1) B_o	(2) $\frac{1}{B_g}$	(3) R_s	(4) μ_o	(5) μ_g	(6) $\frac{\mu_o}{\mu_g}$	(7) $\Delta\frac{1}{B_g}$	(8) $\frac{B_o}{B_g}$	(9) $\left(\frac{B_o}{B_g}-R_s\right)$	(10) $\Delta\left(\frac{B_o}{B_g}-R_s\right)$	(11) $B_{ob}\Delta\frac{1}{B_g}$
1225	1.18	470	550	1.820	0166	109.5	0	555	5	0	0
1150	1.175	442	518	1.832	.0163	112.5	−28	520	2	−3	−33.0
1050	1.167	403	477	1.855	.0159	116.5	−39	470	−7	−9	−46.0
900	1.159	345	413	1.900	.0152	125.0	−58	400	−13	−6	−68.44
800	1.153	306	372	1.942	.0148	131.2	−39	354	−18	−5	−46.0
700	1.147	267	330	1.991	.0143	139.2	−39	306	−24	−6	−46.0
600	1.141	228	288	2.050	.0138	148.5	−39	260	−28	−4	−46.0
500	1.134	190	245	2.118	.0133	159.5	−38	216	−29	−1	−44.8
400	1.127	151	203	2.188	.0128	165.0	−39	170	−33	−4	−46
300	1.120	112	161	2.265	.0123	184.2	−39	125	−36	−3	−46
140	1.103	53	90	2.418	.0111	218.0	−59	58.5	−31.5	+4.5	−69.6
40	1.075	18	30	2.520	.0104	242.5	−35	19.4	−10.6	+20.9	−41.3

Column — Description

(12) $\Delta(N_p/N)$. The estimated production (as a fraction of oil in place at the bubble point) during a pressure decrement. The value for the first pressure decrement may be based on previous experience, and for subsequent decrements $\Delta(N_p/N)$ may be estimated from the foregoing trend.

(13) $(N_p/N)_n$. The fractional cumulative oil recovery at the start of a pressure decrement. At any pressure level this recovery equals $\Sigma\Delta(N_p/N)$ for the previous intervals.

(14) $[1-(N_p/N)_n]$. The fraction of original oil (in place at the bubble point) still in the reservoir at the start of a decrement.

(15) $[1-(N_p/N)_n]\,\Delta[(B_o/B_g)-R_s]$. This is the first term of the numerator of equation (6) and equals Column 14 times Column 10.

(16) $[1-(N_p/N)_n]\Delta[(B_o/B_g)-R_s]-[B_{ob}\,\Delta(1/B_g)]$. This is the numerator of equation (6); it equals Column 15 minus Column 11.

(17) $[1-(N_p/N)_{n+1}]$ is the fraction of oil left in the reservoir at the end of the pressure decrement and is a useful intermediate step in calculating S_g in the next step.

(18) $S_g=\{1-[1-(N_p/N)_{n+1}](B_o/B_{ob})\}(1-S_{wi})$. This is equation (4a), for calculating the gas saturation at the end of the pressure decrement as a fraction of total pore volume. $(N_p/N)_{n+1}=(N_p/N)_n+\Delta(N_p/N)$.

(19) k_g/k_o. The gas-oil relative-permeability ratio is read from Fig. 8 at the calculated gas saturation (step 18).

(20) $(k_g/k_o)(\mu_o/\mu_g)(B_o/B_g)$. The flowing gas-oil ratio in the reservoir at the end of the pressure decrement equals the product of Columns 6, 8, and 19.

(21) R_{n+1}. The producing gas-oil ratio at the end of the pressure decrement equals the flowing GOR plus the solution GOR, Column 20 plus Column 3.

(22) $(R_n+R_{n+1})/2$. The average gas-oil ratio for the pressure decrement; the arithmetic average of the GOR's at the start and end of a pressure decrement.

(23) $[(B_o/B_g)-R_s]_{n+1}+[(R_n+R_{n+1})/2]$. The denominator of equation (6) equals Column 9 (at the lower pressure) plus Column 22.

(24) $\Delta(N_p/N)$. The oil production for a pressure decrement calculated from equation (6) equals Column 16 divided by Column 23. If the calculated oil production differs from the value assumed in Column 12, use this calculated value in Column 12 and repeat until Columns 12 and 23 agree to the third significant figure.

2. MUSKAT* DIFFERENTIAL EQUATION

The recovery performance of a solution-gas-drive field can be predicted directly with a differential form of the material balance equation. The most widely used form is the Muskat equation,

$$\frac{dS_o}{dp}=\frac{S_o\frac{B_g}{B_o}\frac{dR_s}{dp}+\frac{k_g}{k_o}\frac{\mu_o}{\mu_g}\frac{S_o}{B_o}\frac{dB_o}{dp}+(1-S_w-S_o)\,B_g\frac{d\left(\frac{1}{B_g}\right)}{dp}}{1+\frac{k_g}{k_o}\frac{\mu_o}{\mu_g}} \qquad (7$$

Equation (7) is simply a combination of equation (6), (3a), and (4a), written in differential form. very small pressure increments, such as one-half one psi, are used, the values of S_o, B_g, B_o, μ_o, and change insignificantly during the period. (Sometim even larger pressure increments can be used with s

TABLE 1-B. Calculation of Oil Recovery for Example 4.

pressure, psig	(12) $\Delta\frac{N_p}{N}$	(13) $\left(\frac{N_p}{N}\right)_n$	(14) $1-\left(\frac{N_p}{N}\right)_n$	(15) (14) × (10)	(16) (15) − (11)	(17) $1-\left(\frac{N_p}{N}\right)_{n+1}$	(18) S_o, % PV	(19) k_o/k_o	(20) (19) × (6) × (8)	(21) R_{n+1} (20) + (3)	(22) $\frac{R_{n+1}+R_n}{2}$	(23) (9) + (22)	(24) (16) ÷ (23)
1225	0	0	1.0	0	0	0	0	0	0	550	—	—	0
1150	0.0700	0	1.0	−3	30	0.930	5.18	0	0	518	534	536	0.0560
	0.0560					0.944	4.24	0	0	518	534	536	0.0560
1050	0.0500	0.0560	0.9440	−8.50	37.50	0.8940	8.11	0.0095	520	997	758	751	0.0500
900	0.0400	0.1060	0.8940	−5.36	63.08	0.8540	11.28	0.0245	1225	1638	1318	1305	0.0483
	0.0440*					0.8500	11.56	0.0270	1350	1763	1380	1367	0.0461
	0.0461					0.8479	11.70	0.0285	1425	1838	1418	1405	0.0449
	0.0449					0.8491	11.62	0.0277	1385	1798	1398	1385	0.0455
	0.0455					0.8485	11.66	0.0280	1400	1813	1405	1392	0.0453
	0.0453					0.8487	11.65	0.0280	1400	1813	1405	1392	0.0453
800	0.0200	0.1513	0.8487	−4.24	41.76	0.8287	13.32	0.0465	2160	2532	2173	2155	0.0194
	0.0194					0.8293	13.28	0.0465	2160	2532	2173	2155	0.0194
700	0.0150	0.1707	0.8293	−4.98	41.02	0.8143	14.60	0.066	2811	3141	2837	2813	0.0146
	0.0146					0.8147	14.56	0.066	2811	3141	2837	2813	0.0146
600	0.0120	0.1853	0.8147	−3.26	42.74	0.8027	15.67	0.090	3475	3763	3452	3424	0.0125
	0.0125					0.8022	15.70	0.090	3475	3763	3452	3424	0.0125
500	0.0100	0.1978	0.8022	−0.80	44.00	0.7922	16.71	0.118	4065	4310	4037	4008	0.0110
	0.0110					0.7912	16.77	0.119	4100	4345	4054	4025	0.0109
	0.0109					0.7913	16.77	0.119	4100	4345	4054	4025	0.0109
400	0.0100	0.2087	0.7913	−3.17	42.83	0.7813	17.77	0.160	4488	4691	4518	4485	0.0095
	0.0095					0.7818	17.73	0.160	4488	4691	4518	4485	0.0095
300	0.0100	0.2182	0.7818	−2.35	43.65	0.7718	18.72	0.200	4605	4766	4729	4693	0.0093
	0.0093					0.7725	18.68	0.200	4605	4766	4729	4693	0.0093
140	0.0150	0.2275	0.7725	3.48	73.08	0.7575	20.44	0.335	4272	4362	4564	4532	0.0161
	0.0161					0.7564	20.51	0.335	4272	4362	4564	4532	0.0161
40	0.0150	0.2436	0.7564	15.81	57.11	0.7414	22.72	0.565	2658	2688	3525	3514	0.0163
	0.0163					0.7401	22.81	0.565	2658	2688	3525	3514	0.0163

Ultimate Recovery at 40 psig = 0.2599

*When the assumed and calculated values of $\Delta(N_p/N)$ differ by more than 10 percent, use an average of the two for the next assumed value of $\Delta\frac{N_p}{N}$ to reduce the number of trials.

ficient accuracy.) Thus, the oil saturation and pressure-dependent values at the start of the period can be used and the trial-and-error procedure is eliminated. This type of calculation is restricted to high-speed computers because of the numerous calculations required. Programs are available for the Muskat solution. For details, see computer program manuals.

Although the Muskat equation can be used for hand calculation by taking larger pressure increments, the Pirson Method, using equations (6), (3a), and (4a), is recommended.

D. Numerical Prediction Methods

Numerical methods for predicting the performance of solution-gas-drive reservoirs in one or two dimensions are available. The one-dimensional method for a single well, described by Dalton and Greene[2], accounts for pressure and saturation gradients in the wellbore drainage area. By contrast, the material-balance prediction methods (e.g., Pirson or Muskat) assume constant pressure and saturation throughout the reservoir. These two concepts of pressure and saturation profile are illustrated in Fig. 2.

The one-dimensional method provides a sound basis for determining the effects of well spacing or producing rate on solution-gas-drive performance. Example calculations show that gas-oil ratio behavior is affected by well spacing and producing rate, even though ultimate recovery remains essentially constant. The calculated performance of an intermittently produced well shows that although the gas-oil ratio can be temporarily reduced by a shut-in period, there is no permanent increase in oil recovery. Since the one-dimensional method has shown that ultimate oil recovery is not significantly affected by saturation gradients, the Pirson or Muskat methods are recommended for general use.

The two-dimensional analysis will allow one to determine the effect of areal variations in sand quality throughout the reservoir. This method has been used to determine oil migration between leases and to evaluate infill drilling in solution-gas-drive fields. The two-dimensional method can also be used to evaluate gravity drainage by modeling a vertical cross section of a reservoir that is either homogeneous or stratified. This application will be discussed in more detail later.

E. Short-Cut Prediction Methods

The previously discussed methods for predicting the performance of a solution-gas-drive reservoir are lengthy to apply. If data on a reservoir are sparse or a recovery estimate is needed quickly, the use of a short-cut method may be justified. If complete data are available on a reservoir, however, the short-cut methods should be avoided and a complete prediction made. Some acceptable short-cut methods are discussed below.

1. RECOVERY EFFICIENCY BASED ON ACTUAL FIELD RESULTS

The producing histories of 68 solution-gas-drive fields have been analyzed to determine what factors influence recovery efficiency. One of our analyses resulted in a linear equation for the oil recovered during pressure reduction below the bubble point. The coefficients for each term in the equation were calculated from data on the 68 fields by the method of least squares fit.

$$\left[\begin{array}{c}\text{Recovery Efficiency}\\ \text{(Percent of Original}\\ \text{Oil in Place)}\end{array}\right] = 7.93 \log\left(\frac{k}{\mu_o}\right) + 0.373\left(\frac{p_b}{p_a}\right) + 0.182\, S_{wi} + 0.149\,\varphi - 0.0006d - 0.0045\left(\frac{R_{sb}}{B_{ob}}\right), \quad (8)$$

where

(k/μ_o) = dry air permeability (md) divided by the oil viscosity (cp) at the bubble point,

(p_b/p_a) = bubble-point pressure (psia) divided by the abandonment pressure (psia),

S_{wi} = connate water saturation, % PV,

φ = porosity, %,

d = reservoir depth, ft subsurface, and

(R_{sb}/B_{ob}) = solution-gas-oil at the bubble point (scf/STB) divided by the oil volume factor at the bubble point (res B/STB).

For each of the 68 fields, the recovery calculated by equation (8) was compared with the actual recovery. This comparison is evaluated by the confidence-limit lines in Fig. 9. The confidence-limit lines show that in 70 percent of the fields, the calculated recovery was within 25 percent of the actual value, while in 31 percent of the cases, the error was less than 10 percent. These results are fair, even though relative permeability—one of the most important factors in oil recovery—does not enter into equation (8) directly. The fields where calculated recovery is in error by 2 percent or more of the actual value probably have unusually favorable or unfavorable relative-permeability characteristics. The ranges of data used in this study are as follows: $\log(k/\mu_o)$ (0.86 to 3.080); p_b/p

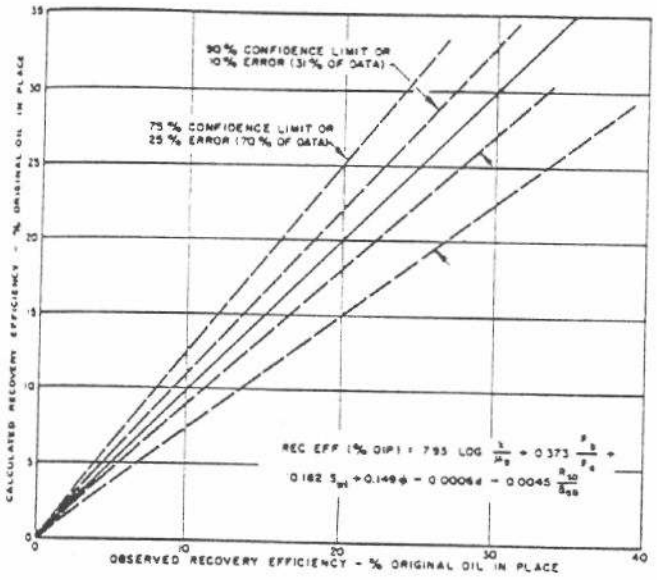

FIG. 9. Comparison of observed with empirically calculated oil recovery for 68 solution-gas-drive sandstone fields.

(1.56 to 33.5); S_{wi} (8.9 to 50.0); φ (9.0 to 28.9); d (1500 ft to 11,500 ft); and R_{sb}/B_{ob} (57.1 to 980 scf/res bbl).

2. ULTIMATE RECOVERY FROM DECLINE CURVES

If a solution-gas-drive reservoir has been producing at capacity, its ultimate recovery can be estimated by extrapolating the production decline curve. This curve will usually approach a straight line if the logarithm of the producing capacity is plotted against cumulative oil production. Details of decline-curve analysis are discussed in Chapter 5-8.

3. ALTERNATE METHODS FOR ESTIMATING RECOVERY

A quick estimate of ultimate recovery of a solution-gas-drive reservoir based on the Muskat Method can be made from reference 14. This reference contains figures prepared from calculations using varying fluid properties and relative-permeability characteristics. To use the method for a specific reservoir, choose the figure that most nearly matches the field (stock-tank-oil viscosity, connate water, and relative-permeability-ratio curve). The actual determination of ultimate oil recovery from bubble-point fluid characteristics is illustrated on each figure.

Roberts and Ellis[10] propose a method for using the early history of a solution-gas-drive sandstone reservoir to predict the future performance. They extended the work of Arps and Roberts[1] to show the predicted gas-oil ratio trends for a variety of solution gas-oil ratios, oil gravities, and sandstone relative-permeability characteristics. If the oil gravity and solution gas-oil ratio of a reservoir are known, the trend of the producing gas-oil ratio can be matched with the published predictions to determine the approximate relative-permeability characteristics. The future gas-oil ratio trend and recovery can be estimated by extrapolating the history along the calculated GOR trend. Although the work presents predictions for only a few oil gravities, solution GOR's, and sand qualities, a reasonable prediction can be made by interpolating between the published curves.

V. PERFORMANCE PREDICTIONS ON A TIME BASIS

The material-balance methods for predicting solution-gas-drive recovery give recovery as a function of average reservoir pressure. A detailed economic analysis of the future worth of a reservoir requires that the predicted recovery be put on a time basis. This, in turn, requires that the field producing rate be determined as a function of reservoir pressure.

Forecasting field producing rates requires a prediction of the maximum or capacity producing rate together with a knowledge of the government-regulated, market-demand proration rules. An example of calculating the maximum producing rate of a well for any stage of reservoir pressure is presented in this section. The maximum rate for a field is the summation of the individual well rates. Proration rules vary considerably between states. Some of the large producing states, including California and Illinois, have no compulsory proration. Most of the other states have proration formulas, which may include well depth, spacing, and well potential. The basis of proration for individual states is discussed in Chapter 2-6, Conservation Practices in the U. S. A.

A. Calculating Well and Field Productivities

An individual well's maximum producing rate in stock-tank barrels per day can be calculated by the following equation for pseudo-steady-state flow:

$$q_o = \frac{0.00708\ (\bar{p}_R - p_{wf})\, k\, k_{ro}\, h}{B_o\, \mu_o\, [\ln(r_e/r_w) - 0.75]} \qquad (9)^*$$

where

$\bar{p}_R$ = average reservoir pressure of drainage area, psig,

p_{wf} = flowing pressure at the wellbore sandface, psig,

k = absolute permeability, md,

*The term $[\ln(r_e/r_w) - 0.75]$ is used when the average pressure of the well drainage area $\bar{p}_R$, is used. If p_e, the pressure at r_e, is used, this term becomes $[\ln(r_e/r_w) - 0.5]$.

k_{ro} = relative permeability to oil at the existing gas saturation,

h = pay thickness, ft,

B_o = oil formation volume factor, res B/STB,

μ_o = oil viscosity, cp,

r_e = external well drainage radius, ft, and

r_w = wellbore radius, ft.

If productivity index (PI) data on a well are available, they should be used to evaluate the group of terms, $\frac{kh}{[\ln(r_e/r_w) - 0.75]}$, in equation (9).

This and other details of determining well productivity are covered in Chapters 2-1, Oil Well Productivity.

Shown also in Chapter 2-1 are examples to illustrate how producing rate affects such factors as (1) the tubing pressure drop in a flowing well, and (2) pressure and saturation gradients resulting from well drawdown.

The following simplified example for calculating well producing rates is presented to achieve continuity between Example 4, the Pirson prediction, and Example 9, which analyzes the economics of well spacing. We will predict, in the following example, the maximum production rate for a pumping well as a function of reservoir pressure. In determining fluid properties and relative permeability, an average value for reservoir pressure and gas saturation will be assumed to exist throughout the well drainage area. We will further assume that the well will always be pumped down, so that no pressure (0 psig) exists at the wellbore sand face.

Example 5 Predicting Maximum Well Producing Rate

Problem: Calculate the maximum producing rate as a function of reservoir pressure for the average well located on 80-acre spacing in the reservoir of Example 4. Use the same pressure steps as used in Examples 3 and 4. Information available includes:

B_o and μ_o vs pressure—Table I-A, Columns 1 and 4

Gas saturation vs pressure—Table I-B, Column 18; k_{ro} vs gas saturation—Fig. 10

k = 20 md

h = 20 ft

r_w = 1 ft

Solution: Calculate r_e and simplify equation (9) by grouping the constant terms; r_e can be approximated as the radius of an 80-acre circle:

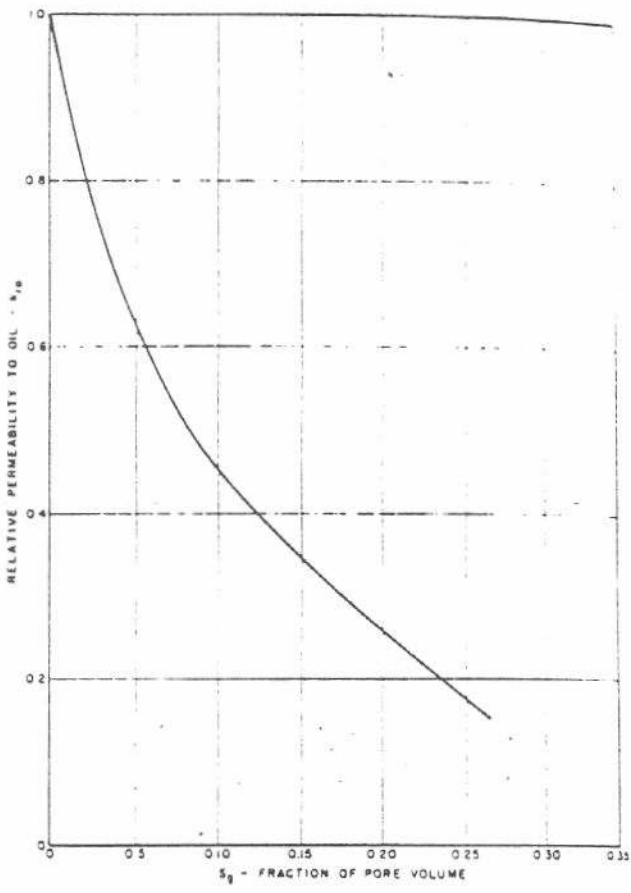

FIG. 10. Relative permeability to oil vs gas saturation — Example 5.

$$r_e = \sqrt{\frac{80 \times 43{,}560}{\pi}} = 1053 \text{ ft}$$

$$q_o = \frac{0.00708\,(\bar{p}_R - 0)\,(20)\,k_{ro}\,(20)}{B_o\mu_o\left[\ln\left(\frac{1053}{1}\right) - 0.75\right]} = 0.455\,\frac{\bar{p}_R\,k_{ro}}{B_o\mu_o}$$

Tabulate as a function of pressure: $B_o\mu_o$ (from Table I-A), S_g (from Table I-B), and k_{ro} (Fig. 10). With these data, the maximum production rate is calculated (Column 5, Table II).

The calculations for the maximum production rate for an average well in a reservoir are based on the average permeability and pay thickness. The maximum field rate can then be calculated best by putting the average well producing rate on a time basis and accounting for field development time.

B. Converting Maximum Producing Rate to a Time Basis

To determine the average well's capacity on a time basis, we must determine the volume of oil produced during each pressure decrement. For this, the volume of oil in place for the drainage area of an average well

TABLE II. Calculation of Maximum Producing Rate. (average well on 80-acre spacing)

(1) Pressure, psig	(2) $B_o \mu_o$	(3) S_g, % PV	(4) k_{ro}	(5) $q_o = 0.455 \frac{\bar{p}_R k_{ro}}{B_o \mu_o}$ STB/D
1300	2.15	0	1.0	275.1
1225	2.148	0	1.0	259.5
1150	2.153	4.24	0.670	162.8
1050	2.165	8.11	0.500	110.4
900	2.202	11.65	0.415	77.5
800	2.239	13.28	0.380	61.8
700	2.284	14.56	0.360	50.2
600	2.339	15.70	0.335	39.1
500	2.402	16.77	0.310	29.4
400	2.466	17.73	0.300	22.1
300	2.537	18.68	0.280	15.0
140	2.667	20.51	0.250	5.9
40	2.709	22.81	0.210	1.4

must be calculated first. Then, the fractional oil recovery for a pressure decrement (as shown in Table I-B, Column 12) times the oil in place gives the barrels of oil recovered for the period. The number of days in the period equals the oil produced divided by the average producing rate. This procedure is demonstrated in the following example:

Example 6 Well Producing Rate Placed on a Time Basis

Problem: Put the producing rate schedule calculated in Example 5 on a time basis if the oil recovery versus pressure history is as given in Table I-B (Column 13), $\varphi = 15\%$, and $S_{wi} = 30\%$.

Solution: Calculate the oil in place for the drainage area of the average well on 80-acre spacing.

$$N = \frac{(80 \text{ acres})(7758 \text{ bbl/acre-ft})(\varphi)(1-S_{wi})(h \text{ ft})}{(B_{oi} \text{ res B/STB})}$$

$$= \frac{(80)(7758)(0.15)(1-0.30)(20)}{1.1795}$$

$$= 1{,}105{,}000 \text{ STB}.$$

For the pressure decrements used in Example 5, tabulate the oil produced in percent of oil in place (Table I-B, Column 12) and in stock-tank barrels. Calculate and list the average producing rate for the period, assuming an arithmetic average of the rate at the start and at the end of the interval. This is shown in Table III.

The maximum producing rate for the average well is plotted against time in Fig. 11. Here, the instantaneous rates at pressure values (Column 5, Table II) are plotted against the cumulative time values calculated above. For example, when the rate is 275.1 STB/D at 1300 psig, the cumulative producing time is zero; at 1225 psig when the rate is 259.5 STB/D, there have

TABLE III. Well Production Rate Placed On a Time Basis

(1) Pressure Decrement, psig	(2) Oil Produced % OIP*	(3) Oil Produced STB	(4) Avg. Prod. Rate, STB/D†	(5) Duration of Period, Days‡	(6) Cumulative Producing Time, Yrs.
1300–1225	0.15	1,658	267.3	6.2	0.02
1225–1150	5.60	61,880	211.2	293.0	0.82
1150–1050	5.00	55,250	136.6	404.5	1.93
1050–900	4.53	50,057	94.0	532.5	3.39
900–800	1.94	21,437	69.7	307.6	4.23
800–700	1.46	16,133	56.0	288.1	5.02
700–600	1.25	13,813	44.7	309.0	5.87
600–500	1.09	12,045	34.3	351.2	6.83
500–400	0.95	10,498	25.8	406.9	7.94
400–300	0.93	10,277	18.6	552.5	9.45
300–140	1.61	17,791	10.5	1694.4	14.09
140–40	1.63	18,012	3.7	4868.1	27.43

*For 1300 to 1225 psig, see Example 3; for 1225 to 40 psig, see Column 12, Table I-B.

†Avg. of rates in Column 5, Table II, for the start and end of a pressure period.

‡Oil produced during period divided by average rate. Column 3 divided by Column 4.

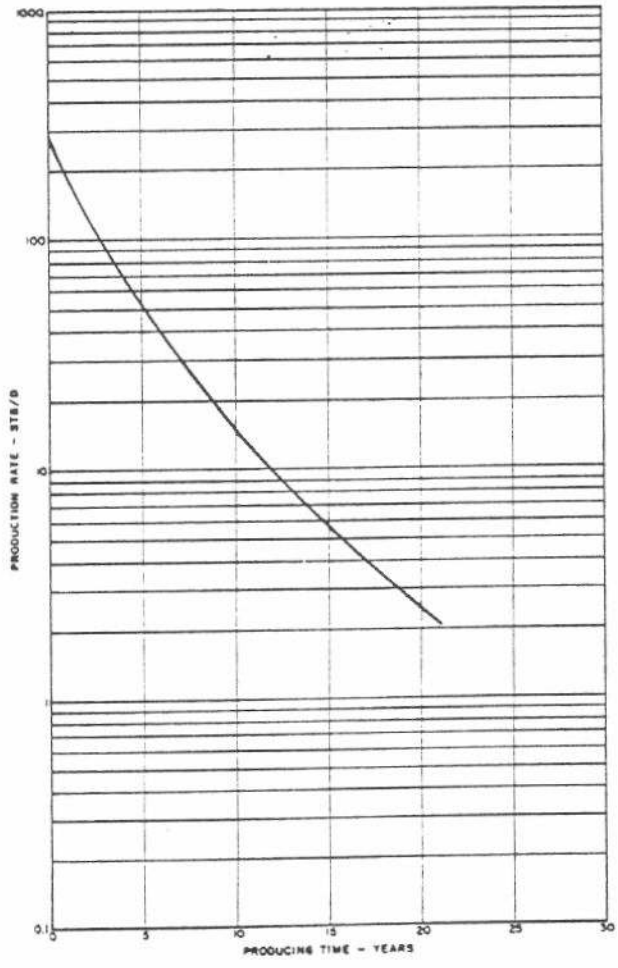

FIG. 11. Maximum producing rate decline — average well, 80-acre spacing.

been 0.02 cumulative years of production. The production curve, when coupled with a reasonable development schedule, can be the basis for predicting a field's capacity producing rates. The prediction of the field's maximum producing rate from an average well rate curve is illustrated later (Example 9).

VI. RESERVOIR CONTROL

Our discussion so far on the solution-gas-drive mechanism neglects the effects of gravity; so, recovery is not rate-sensitive. In a thick reservoir, or a steeply dipping formation, gravity may or may not be important. If it is, ultimate recovery might be enhanced by cutting back producing rates so that the benefits of gravity can be realized.

In reservoirs under gravity control Joslin[4] points out that high initial producing rates may decrease the breakthrough recovery to updip wells by elongating the thickness of the transition zone from high to low oil saturations in the gas cap. The lengthened transition zone results in a higher oil saturation in the gas cap if the gas front breaks through to the updip wells high withdrawal rates. However, theoretical analyses (Hicks et al.[3]) and laboratory experiments on gravity drainage of sandpacked columns have shown that fluids can distribute themselves rapidly to account for changes in withdrawal rates if gas production is not continued after breakthrough. Therefore, the ultimate recovery from a reservoir having good vertical segregation characteristics and large closure may not be affected by intermediate producing rates. This recovery, however, is a function of the producing rate and the rate of gas-oil contact advance just prior to gas breakthrough in the last row of downdip wells. Thus, in some reservoirs where good gravity segregation is obtained recoveries are not significantly influenced within a practical range of production rates.

Two-dimensional analyses are the best ways to evaluate gravity, but some simple ways of estimating the importance of gravity are available and are presented below.

Even when gravity is not significant, field producing rates are important because they are tied in closely with well spacing. This section, therefore, includes an example to show the economic advantage of wide well spacing for a solution-gas-drive reservoir.

A. Influence of Gravity on Solution-Gas Drive

As already pointed out, the influence of gravity on reservoir performance can best be evaluated by a two-dimensional study of a vertical cross section of the reservoir. This has been done successfully for several fields. However, to determine quickly whether or not gravity may be significant, one of the following simplified procedures is recommended. These simplified methods should be used to determine if a two-dimensional study of a field might be worthwhile.

1. DIPPING RESERVOIRS

In a dipping reservoir, the difference between the densities of oil and gas will tend to cause oil to flow downdip and gas updip. The degree of gravity flow will depend on the reservoir's geometry and permeability. The importance of gravity in a dipping reservoir can be determined from the following equation:

$$q = 0.000487 \frac{k k_{ro} A \, \Delta\rho \sin \alpha_d}{B_o \mu_o}, \qquad (10)$$

where

q = downdip oil flow rate, STB/D,

A = the average cross-sectional reservoir area open to flow, sq ft,

$\Delta\rho$ = the average density difference between oil and gas at reservoir conditions, gm/cc, and

α_d = the reservoir dip angle, degrees.

Equation (10) is a linear flow equation in which the gravity gradient in the direction of flow [equation (11)] is substituted for the flow gradient, dp/dx:

$$\frac{dp}{dx} = 0.433 \, \Delta\rho \sin \alpha_d. \qquad (11)$$

Equation (10) shows the rate in stock-tank barrels per day at which gravity will cause oil to flow downdip. The flow rate varies with the value of k_{ro}, which is a function of gas saturation. Gravity cannot be effective unless the oil moving downward is replaced by gas moving upward. This may occur as gas moves through a thin zone of high gas saturation near the top of porosity, or as gas moves vertically to an overlying gas cap. The maximum rate of oil movement downdip could be expected to occur when the average gas saturation is slightly in excess of the equilibrium saturation. The following example illustrates how the rate of oil flow downdip is calculated.

Example 7 Determine the Rate of Oil Flow Downdip

Problem: Calculate the rate at which oil will flow downdip for the reservoir in the previous example when reservoir pressure is 900 psig. Assume that the reservoir is a monocline and that the following are known:

$\alpha_d = 15°$

$\Delta\rho = 0.71$ gm/cc

B_o and μ_o vs pressure—Table I-A

k_{ro} vs gas saturation—Fig. 10

$k = 20$ md

Average width perpendicular to direction of dip = 12,000 ft

Average pay thickness = 20 ft

Solution: Use equation (10), substituting the appropriate values at 900 psig.

From Table I-A, $B_o = 1.159$, $\mu_o = 1.900$

From Table I-B, Column 18, $S_g = 11.65\%$ PV

From Fig. 10, $k_{ro} = 0.415$

Substituting in equation (10),

$$q = 0.000487\left[\frac{(20)(0.415)(12{,}000\times 20)(0.71)(0.259)}{(1.159)(1.900)}\right]$$

$= 81$ STB/D.

The rate of oil flow downdip at a reservoir pressure of 900 psi is 81 STB/D. A reservoir with the dimensions used in Example 7 would contain at least 20 wells (160-acre spacing), so the gravity rate would average only 4 STB/D per well. As shown in Example 5, the capacity of the average well at 900 psig is 77.5 STB/D, so gravity is not very important, even with a comparatively steep dip of 15°. The downdip flow rate will decrease as pressure declines and gas saturation increases, because k_{ro} will become smaller.

Permeability is the most important factor affecting downdip flow in a dipping reservoir. Although gravity was not important for the reservoir used in Example 7, a higher permeability would change this completely. If permeability were 200 md instead of 20 md, the gravity rate would be 40 STB/D per well. Of course, the well capacity would also be higher. However, for the high-permeability case, the operator might consider restricting production to achieve more efficient recovery. A detailed study would be necessary to determine the optimum producing rate.

2. THICK HORIZONTAL RESERVOIR

In a thick reservoir, gravity will tend to segregate oil and gas vertically, resulting in a high gas saturation near the top of the pay. This gravity process will take place in a horizontal reservoir, or it will augment the downdip flow of oil discussed above. The most influential factor for vertical gravity flow is vertical permeability, but oil viscosity and pay thickness are also significant. Vertical permeability is usually much lower than the average horizontal permeability, and values of 10 percent to 20 percent are common. On the other hand, vertical permeability averages 50 to 70 percent of horizontal permeability in some major reservoirs in the Lake Maracaibo area. The best completion interval for producing wells depends on the degree of gravity segregation. If gravity is important, wells should be open only in the lower part of the pay to prevent excess gas production. On the other hand, if gravity can be neglected, the entire pay section can be exposed for maximum productivity.

Vertical gravity flow is sometimes an important producing mechanism in thick pressure-depleted reservoirs, such as Coalinga, Oklahoma City, and Healdton. Matthews and Lefkovits[5] studied the gravity drainage process in these fields and showed that a well's producing rate from this process is:

$$q = 0.000487\,\frac{kk_{ro}\Delta\rho h^2}{B_o\mu_o\,[ln\,(r_e/r_w) - 0.5]}, \qquad (12)$$

where q = maximum production rate from gravity drainage when gas saturation is evenly distributed, STB/D; and h = the height of oil in the formation above the level in the wellbore, ft; other factors have been defined previously.

The maximum gravity drainage rate will occur when a well is pumped down to the base of the pay zone. In this case, h equals the pay thickness less the thickness of the high-gas-saturation zone at the top. The following example shows how equation (12) can be used to appraise the potential of a well to produce by gravity drainage. Of course, gravity drainage cannot be effective unless the formation has continuous vertical permeability to allow continuity of gravity forces.

Example 8 Estimating a Well's Potential for Gravity Drainage

Problem: Estimate the gravity drainage rate for the well of Examples 5 and 7 when reservoir pressure is 900 psig. Assume the well is pumped to the base of the pay and no high gas saturation zone exists. Use needed reservoir and fluid data from Examples 5 and 7.

Solution: From Example 7, $k = 20$ md, $k_{ro} = 0.415$, $B_o = 1.159$, $\mu_o = 1.900$ cp, $\Delta\rho = 0.71$ gm/cc.

From Example 5, $(r_e/r_w) = 1053$, $h = 20$ ft.

Substitute the appropriate values in equation (12):

$$q = 0.000487\left[\frac{(20)(0.415)(0.71)(20)^2}{(1.159)(1.9)[ln\,1053 - 0.5]}\right]$$

$= 0.0807$ STB/D.

This calculated gravity drainage rate of about 0.1 STB/D will decline as the reservoir gas saturation increases; so, for our example reservoir, vertical gravity segregation can be considered to be unimportant. For a reservoir with high permeability and thick pay, however, the calculated gravity drainage rate per well could be high. Gravity drainage rates of 50 STB/D or more have been observed in the Coalinga and Oklahoma City fields.

Although the calculated gravity rates were small for both Examples 7 and 8, there is about a factor of forty between them. In Example 7, the reservoir was assumed to dip 15° and downdip flow contributed about 4 STB/D. By contrast, Example 8 assumed a level reservoir so the only benefit of gravity was vertical movement of oil and gas, which contributed less than 0.1 STB/D. Since the same reservoir and fluid data were used in both examples, the difference in gravity effects is attributed to the reservoir's dip angle.

3. GRAVITY SEGREGATION FROM FIELD PERFORMANCE

The gravity segregation of oil and gas in the reservoir can often be inferred from the field's gas-oil ratio performance. If gravity is important, the rate of increase in the field-observed gas-oil ratio will be reduced. A comparison of the production histories of two Venezuelan fields, Fig. 12 and Fig. 13, illustrates the effect of gravity on gas-oil ratio performance. The performance of reservoir A, shown in Fig. 12, is typical of a dissolved-gas drive without gravity effects. The producing gas-oil ratio has increased rapidly to a value of about five times the initial ratio and is still climbing. At the same depletion stage, reservoir B (Fig. 13) has a much different gas-oil ratio history. The producing ratio is only about twice the initial value and has not increased much for several years.

The reservoirs are very similar except for one thing, the A sand is lenticular, while the B sand has continuous permeability. Both of the reservoirs are fault blocks having about 500 feet of closure and a dip of about 400 feet per mile. The lenticular nature of the A reservoir reduces vertical permeability and the related effect of gravity. The difference in gravity effect cannot be attributed to producing rate since the fields produced roughly the same amount of the oil in place, about six percent, during the first 10 years of their producing lives. The gravity segregation in reservoir B can also be seen on an individual well basis. Some high-structure wells have experienced high gas-oil ratios while downdip wells produce little or no free gas.

B. Thin, Horizontal Reservoirs — Economic Analysis

Well spacing is one of the most important factors that an operator of a dissolved-gas-drive field might control. If gravity is unimportant, the field can be produced as fast as well potentials and state proration rules (if applicable) will permit. Whether prorated or not, field producing rates are generally higher for close well spacing. The well spacing and market-demand proration rules for individual states are reviewed in Chapter 2-6, Conservation Practices in the U. S. A.

The optimum well spacing for a field must be de-

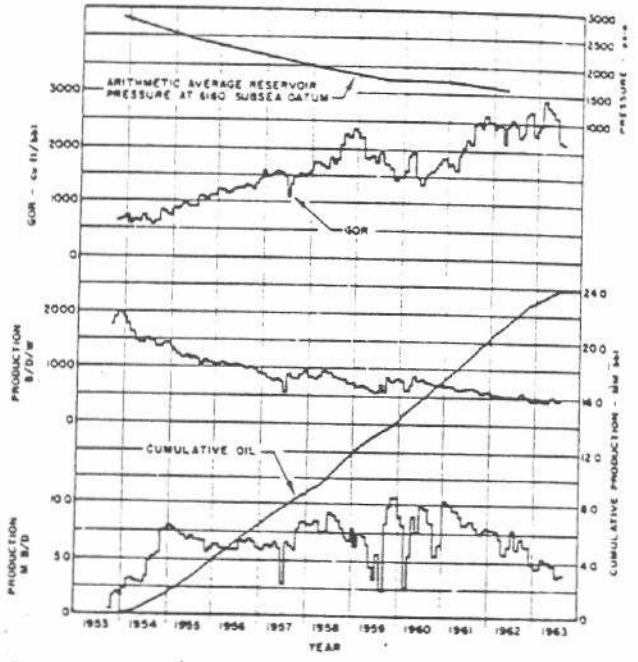

FIG. 12. Production history, reservoir A.

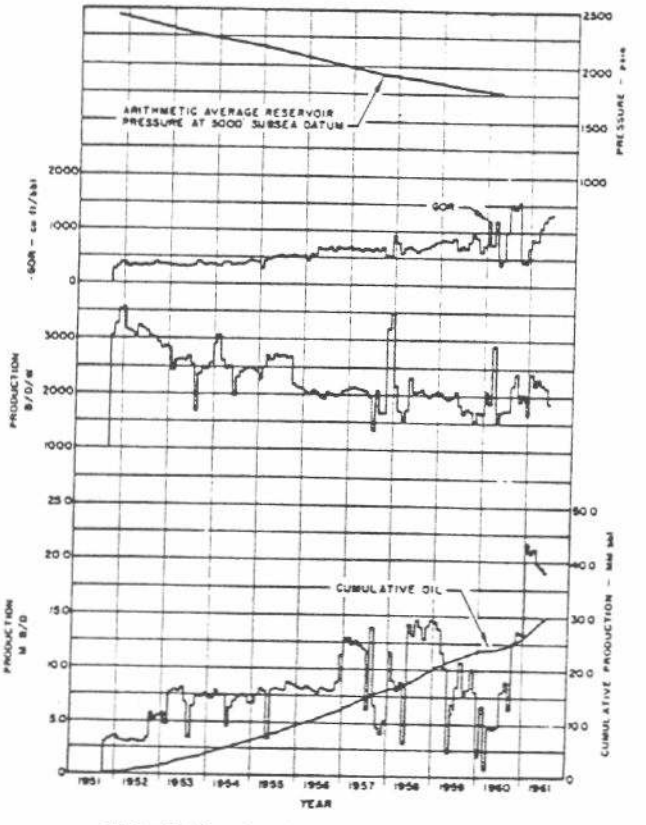

FIG. 13. Production history, reservoir B.

termined from an economic study. In the U. S. most states have maximum and minimum well spacings which limit the spacing cases that must be studied. For capacity operation (and to a certain extent prorated operation), closer well spacing will shorten operating life. This, in turn, gives a higher present value for the reserves. On the other hand, every well drilled adds to the investment. In most cases, economics favor the widest possible well spacing that will effectively drain the reservoir in a reasonable time period. The trend in the industry is toward wider well spacing.

Example 9 compares the economics of developing a U. S. field on 80-acre and on 160-acre well spacing. Capacity production is assumed and the producing rate for the average well versus time is calculated as in Examples 5 and 6. A reasonable development schedule is assumed for each spacing, and the corresponding schedule for the field producing rate is determined. A yearly economic analysis is made including the value of oil produced, all investment and operating expenses, and income tax. A present-value profile is made by applying various discount factors to the net profit for each year, and the discounted cash flow (DCF) rate of return is determined for each spacing. The particular manner in which cost features are handled in Example 9 is only one way of considering the economics of a proposal. Other and sometimes more complex procedures are frequently used to provide more realistic or detailed monetary breakdowns.

Chapter 5-1, Economic Analyses, provides a more comprehensive discussion of profitability yardsticks and economic criteria for determining the value of an operation.

Example 9 Economic Analysis of Well Spacing

Problem: Assuming maximum producing rates, make a present-value economic analysis for developing a 3200-acre field on 80-acre and 160-acre spacing. The field is located in the U. S. Reservoir and fluid properties are the same as described in Examples 1 through 4. For the producing-rate schedule of a well on 80-acre spacing, see Examples 5 and 6.

The development schedule is: assume 6 wells in the first year for 80-acre and 4 for 160-acre spacing. After the first year, 12 wells can be drilled per year for 80-acre and 8 per year for 160-acre spacing until the development is complete. Although this development schedule is somewhat arbitrary, it is realistic.

Economic factors are:

1. Investment and Well Expenses:
   Drill and Complete Well: $500,000
   Pumping Equipment—per well: $ 75,000
   Direct Operating Expense—per well per month: $ 400
   Overhead—on gross income after royalty: (other bases are also used) 8%
2. Revenue and Taxes:
   Gross Value of Oil (after 1/8 royalty)/STB: $2.80
   Production Tax—on gross income after royalty: 5%
   Ad Valorem Taxes: 2%
   Depreciation: 25% of well costs on a unit of production basis
   Depletion Allowance: the lesser of 27½% of gross income or 50% of net income (see Column 11, Table VI-A)
   Federal Income Tax Rate: 50%. Assume 7% tax credit on tangible investment in year spent.

Solution: The maximum producing rate versus time for the 80-acre case is shown in Fig. 11. For the 160-acre spacing the rate is (0.423/0.455) or 0.95 times the 80-acre rate at any pressure stage (see Example 5). The lower producing rate on wide spacing results from the higher value for r_e [see equation (9)]. This comparison of producing rates may not be strictly valid because of the difficulty in computing or estimating the true value for r_e for typical wells in heterogeneous formations. Nevertheless, it is believed to be a good approximation as the average travel distance for produced oil is greater for more widely spaced wells. Similarly, for a given drop in the reservoir pressure, a well on 160-acre spacing must produce twice as much oil as for the 80-acre case. Thus, the time to reach a given pressure stage is 2/0.95 or 2.1 times as long for the 160-acre case. The producing rate for the average 160-acre well determined from the foregoing conditions is shown in Fig. 14.

The economic limit for producing a well is the rate at which income after overhead and local taxes just equals the operating expense. Sometimes the economic limit of a well is established when the expenses directly chargeable to the well exceed revenue from the well. This tends to increase the producing life of a well over that obtained by assigning a fixed cost for operating the well. Partly for simplicity, the fixed-cost approach

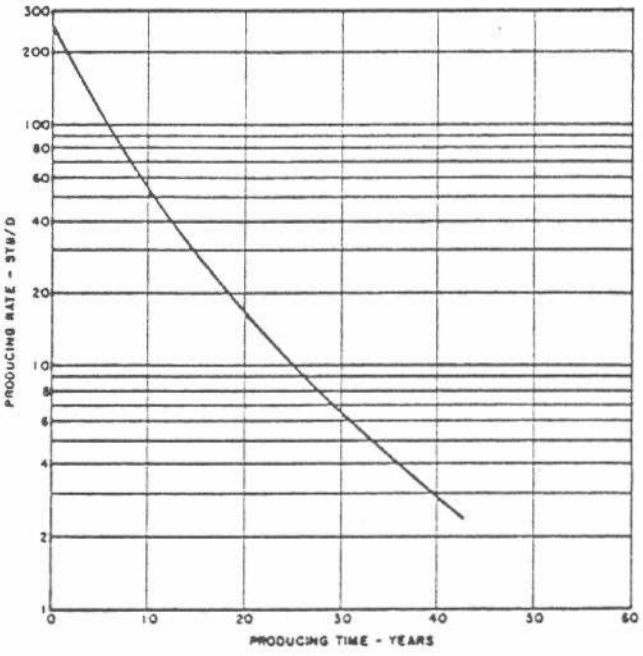

FIG. 14. Maximum producing rate decline — average well, 160-acre spacing.

TABLE IV. Calculated Maximum Production Schedule for an Average Well

Year	Production STB/yr 80-acre	160-acre
1	82,200	89,700
2	56,300	73,000
3	40,500	60,400
4	29,600	51,200
5	22,500	43,000
6	17,000	36,500
7	13,150	31,400
8	10,220	27,400
9	8,200	20,800
10	6,600	18,300
11	5,300	17,200
12	4,300	16,100
13	3,500	13,900
14	2,920	12,400
15	2,410	11,150
16		10,000
17		8,770
18		7,900
19		7,140
20		6,450
21		5,850
22		5,200
23		4,750
24		4,300
25		3,900
26		3,500
27		3,200
28		2,920
29		2,700
30		2,450
31		2,260
Ultimate Recovery	304,700	603,740

is used in this example. The equation for the p
ducing rate at the economic limit is:

$$2.80\, q_o\,(1 - \text{Overhead} - \text{Production Tax} - \text{Ad Valorem Tax}) = \text{Operating Expense.} \qquad (1$$

$$q_o = \frac{\$400/\text{well-month}}{\frac{30.4\ \text{days}}{\text{month}}\ \frac{\$2.80}{\text{STB}}\ (1 - 0.08^a - 0.05^b - 0.02^c}$$

$$= 5.54\ \text{STB/D},$$

where superscripts

a = Overhead,

b = Producing Tax,

c = Ad Valorem Tax.

Table IV shows the oil production per year fro
completion to the economic limit for one well on 8

TABLE V-A. Schedule of Total Oil Recovery for 160-Acre Spacing

Year	Wells Drilled During Year	Wells Producing	Production—MSTB From Wells Drilled in Year 1	2	3	Field Total
1	4	4	358.8			358.8
2	8	12	292.0	717.6		1009.6
3	8	20	241.6	548.0	717.6	1543.2
4		20	204.8	483.2	584.0	1272.0
5		20	172.0	409.6	483.2	1064.8
6		20	146.0	344.0	409.6	899.6
7		20	125.6	292.0	344.0	761.6
8		20	109.6	251.2	292.0	652.8
9		20	83.2	219.2	251.2	553.6
10		20	73.2	166.4	219.2	458.8
11		20	68.8	146.4	166.4	381.6
12		20	64.4	137.6	146.4	348.4
13		20	55.6	128.8	137.6	322.0
14		20	49.6	111.2	128.8	289.6
15		20	44.6	99.2	111.2	255.0
16		20	40.0	89.2	99.2	228.4
17		20	35.1	80.0	89.2	204.3
18		20	31.6	70.2	80.0	181.8
19		20	28.6	63.2	70.2	162.0
20		20	25.8	57.2	63.2	146.2
21		20	23.4	51.6	57.2	132.2
22		20	20.8	46.8	51.6	119.2
23		20	19.0	41.6	46.8	107.4
24		20	17.2	38.0	41.6	96.8
25		20	15.6	34.4	38.0	88.0
26		20	14.0	31.2	34.4	79.6
27		20	12.8	28.0	31.2	72.0
28		20	11.7	25.6	28.0	65.3
29		20	10.8	23.4	25.6	59.8
30		20	9.8	21.6	23.4	54.8
31		20	9.0	19.6	21.6	50.2
32		16		18.0	19.6	37.6
33		8			18.0	18.0
Ultimate Recovery			2415.0	4830.0	4830.0	12,075.0

TABLE V-B. Schedule of Total Oil Recovery for 80-Acre Spacing

Year	Wells Drilled During Year	Wells Producing	Production—MSTB: From Wells Drilled in Year 1	2	3	4	Field Total
1	6	6	493.2*				493.2
2	12	18	337.8	986.4			1324.2
3	12	30	243.0	675.6	986.4		1905.0
4	10	40	177.6	486.0	675.6	822.0	2161.2†
5		40	135.0	355.2	486.0	563.0	1539.2
6		40	102.0	270.0	355.2	405.0	1132.2
7		40	78.9	204.0	270.0	296.0	848.9
8		40	61.3	157.8	204.0	225.0	648.1
9		40	49.2	122.6	157.8	170.0	499.6
10		40	39.6	98.4	122.6	131.5	392.1
11		40	31.8	79.2	98.4	102.2	311.6
12		40	25.8	63.6	79.2	82.0	250.6
13		40	21.0	51.6	63.6	66.0	202.2
14		40	17.5	42.0	51.6	53.0	164.1
15		40	14.5	35.0	42.0	43.0	134.5
16		34‡		29.0	35.0	35.0	99.0
17		22			29.0	29.2	58.2
18		10				24.1	24.1
Ultimate Recovery			1828.2	3656.4	3656.4	3047.0	12,188.0

*First year of production for 6 wells on 80-acre spacing. 82,200 STB/yr (Table IV) × 6 wells = 493.2 MSTB/yr.

†Fourth year of production for 6 wells, third year for 12 wells, second year for 12 wells, plus first year for 10 wells. (29.6)(6) + (40.5)(12) + (56.3)(12) + (82.2)(10) = 2161.2 STB/yr.

‡Wells are abandoned after producing 15 years.

acre spacing and one on 160-acre spacing. The production figures were obtained by reading the mid-year rate from Fig. 11 (80-acre) and Fig. 14 (160-acre), and multiplying by 365. As shown in Table IV, the economic, ultimate recovery per acre is slightly less for the wider spacing. This is caused by the lower productivity index for the wider spacing resulting from a higher value of r_e.

The development of the field covers 3 years on 160-acre spacing and 4 years on 80-acre. Tables V-A and V-B show the schedule of total oil recovery for the 160-acre and 80-acre cases, respectively. Wells drilled after the first year were assumed to have the same recovery curve as first-year wells. This would not be the case if production from the early wells lowered the reservoir pressure beyond the assumed drainage area (80 or 160 acres). However, no error in ultimate oil recovery is introduced by the assumption.

The economic summary for the field is shown in Table VI-A for the 160-acre case and in Table VI-B for the 80-acre case. The economic producing life totals 33 years and 18 years, respectively. All money figures are in thousands of dollars. The significance of each column in Tables VI-A and VI-B is as follows:

Column	Description
(1)	Oil production schedule from Table V-A or V-B.
(2)	Gross income. Column 1 times $2.80 (the value of the oil after deducting one-eighth royalty). The actual sale price of the oil is $3.20/bbl.
(3)	Average number of wells for each year from Table V-A or V-B.
(4)	Lease and well operating expense. (Column 3) ($400/well-mo) (12 mo/yr).
(5)	Production and ad valorem taxes. (Column 2) (0.07).
(6)	Overhead. (Column 2) (0.08).
(7)	Total operating expense. Sum of Columns 4, 5, and 6.
(8)	Operating profit. (Column 2 minus Column 7).
(9)	Intangible investment. (Wells drilled per year —from Table V-A or V-B) (0.75) ($575,000 —the cost per well including pumping equipment.)
(10)	Depreciation of tangible investment. The investment not included in Column 9 (i.e., 25 percent of investment) is depreciated on a per barrel basis. Column 10 = $\text{Col. 1}\left[\frac{(0.25)(\$575{,}000)(\text{total wells drilled})}{(\text{ultimate oil produced})}\right]$.
(11)	Net for depletion limitation. (Column 8 less Columns 9 and 10.)

TABLE VI-A. Economic Summary — 160-Acre Spacing

Year	(1) Oil Production, MSTB	(2) Gross Income, M $	(3) No. Wells	Operating Expenses, M $ (4) L & W	(5) Production Ad Valorem Taxes (7% Gross)	(6) Overhead* (8% Gross)	(7) Total	(8) Operating Profit, M $	(9) Intangible Investment, M $
1	358.8	1,004.6	4	19.2	70.3	80.4	169.9	$34.7	1,725.0
2	1,009.6	2,826.9	12	57.6	197.9	226.2	481.7	2,345.2	3,450.0
3	1,543.2	4,321.0	20	96.0	302.5	345.7	744.2	3,576.8	3,450.0
4	1,272.0	3,561.6	20	96.0	249.3	284.9	630.2	2,931.4	0
5	1,064.8	2,987.4	20	96.0	208.7	238.5	543.2	2,438.2	
6	899.6	2,518.9	20	96.0	176.3	201.5	473.8	2,045.1	
7	761.6	2,132.5	20	96.0	149.3	170.6	415.9	1,716.6	
8	652.8	1,827.8	20	96.0	127.9	146.2	370.1	1,457.7	
9	553.6	1,550.1	20	96.0	108.5	124.0	328.5	1,221.6	
10	458.8	1,284.6	20	96.0	89.9	102.8	288.7	995.9	
11	381.6	1,068.5	20	96.0	74.8	85.5	256.3	812.2	
12	348.4	975.5	20	96.0	68.3	78.1	242.4	733.1	
13	322.0	901.6	20	96.0	63.1	72.1	231.2	670.4	
14	289.6	810.9	20	96.0	56.8	64.9	217.7	593.2	
15	255.0	714.0	20	96.0	50.0	57.1	203.1	510.9	
16	228.4	639.5	20	96.0	44.8	51.2	192.0	447.5	
17	204.3	572.0	20	96.0	40.0	45.7	181.7	390.3	
18	181.8	509.0	20	96.0	35.6	40.7	172.3	336.7	
19	162.0	453.6	20	96.0	31.8	36.3	164.1	289.5	
20	146.2	409.4	20	96.0	28.7	32.8	157.5	251.9	
21	132.2	370.2	20	96.0	25.9	29.6	151.5	218.7	
22	119.2	333.8	20	96.0	23.4	26.7	146.1	187.7	
23	107.4	300.7	20	96.0	21.1	24.1	141.2	159.5	
24	96.8	271.0	20	96.0	19.0	21.7	136.7	134.3	
25	88.0	246.4	20	96.0	17.2	19.7	132.9	113.5	
26	79.6	222.9	20	96.0	15.6	17.8	129.4	93.5	
27	72.0	201.6	20	96.0	14.1	16.1	126.2	75.4	
28	65.3	182.8	20	96.0	12.8	14.6	123.4	59.4	
29	59.8	167.4	20	96.0	11.7	13.4	121.1	46.3	
30	54.8	153.5	20	96.0	10.7	12.2	118.9	34.6	
31	50.2	140.6	20	96.0	9.8	11.2	117.0	23.6	
32	37.6	105.3	16‡	76.8	7.4	8.5	92.7	12.6	
33	18.0	50.4	8	38.4	3.5	4.0	45.9	4.5	
	12,075.0	33,810.0		2,976.0	2,366.7	2,704.8	8,047.5	25,762.5	8,625.0

*For this example, actual overhead is assumed to equal tax overhead (8% of gross income). In actual practice this may not be true.
**The lesser of 27½% of gross income or 50% of net income (Column 11).
†Negative values of income tax are assumed to be tax credits applicable to other company projects.
‡Wells are abandoned after producing 31 years.

TABLE VI-B. Economic Summary — 80-Acre Spacing

Year	(1) Oil Production, MSTB	(2) Gross Income, M $	(3) No. Wells	Operating Expenses, M $ (4) L & W	(5) Production Ad Valorem Taxes (7% Gross)	(6) Overhead* (8% Gross)	(7) Total	(8) Operating Profit, M $	(9) Intangible Investment, M $
1	493.2	1,381.0	6	28.8	96.7	110.5	236.0	1,145.0	2,587.5
2	1,324.2	3,707.8	18	86.4	259.5	296.6	642.5	3,065.3	5,175.0
3	1,905.0	5,334.0	30	144.0	373.4	426.7	944.1	4,389.9	5,175.0
4	2,161.2	6,051.4	40	192.0	423.6	484.1	1,099.7	4,951.7	4,312.5
5	1,539.2	4,309.8	40	192.0	301.7	344.8	838.5	3,471.3	0
6	1,132.2	3,170.2	40	192.0	221.9	253.6	667.5	2,502.7	
7	848.9	2,376.9	40	192.0	166.4	190.2	548.6	1,828.3	
8	648.1	1,814.7	40	192.0	127.0	145.2	464.2	1,350.5	
9	499.6	1,398.9	40	192.0	97.9	111.9	401.8	997.1	
10	392.1	1,097.9	40	192.0	76.9	87.8	356.7	741.2	
11	311.6	872.5	40	192.0	61.6	69.8	323.4	549.1	
12	250.6	701.7	40	192.0	49.1	56.1	297.2	404.5	
13	202.2	566.1	40	192.0	39.6	45.3	276.9	289.2	
14	164.1	459.5	40	192.0	32.2	36.8	261.0	198.5	
15	134.5	376.6	40	192.0	26.4	30.1	248.5	128.1	
16	99.0	277.2	34‡	163.2	19.4	22.2	204.8	72.4	
17	58.2	162.9	22	105.6	11.4	13.0	130.0	32.9	
18	24.1	67.5	10	48.0	4.7	5.4	58.1	9.4	
	12,188.0	34,126.6		2,880.0	2,389.4	2,730.1	7,999.5	26,127.1	17,250.0

*For this example, actual overhead is assumed to equal tax overhead (8% of gross income). In actual practice this may not be true.
**The lesser of 27½% of gross income or 50% of net income (Column 11).
†Negative values of income tax are assumed to be tax credits applicable to other company projects.
‡Wells are abandoned after producing 15 years.

Year	(10) Depreciation, M $	(11) Net for Depletion Limitation, M $	(12) Depletion,** M $	(13) Taxable Income, M $	(14) Income Tax, M $†	(15) 7% Tax Credit	(16) Total Investment, M $	(17) Cash Flow, M $	(18) Status, M $
1	85.4	(975.7)	0	(975.7)	(487.9)	120.8	2,300.0	(856.6)	(856.6)
2	240.4	(1,345.2)	0	(1,345.2)	(672.6)	241.5	4,600.0	(1,340.7)	(2,197.3)
3	367.4	(240.6)	0	(240.6)	(120.3)	241.5	4,600.0	(661.4)	(2,858.7)
4	302.9	2,628.5	979.4	1,649.1	824.6		0	2,106.8	(751.9)
5	253.5	2,184.7	819.9	1,364.8	682.4			1,755.8	1,003.9
6	214.2	1,840.9	692.7	1,138.2	569.1			1,476.0	2,479.9
7	181.3	1,535.3	586.4	948.9	474.4			1,242.2	3,722.1
8	155.4	1,302.3	502.6	799.7	399.9			1,057.8	4,779.9
9	131.8	1,089.8	426.3	663.5	331.7			889.9	5,669.8
10	109.2	886.7	353.3	533.4	266.7			729.2	6,399.0
11	90.9	721.3	293.8	427.5	213.8			598.4	6,997.4
12	83.0	650.1	268.3	381.8	190.9			542.2	7,539.6
13	76.6	583.8	247.9	345.9	172.9			497.5	8,037.1
14	69.0	524.2	223.0	301.2	150.6			442.6	8,479.7
15	60.7	450.2	196.4	253.8	126.9			384.0	8,863.7
16	54.4	393.1	175.9	217.2	108.6			338.9	9,202.6
17	48.6	341.7	157.3	184.4	92.2			298.1	9,500.7
18	43.3	293.4	140.0	153.4	76.7			260.0	9,760.7
19	38.6	250.9	124.7	126.2	63.1			226.4	9,987.1
20	34.8	217.1	108.6	108.5	54.3			197.6	10,184.7
21	31.5	187.2	93.6	93.6	46.8			171.9	10,356.6
22	28.4	159.3	79.6	79.7	39.8			147.9	10,504.5
23	25.6	133.9	67.0	66.9	33.5			126.0	10,630.5
24	23.0	111.3	55.6	55.7	27.8			106.5	10,737.0
25	21.0	92.5	46.3	46.2	23.1			90.4	10,827.4
26	19.0	74.5	37.2	37.3	18.7			74.8	10,902.2
27	17.1	58.3	29.2	29.1	14.5			60.9	10,963.1
28	15.5	43.9	22.0	21.9	11.0			48.4	11,011.5
29	14.2	32.1	16.0	16.1	8.0			38.3	11,049.8
30	13.0	21.6	10.8	10.8	5.4			29.2	11,079.0
31	12.0	11.6	5.8	5.8	2.9			20.7	11,099.7
32	9.0	3.6	1.8	1.8	0.9			11.7	11,111.4
33	4.3	0.2	0.1	0.1	0.1			4.4	11,115.8
	2,875.0	14,262.5	6,761.5	7,501.0	3,750.5	603.8	11,500.0	11,115.8	

Year	(10) Depreciation, M $	(11) Net for Depletion Limitations, M $	(12) Depletion,** M $	(13) Taxable Income, M $	(14) Income Tax, M $†	(15) 7% Tax Credit	(16) Total Investment, M $	(17) Cash Flow, M $	(18) Status, M $
1	232.8	(1,675.2)	0	(1,675.2)	(837.6)	181.1	3,450.0	(1,286.3)	(1,286.3)
2	624.7	(3,734.4)	0	(3,734.4)	(1,867.2)	362.3	6,950.0	(1,605.2)	(2,891.5)
3	898.7	(1,583.8)	0	(1,583.8)	(791.9)	362.3	6,900.0	(1,355.9)	(4,247.4)
4	1,019.6	(380.4)	0	(380.4)	(190.2)	301.9	5,750.0	(306.2)	(4,553.6)
5	726.1	2,745.2	1,185.2	1,560.0	780.0		0	2,691.3	(1,862.3)
6	534.1	1,968.6	871.8	1,096.8	548.4			1,954.3	92.0
7	400.5	1,427.8	653.6	774.2	387.1			1,441.2	1,533.2
8	305.8	1,044.7	499.0	545.7	272.9			1,077.6	2,610.8
9	235.7	761.4	384.7	376.7	188.3			808.8	3,419.6
10	185.0	556.2	278.1	278.1	139.1			602.1	4,021.7
11	147.0	402.1	201.1	201.0	100.5			448.6	4,470.3
12	118.2	286.3	143.1	143.2	71.6			332.9	4,803.2
13	95.4	193.8	96.9	96.9	48.4			240.8	5,044.0
14	77.4	121.1	60.6	60.5	30.3			168.2	5,212.2
15	63.5	64.6	32.3	32.3	16.2			111.9	5,324.1
16	46.7	25.7	12.8	12.9	6.4			66.0	5,390.1
17	27.5	5.4	2.7	2.7	1.3			31.6	5,421.7
18	11.4	(2.0)	0	(2.0)	(1.0)			10.4	5,432.1
	5,750.0	3,127.1	5,421.9	(2,194.8)	(1,097.4)	1,207.6	23,000.0	5,432.1	

(12) Depletion. The lesser of (0.275) (Column 2) or (0.5) (Column 11). Never less than zero.

(13) Taxable income. (Column 11 minus Column 12.)

(14) Income tax. (0.50) (Column 13).

(15) In the U. S. a tax credit of 7% of the tangible investment is allowed in the year the investment is made.

(16) Total investment. (Wells drilled) ($575,000).

(17) Cash flow. Column 8 plus Column 15, minus Columns 14 and 16.

(18) Status. Accumulation of Column 17.

The 80-acre spacing case doesn't pay out until the end of the sixth year, and the ultimate profit is only $5,432,100, or $0.24 per dollar invested. By comparison, the 160-acre case will pay out in the fifth year and have an ultimate profit of $11,115,800 or $0.97 per dollar invested.

One of the best measures of the economics of a project is the discount cash flow (DCF) rate of return. The DCF rate of return represents the percent return that an investor may expect on the unrecovered funds left at risk each year over the life of the project. The DCF return is obtained, first, by determining the present value of the cash flow for each year for various interest or discount rates. Then, a present-value profile for a project, a plot of present value vs the discount (or interest) rate, is prepared. The point at which the present value is zero gives the DCF rate of return. The present value of the cash flow for any year is determined by the following equation:

$$\text{Present Value} = \frac{(\text{Cash Flow})_n}{(1+i)^n}, \qquad (14)$$

where

n = the year from project start,

i = the fractional rate of interest.

The present-value profiles for the two spacing cases are shown in Fig. 15. The DCF rate of return for the 80-acre case is about 19 percent, while 160-acre spacing shows a 34 percent rate of return. Since the present-value profiles do not cross, the additional investment for 80-acre spacing above that for 160-acre will not pay out on an incremental basis (see Chapter 5-1, Economic Analyses). This example is a case where the wider spacing (160-acre) has an economic advantage over the closer spacing (80-acre).

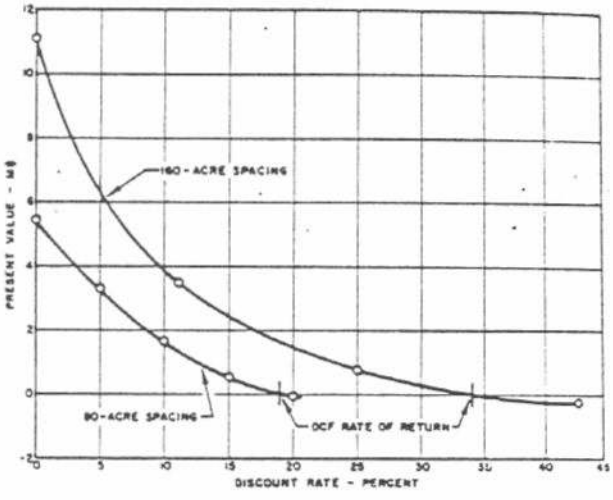

FIG. 15. Present-value profile — Example 6.

REFERENCES

1. Arps, J. J., and Roberts, T. G.: "The Effect of the Relative Permeability Ratio, the Oil Gravity, and the Solution-Gas-Oil Ratio on the Primary Recovery from a Depletion Type Reservoir," *Trans. AIME*, v. 204, 1955, p 120.

2. Dalton, R. L., and Greene, H. W.: "Predicting Dissolved-Gas-Drive Behavior of a Single Well," JR61:46-4140, October 1961.

3. Hicks, A. L., Fisher, W. G., and Knutson, W. G.: "Calculations of Oil Recovery by Variable-Rate Gas or Water Injection," JPRCo Technical Service Report No. 3925, December 1960.

4. Joslin, W. J.: "Applying the Frontal Advance Equation to Vertical Segregation Reservoirs," *Jour. Pet. Tech.*, January 1964, p 87.

5. Matthews, C. S., and Lefkovits, H. C.: "Gravity Drainage Performance of Depletion-Type Reservoirs in the Stripper Stage," *Trans. AIME*, v. 207, 1956, p 265.

6. Muskat, M.: *Physical Principles of Oil Production*, McGraw-Hill, New York, 1949.

7. Pirson, S. J.: *Elements of Oil Reservoir Engineering*, McGraw-Hill, New York, 1950.

8. Quarterly Progress Report, Service, Research, & Development, Imperial Oil Limited, v. 3, No. 1, March 1963.

9. Reservoir Status Report B-6-X.22, B-5-X.3, B-5-X.4, B-7-X.21 and Basic Data B-5-X.3, B-5-X.4, B-7-X.21, Creole PE Report, July 1962, p 21ff.

10. Roberts, T. G., and Ellis, H. E., Jr.: "Correlation of Gas-Oil Ratio History in a Solution-Gas-Drive Reservoir," *Jour. Pet. Tech.*, v. 14, June 1962, p 595.

11. Schilthuis, R. J.: "Active Oil and Reservoir Energy," *Trans. AIME*, v. 118, 1936, p 33.

12. "Status Report and Depletion Study B-5-X.1 and B-5-X.9 Reservoirs," Creole PE Report, November 1963, p 25ff.

13. Tracy, G. W.: "Simplified Form of the Material Balance Equation," *Trans. AIME*, v. 204, 1955, p 243.

14. Wahl, W. L., et al.: "Estimation of Ultimate Recovery from Solution-Gas Drive Reservoirs," *Jour. Pet. Tech.*, June 1958, p 132.

CHAPTER 3-5

Water-Drive Reservoirs

CONTENTS

I. INTRODUCTION

This chapter discusses the engineering techniques used to evaluate and predict the performance of water-drive reservoirs. The techniques are applicable to natural water drive or to natural water drive supplemented by flank-water injection. (Pattern waterfloods are discussed in Chapter 4-1, Waterflood Field Predictions.) Since solution-gas drive often occurs in conjunction with the water-drive mechanism, the techniques described in this chapter include treatment of gas liberated from solution and free gas production. They do not consider gas-cap drive or the possible formation of a secondary gas cap; methods for handling these more complex situations are covered in Chapter 3-6, Gas-Cap and Combination-Drive Reservoirs.

To determine the most efficient and economic method of reservoir depletion, it is usually necessary to predict water-drive behavior for several possible methods of operation. The various possibilities may involve different schedules of production rates, different reservoir pressure levels, or a comparison of natural depletion versus pressure maintenance. Ranges of possible operating conditions and their comparative economics are normally investigated during a detailed reservoir study.

A basic technique for predicting pool-wide behavior is discussed in detail in this chapter. While the method is simple enough to be handled with desk calculators, it is capable of giving good practical results for many water-drive reservoirs. Furthermore, the basic technique will provide a foundation for modifications designed to meet the requirements of particular reservoirs. Some of these modifications are presented in this chapter. The particular technique for a given reservoir study depends on the quality of the available data and the time allotted for the study.

When sufficient time and money are available for a detailed reservoir study, the engineer should consider high-speed computer techniques. Several of the programs will expedite water-drive studies. Some programs follow the basic technique presented in this chapter. Chapter 5-10, Numerical Prediction Methods, discusses computer techniques used for reservoir studies.

II. WATER-DRIVE RESERVOIR CHARACTERISTICS

A. Water-Drive Mechanism

Many oil fields grade downstructure into a water zone or aquifer that may provide an important source of producing energy. The vertical transition from the oil-productive section to a zone of 100 percent water saturation can vary from a few feet to many feet. A discussion of the gravity and capillary forces involved in this water-oil transition zone is presented in Chapter 1-2, Rock Properties, and Chapter 1-9, Fluid Distributions. The expansion of water in the aquifer may constitute a great source of potential reservoir energy. When oil is produced from the reservoir, the pressure drops. As the pressure decline reaches the aquifer, the water expands and flows into the oil zone.

The two factors most important in determining the effectiveness of a water drive are the size of the aquifer and the permeability of the formation. The overall compressibility of water and formation rock is of the order of 10^{-5} volumes per volume per psi. Thus, for each barrel of oil produced, the aquifer must contain a minimum of *several* thousand barrels of water if natural water drive is to maintain pressure near the original value. The size of an aquifer relative to a reservoir can be roughly described by the dimensionless ratio $r_D = r_a/r_R$ — that is, the ratio of the aquifer radius to the reservoir radius. Usually r_D must be at least 40 for strong natural water drives. Often an aquifer is considered to be infinite in size because it is so big that production from the reservoir can never affect the pressure at the aquifer boundary. Another type of "infinite" aquifer is one that outcrops in an area where it is continually recharged with surface water.

No matter how big the aquifer is, however, it will not be effective in maintaining reservoir pressure unless the formation permeability is high enough to allow rapid communication throughout the aquifer and the reservoir. In some cases, a fracture system in the aquifer has provided extremely good communication even though core analysis shows permeabilities to be low or moderate. Most water-drive fields are rate-sensitive because formation permeability is not high enough to allow instantaneous communication.

A reservoir can receive essentially all of its producing energy from a water drive if no gas cap is present and if reservoir pressure stays above the bubble point. Many small reservoirs achieve complete water drives, but in a large reservoir the pressure generally falls below the bubble point, resulting in some solution-gas-drive energy. Water injection is often used to augment natural water influx in order to maintain pressure at or near the bubble point.

Most water-drive fields can be classified as flank- or bottom-water drives (Fig. 1). In general, for a flank-water-drive field, the formation thickness is small compared to the reservoir area. By contrast, for a bottom-water-drive field, where the entire oil zone

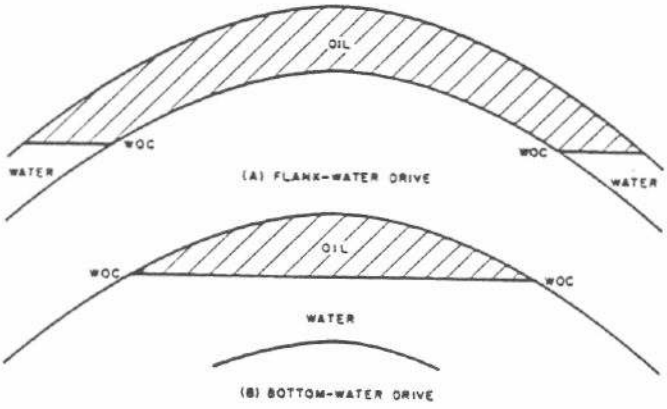

FIG. 1. Example of flank- and bottom-water drives.

is originally underlain by water, the formation is usually very thick or the reservoir area small. The East Texas field is an example of a strong flank-water drive, while the Leduc D-3 reservoir in Canada illustrates a strong bottom-water drive.

An unusual type of water drive is associated with the subsidence of the land surface overlying an oil field. In this case, the unconsolidated rock in the reservoir and overlying formations is compacted as oil is produced. The compaction, in turn, causes the surface to subside. Generally accepted theories submit that the squeezing of water from unconsolidated shales into the oil reservoir compacts the shales and accounts for much of the subsidence. However, part of the compaction may be the result of sand grains breaking in the reservoir. Although such a "compaction drive" may be effective considering only the reservoir performance, serious problems can be encountered at the surface. Land subsidence has been noted above several oil fields in the Lake Maracaibo area of Venezuela, but the most famous case of surface subsidence is near Long Beach, California. In this area, buildings and other surface facilities have slowly fallen below sea level. After more than 20 years of continued subsidence, large-scale water injection has been started in an attempt to stop the subsidence.

B. Performance Characteristics

Fig. 2 shows the general pressure and production performance to be expected from a water-drive field produced at capacity rates above the saturation pressure. The reservoir pressure at depletion in this example is more than 60 percent of the initial value.

Where the aquifer is unlimited, the rate of pressure decline generally becomes lower with time, because the average rate of water influx increases as the total pressure differential between the field and the aquifer

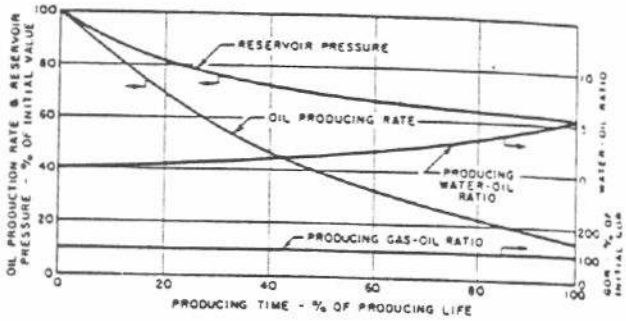

FIG. 2. Performance of example water-drive reservoir produced at capacity.

increases. If the water influx rate becomes equal to the fluid production rate, the reservoir pressure becomes constant with time. If the production rate of a strong water-drive field is drastically reduced or if the field is shut in for a long period, reservoir pressure may actually increase significantly. The prediction of water influx rates and pressure performance of a water-drive field is described in the example of Section VIII.

The production performance of a water-drive field is generally characterized by a slow but steady decline in oil-producing rate and a continual increase in water production. The producing gas-oil ratio will remain constant and equal to the solution gas-oil ratio as long as production stays above the bubble point. The production curve shown in Fig. 2 is typical for a domestic field where the entire productive area is producing. As water encroaches upon the wells, the oil production rate goes down and the water production rate goes up. If the water and oil have about the same mobility, total fluid production declines very slowly unless wells are abandoned. Excess water production can be prevented by unitizing a field, and shutting in wells with high water-oil ratios. Many of the large foreign fields such as Abqaiq and Ghawar in Arabia and Zelten in Libya were developed in anticipation of a water drive. Therefore, few wells were drilled close to the water-oil contact. These fields should produce for many years before water production becomes a problem.

The water drive in most fields is not strong enough to maintain pressure above the bubble point at the desired producing rates. However, the rate of pressure drop may be greatly reduced when the bubble-point pressure is reached, as expansion of the released gas adds to the reservoir energy. If the reservoir pressure drops very far below the bubble point, the producing gas-oil ratio may increase. However, unless the water drive is very weak, the ratio probably will not increase to more than twice the original solution gas-oil ratio.

. Field Examples of Water-Drive Recovery

Table I shows the reservoir characteristics and erformance data on some of Exxon's foreign water-rive fields. The recovery efficiencies shown in the able are in line with data submitted by the industry o the API Subcommittee on Recovery Efficiency. his Subcommittee, which has data on 66 predominantly water-drive fields, reports that recovery efficiencies average 53 percent of the oil in place and ange from 20 percent to more than 90 percent of the il in place. The Subcommittee is using the data to evelop a correlation between recovery efficiency and arious reservoir and fluid parameters. Preliminary esults have shown that high permeability and low oil iscosity are the two most important factors associated with fields with high oil recovery. Significantly, 44 ercent of the fields had an average permeability in xcess of one darcy and 91 percent had an average ermeability of more than 100 md. This illustrates he importance of permeability to water drive. Work o date shows that recovery correlations based on ommonly measured reservoir and fluid properties uch as dry air permeability, porosity, connate -, oil viscosity, formation volume factor, etc., nay be seriously in error if applied to a specific field. The actual recovery efficiency is controlled by water-il relative permeability characteristics (not reported for most of the fields), which are only roughly elated to permeability and porosity. A study of previously submitted API field data resulted in the Guthrie-Greenberger[4] equation relating recovery to ermeability, porosity, connate water, oil viscosity, tc. This equation will be superseded when the present orrelative studies are completed.

Some of the extremely high recovery efficiencies hat were reported can be explained only as the result f gravity causing a slow upward movement of oil in he water-invaded zone. As the water-oil contact ises, the difference in gravity head between the oil nd the water causes the oil to flow upward, thus ecreasing the residual oil saturation and increasing he recovery efficiency above that which could be chieved by horizontal water displacement. Humble as experimental evidence of this process.[10] Cores rom water-swept sections of the East Texas, Conroe, an, and Friendswood fields had low residual oil aturations (6 to 10 percent). On the other hand, aboratory waterfloods on cores from all these fields residuals ranging from 15 to 20 percent.

Gravity-induced migration can be effective only in igh-closure reservoirs with good vertical permeability. The maximum gravity force possible is proportional to the density difference between the oil and the water times the vertical distance through which

TABLE I — Characteristics of Selected Water-Drive Pools

Field	Date of Initial Production	Predominant Lithology	Type of Water Drive	Oil Characteristics		Formation Characteristics			Orig. Oil in Place, MMSTB	Recovery Factor, % OIP	Cumulative Production to 3/1/64, MMSTB	Current Production Rate, STB/D	Avg. Depletion Rate, % Reserves/Yr
				Gravity, °API	Viscosity, cp	Permeability, md	Avg. Porosity	Avg. Connate Water, % PV					
Canada													
R1	1948	Ls	Bottom	34	3	500	6.5	25	1275	64	280	31,000	1.4
R2	1958	Ls	None—Flank Inj.	42	0.3	43	9.3	16.5	840	47	14	17,000	1.6
R3	1949	Ls	Bottom	35	1	1000	5.5	15	37	70	11	1,000	1.4
France													
R4	1954	Ls	Bottom + Inj.	37	2	Less than 100*	13.0	30	617	30	75	27,500	4.0
Sumatra													
R5	1957	Ss	Bottom	36	5	1680	25.2	18.1	234	50	42	15,000	6.0
Venezuela													
R6	1955	Ss	Flank	22.0	2	1400	29.0	23.6	1102	55	110	57,000	1.8
R7	1951	Ss	Flank	22.6	2	1460	34.1	25.0	1239	55	67	17,000	0.8
R8	1952	Ss	Flank	22.0	3	1826	30.7	22.0	606	45	40	18,000	1.2
R9	1952	Ss	Flank	21.9	2	1422	31.8	20.0	544	40	37	16,000	1.8
R10	1956	Ss	Flank	23.6	2	1280	27.7	22.2	468	55	55	41,000	2.6
R11	1947	Ss	Compaction	15.0	58	1610	33.0	22.6	7813	30	550	100,000	1.4

*Core analysis permeability is low but natural fractures or vugs result in very high effective permeability.

permeability is continuous. In Exxon's tests, the low residuals were consistently in cores from thick sections having good vertical permeability. Conversely, cores located immediately below shale barriers had residual oil saturations close to those obtained in the laboratory floods.

III. BASIC RESERVOIR AND AQUIFER DATA NEEDED FOR STUDIES

The data described in this section are desirable for a water-drive study in which reservoir performance is calculated by the basic technique described in this chapter. Engineers are cautioned against the premature conclusion that these data are not available and that a reservoir study is thus impossible. Data can generally be approximated from empirical relationships or by analogy to other fields.

In studying overall pool behavior, average values of porosity, permeability, and other properties are used. An average value of pressure is assumed to apply for the entire field at a given time. Volumetric behavior of the reservoir fluids is computed on the basis of the average field pressure.

Fig. 3 shows a structural map and cross section of a

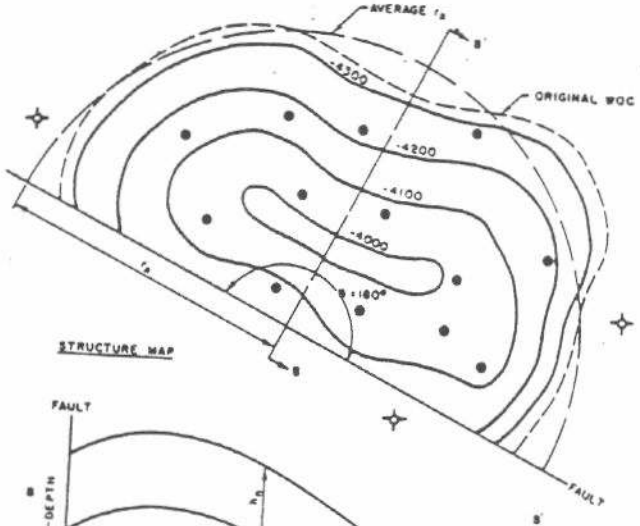

FIG. 3. Structure map and cross section of a water-drive reservoir.

water-drive reservoir which is bounded by a fault on one side and is in contact with an aquifer on the remaining periphery of the pool. The figure illustrates some of the quantities in the following list of data.

A. Characteristics of the Hydrocarbon-B Reservoir

1. Average porosity fraction, $\bar{\varphi}$. (See Chap and 1-3.)
2. Connate water distribution. (See Chapte
3. Average absolute permeability, $\bar{k}$, millid (See Chapters 1-2, 1-3, 2-1, 5-5, and
4. Depth of water-oil contact, feet. (See C 1-9.)
5. Plot of hydrocarbon volume versus depth Chapter 1-3.)
6. Average angle of dip of formation, α_d, de (See Fig. 3.)
7. Original oil in place, N, stock-tank ba (See Section IV of this chapter.)
8. Average radius of the reservoir, r_R feet. Fig. 3.)
9. Reservoir periphery open to water influ degrees. (In Fig. 3, for example, θ = 1
10. Fraction of reservoir periphery open to w influx, $f_R = \theta/360°$. (For Fig. 3, f_R = 180/ = 0.5.)
11. Average area exposed to influx of water, square feet. (In Fig. 3, $A = 2\pi r_R w$.*)

B. Aquifer Characteristics

1. Permeability, millidarcies.
2. Net formation thickness, h_n, feet. (See Chap 1-3 and Fig. 3.)
3. Average external radius of the aquifer, r_a, fe and ratio of aquifer to reservoir radius,
4. Average porosity fraction, $\bar{\varphi}_a$.

C. General Reservoir Rock Properties

1. Relative permeability to oil and water versu water saturation, k_{ro} and k_{rw} versus S_w. (Se Chapters 1-2 and 4-1.)
2. Water-oil relative permeability ratio versu water saturation, k_{ro}/k_{rw} versus S_w. (Se Chapters 1-2 and 4-1.)
3. Drainage and imbibition capillary pressure ver sus water saturation, P_c versus S_w. (See Chapters 1-2 and 1-9.)
4. Rock compressibility, c_f, vol/vol/psi. (See Chapter 1-2.)

*$w = h_n \cos \alpha_d$; for dip less than 10°, $w \approx h_n$.

D. Reservoir Fluid Properties (see Chapter 1-7)

1. Flash liberation data.
2. Differential liberation data.
3. Gas volume factor versus pressure, B_g versus p.
4. Oil viscosity versus pressure, μ_o versus p.
5. Oil specific gravity at reservoir conditions with respect to fresh water, γ_o versus p.
6. Gas viscosity versus pressure, μ_g versus p.
7. Water viscosity versus pressure, μ_w versus p.
8. Water specific gravity at reservoir conditions with respect to fresh water, γ_w.
9. Compressibility of undersaturated oil, c_o, vol/vol/psi.
10. Water compressibility, c_w, vol/vol/psi.

E. Other Data

1. Reservoir production data (oil, water, and gas) by wells (Chapter 1-6).
2. Reservoir pressure data for preparation of isobaric maps at various dates to obtain average reservoir pressures (Chapter 1-6).
3. Maps showing the water-oil ratio status of the wells at various times in the history of the reservoir.
4. Water influx rates for neighboring pools producing from the same formation. This will permit accounting for possible interference effects between pools.

IV. ANALYSIS OF PAST RESERVOIR PERFORMANCE

The reservoir's past performance can be used to evaluate many of the reservoir parameters needed for predicting future performance. It may be possible to evaluate the original oil in place by material balance; water influx values can be calculated and used to estimate the extent of the aquifer, r_D, and the nature of the aquifer as characterized by the constant C in the unsteady-state flow equation; the efficiency of oil displacement by water can be calculated from field performance; and the capacity of the reservoir and wells to produce can be evaluated. This section describes how these calculations are made.

Original Oil in Place

The most reliable means for an early determination of the original oil in place is the volumetric method, provided that the necessary data are available on rock properties and reservoir extent. The oil content cannot be accurately determined unless good data are available on reservoir porosity and water saturation and productive limits have been defined. As an aid in calculating the original oil in place volumetrically, it is sometimes convenient to express the oil content as a hydrocarbon volume distribution curve, as illustrated in Fig. 4. Such a curve should be carefully prepared

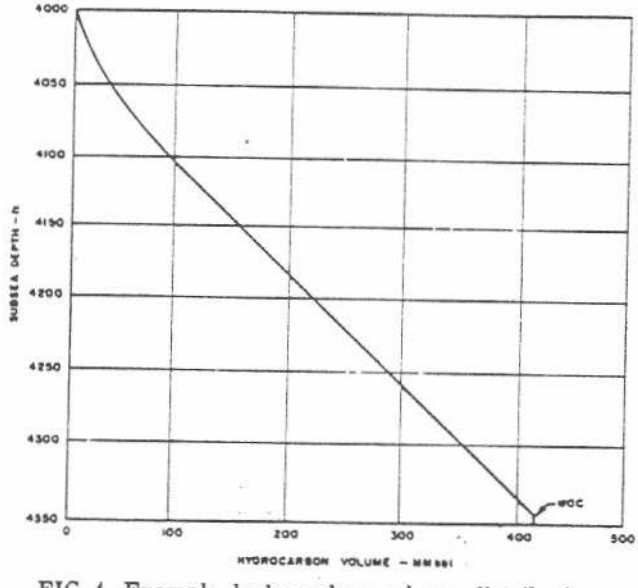

FIG. 4. Example hydrocarbon volume distribution curve.

to account for the variation in oil saturation above the initial water-oil contact; this variation is the result of capillary forces. A detailed discussion of the preparation of the hydrocarbon volume curve is contained in Chapter 1-3. After the reservoir pressure has declined a few hundred psi, the oil in place should be checked by material balance calculations described below.

Alternative methods of calculating oil in place are based on the material balance equation. Material balance is often used to check the volumetric calculation of original oil in place. It is also used on weak water-drive reservoirs when the quality of pressure and production data is superior to the information available on porosity, connate water, and other parameters necessary for the volumetric calculation of oil in place. Considerable caution should be exercised in the use of the material balance method, however, because results are very sensitive to the accuracy of fluid-property and pressure data. Material balance results are most reliable for reservoirs where the ratio of water influx to total withdrawals is relatively low.

The material balance methods of estimating the original oil in place can be derived from the various forms of the material balance equations shown in Chapter 5-4. In computing oil in place for undersatu-

rated reservoirs, it is necessary to account for expansion of the formation rock and connate water. Equation (1) below should be used for pressures above the bubble point.

$$N = \frac{N_p B_o - (W_e - W_p B_w)}{B_o - B_{oi} + \bar{c}_{f+w} B_{oi} (p_i - p)} . \quad (1)$$

For reservoirs without an initial gas cap producing at pressures below the bubble point, equation (2) should be used. It accounts for gas liberated from solution and for free gas production.

$$N = \frac{N_p B_o - N_p R_s B_g + G_p B_g - (W_e - W_p B_w)}{(R_{si} - R_s) B_g - (B_{oi} - B_o)} . \quad (2)$$

Equation (2) is the basic material balance equation of Chapter 5-4 when G, the original free gas in the reservoir, is zero. The symbols of equations (1) and (2) are identified in Chapter 5-4.

In water-drive reservoirs, it is not possible to solve for the oil in place directly from equations (1) or (2) because the water influx, W_e, is a variable, unknown quantity. There are two methods of determining N by material balance.

(1) Set the water influx term, W_e, equal to zero and calculate values for the apparent N at successive time intervals. If a water drive is present, the apparent N should increase with time. Extrapolate the trend of apparent N values back to the time of initial production; this value should approximate the original oil in place.

(2) Solve the material balance equation simultaneously with unsteady-state equations for calculating water influx. To do this, the water influx term is expressed by the following unsteady-state equation (see Chapter 5-5):

$$W_{e,n} = C \sum_{j=1}^{j=n} \Delta p_{j-1} Q_{(tD_n - tD_{j-1})} , \quad (3)$$

where C is a constant which depends on reservoir and aquifer properties. The use of the dimensionless time function, Q_{tD}, is described later in this section and illustrated in Section VIII of this chapter. At this point, we will simply state that it can be determined if the reservoir pressure history and certain aquifer properties are known.

The material balance and unsteady-state equations can then be solved simultaneously at various dates in the reservoir production history, and the best average values for N and C can be determined. This is accomplished by cross-multiplying equation (2), transposing W_e to the left-hand term, substituting for W_e according to equation (3), and dividing through by $(R_{si} - R_s)B_g - (B_{oi} - B_o)$ to obtain:

$$\frac{N_p B_o - N_p R_s B_g + G_p B_g + W_p B_w}{(R_{si} - R_s) B_g - (B_{oi} - B_o)} = N + C \frac{\sum_{j=1}^{j=n} \Delta p_{j-1} Q_{(tD_n - tD_{j-1})}}{(R_{si} - R_s) B_g - (B_{oi} - B_o)} , \quad (4)$$

or

$$\text{Term } A = N + C \text{ (Term } B).$$

Now, plotting Term A against Term B, we obtain N from the intercept and C from the slope as in Fig 5.

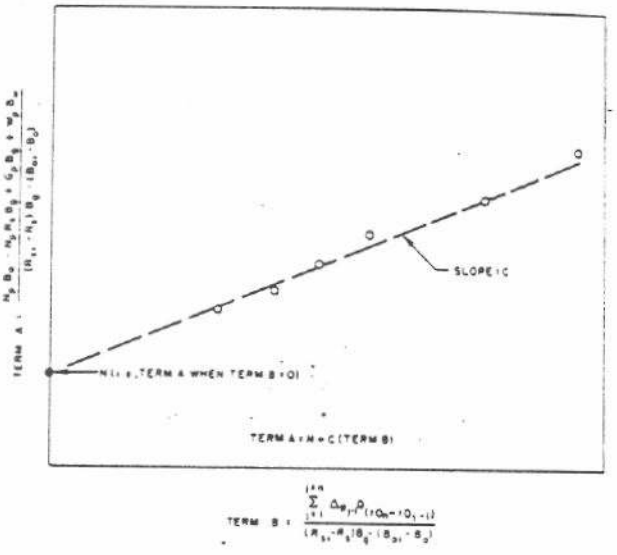

FIG. 5. Graphical material balance evaluation of N and C.

We again emphasize that these material balance methods are generally useless when most of the reservoir energy comes from the water drive. For example, applying either method to the example problem of this chapter (Section VIII) would result in N values that might be 100 percent in error. This is because water encroachment has replaced more than 95 percent of the total reservoir fluid withdrawals in the example.

B. Water Influx Calculations

1. BY MATERIAL BALANCE

The following forms of the material balance equations are convenient for calculating gross water influx: For pressures above the saturation pressure, equation (1) can be solved for water influx, to obtain the following:

$$W_e = NB_{oi} - (N - N_p) B_o - N\bar{c}_{f+w} B_{oi} (p_i - p) + W_p B_w . \quad (5)$$

A variation of equation (5) using the natural depletion function dN_p/dp can be used for predicting

water influx in the case of a weak water drive. The following equation is used and dN_p/dp is established from the very early history:

$$W_e = N_p B_o - \frac{dN_p}{dp} B_{oi} (p_i - p) + W_p B_w . \quad (5a)$$

For pressures below the saturation pressure, solve equation (2) for water influx to get the following equation:

$$W_e = NB_{oi} - (N - N_p) B_o - [NR_{si} - (N - N_p) R_s - G_p] B_g + W_p B_w . \quad (6)$$

Early in the production history of a reservoir, material balance methods may give erratic results for water influx. That is, the results may not be consistent with the water influx principles discussed in this chapter. These erratic results occur because of inaccurate pressure measurements or because average field pressure values may not represent the actual average reservoir pressure if only a few wells are available for pressure measurements. These pressure errors are most serious when the average reservoir pressure is still near the original pressure. In some cases, a negative water influx may be calculated in the early life of a field. This usually indicates nonrepresentative pressure values, since negative influx can occur only under very unusual conditions.

If natural water influx is not sufficient to maintain reservoir pressure and production rates at desired levels, supplementary water injection may be required. Water injected on the flanks of a structure is usually less than 100 percent effective in replacing reservoir withdrawals. About 10 to 30 percent of the injected water is generally ineffective, either because it is lost to the aquifer or because the pressure disturbances due to the injection diminish natural water influx to some extent. If f_i is the fraction of cumulative injected water, W_i, that is effective in maintaining pressure and replacing withdrawals, the following relationships hold:

$$\begin{bmatrix}\text{Gross Water Influx Including}\\ \text{Flank-Water Injection}\end{bmatrix} = W_e + f_i W_i ; \quad (7a)$$

$$\begin{bmatrix}\text{Net Water Influx Including}\\ \text{Flank-Water Injection}\end{bmatrix} = W_e + f_i W_i - W_p B_w . \quad (7b)$$

Material balance equations (5) and (6) may be modified to account for flank-water injection by using the above definitions for gross and net water influx. The natural water influx, W_e, must be evaluated independently by unsteady-state equations if we want to solve for f_i, the injection efficiency. In a similar manner, the natural water-drive methods discussed in the remainder of this chapter may be modified for flank-water injection.

2. UNSTEADY-STATE EQUATIONS

To calculate the flow of water into an oil reservoir from an aquifer, it is necessary to apply unsteady-state flow concepts. Hurst and Van Everdingen[8] published a method that is widely used for water-influx and other unsteady-state calculations. This method is based on the use of graphical solutions to the unsteady-state diffusivity equation. Chapter 5-5 describes the unsteady-state functions of dimensionless time, which are designated Q_{tD}, the dimensionless cumulative water influx. For water-drive reservoirs, Q_{tD} is plotted against dimensionless time, t_D, (see Chapter 5-5, Appendix B). Dimensionless cumulative water influx, Q_{tD}, is related to cumulative influx in barrels, W_e, as follows:

$$Q_{tD} = \frac{W_e}{1.12\, h_n \overline{\varphi}_a\, c_{f+w}\, r_R^2\, \Delta p} . \quad (8)$$

Similarly dimensionless time, t_D, is related to actual time in days, t, as shown below:

$$t_D = \frac{0.00633\, k_w t}{\mu_w\, \overline{\varphi}_a\, c_{f+w}\, r_R^2} . \quad (9)$$

Note that instead of $\bar{c}_{f+w}$ used in equations (1) and (5), c_{f+w} is used in equations (8) and (9). $\bar{c}_{f+w} = (c_f + c_w S_w)/(1 - S_{wi})$ is used in material balance equations because these equations are based on hydrocarbon volumes which constitute only a fraction of the pore volume. The $(1 - S_{wi})$ converts rock and water compressibility from a pore volume basis to a hydrocarbon basis. On the other hand, the water influx equations involve water movement in completely water-saturated porous media. Thus, the system considered is already on a pore volume basis ($S_w = 1.0$) and $c_{f+w} = c_f + c_w$.

Since the Q_{tD} graphs were developed on the basis of a completely radial pool and aquifer, the resulting water influx values must be adjusted by the factor $\theta/360° = f_R$ which is the fraction of the pool periphery open to water influx. Fig. 3 illustrates a field where $\theta = 180°$, thus $f_R = 0.5$. The aquifer constant, C, includes the value of f_R and other aquifer factors as seen by rearranging equation (8). With this modification, equation (8) becomes:

$$W_e = 1.12\, h_n \overline{\varphi}_a\, c_{f+w}\, r_R^2\, f_R\, \Delta p\, Q_{tD} = C\, \Delta p\, Q_{tD} , \quad (10a)$$

where C is the aquifer constant for a specific pool.

Equation (10a) gives the cumulative water influx into an oil reservoir at any time, t, due to an instantaneous reduction in pressure Δp at the radius of the reservoir at zero time. The time, t, is therefore the number of days during which the pressure drop, Δp, has been in effect.

The principle of superposition is applicable to the

water influx problem. This means that the cumulative influx induced by several instantaneous pressure drops can be computed by adding the effects of each pressure drop, if we consider the elapsed time over which each of the pressure drops is effective. Thus,

$$W_e = W_{e,1} + W_{e,2} = C\,[\Delta p_1\, Q_{tD_1} + \Delta p_2\, Q_{tD_2}] \quad (10b)$$

is the cumulative influx at time t due to two pressure drops, Δp_1 and Δp_2, where Δp_1 occurred t_1 days prior to t and Δp_2 occurred t_2 days prior to t.

In applying this method, it is convenient to represent the pressure history of the reservoir by a sequence of constant pressure plateaus separated by a series of instantaneous pressure changes. Fig. 6 shows

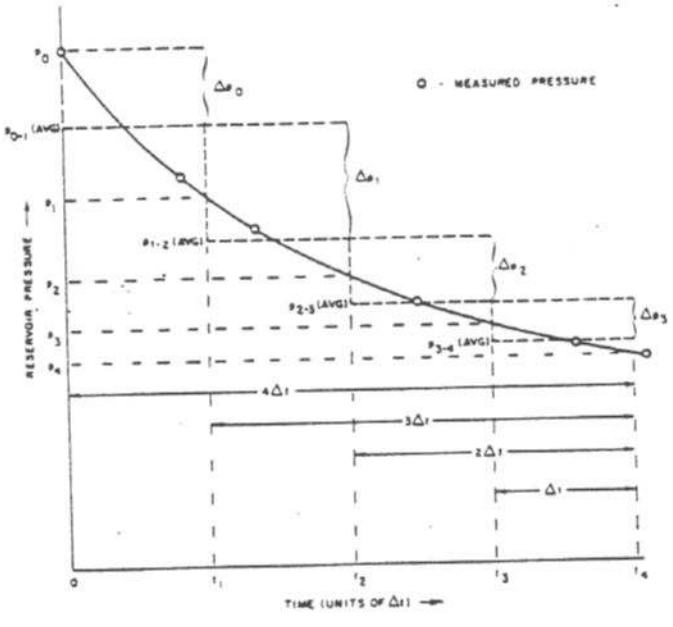

FIG. 6. Stepwise approximation of pressure curve.

the manner in which a smooth pressure decline curve, drawn through observed pressure points, is approximated by a stepwise curve. It should be noted that the plateaus are drawn through the average pressure in each time interval, Δt. Also, note that while it is simpler to use equal time intervals, Δt, as illustrated here, it is not necessary. Equation (10b) will work as well for unequal Δt values. The accuracy of the stepwise approximation will depend upon the length of time increments used. Ordinarily, time increments of three or six months are convenient and give satisfactory results.

The procedure for using equations (10a) and (10b) to calculate the cumulative water influx into a reservoir with the pressure history shown in Fig. 6 is described below. The history is divided into four equal time increments of duration Δt. According to the stepwise curve, only the first pressure drop, Δp_0, has occurred prior to t_1. Since Δp_0 took place at zero time, the cumulative water influx at t_1 is:

$$W_{e,1} = C\,\Delta p_0\, Q_{tD_1}.$$

Four stepwise pressure drops have occurred prior to t_4. The water influx resulting from each can be evaluated independently by accounting for the elapsed time over which each pressure drop is effective. For example, at t_4, the first pressure drop, Δp_0, has been in effect an elapsed time $(t_4 - 0)$ or $4\Delta t$*; Δp_1 has been in effect an elapsed time $(t_4 - t_1)$ or $3\Delta t$; Δp_2 has been in effect for $(t_4 - t_2)$ or $2\Delta t$; and Δp_3 has been in effect an elapsed time $(t_4 - t_3)$ or Δt. Expanding equation (10b) to account for each of the four pressure drops:

$$W_{e,4} = C\,[\Delta p_0\, Q_{tD_4} + \Delta p_1\, Q_{tD_3} + \Delta p_2\, Q_{tD_2} + \Delta p_3\, Q_{tD_1}],$$

where: t_{D_4} corresponds to $4\Delta t$, etc. In general, then, the cumulative water influx at time t_n is as shown previously by equation (3) repeated below:

$$W_{e,n} = C \sum_{j=1}^{j=n} \Delta p_{j-1}\, Q_{(tD_n - tD_{j-1})}.$$

For convenience, equation (3) will be written:

$$W_{e,n} = C \Sigma \Delta p\, Q_{tD}.$$

3. EVALUTION OF THE AQUIFER CONSTANTS, C AND r_D

The application of equation (3) requires the evaluation of the aquifer constant, C:

$$C = 1.12\, h_n \overline{\varphi}_a\, c_{f+w}\, r_R^2\, f_R, \quad (11)$$

and the aquifer extent, r_D:

$$r_D = r_a / r_R. \quad (12)$$

As will be shown in the example of Section VIII, r_D must be evaluated to determine values for Q_{tD} functions.

Although all of the factors involved in the aquifer constant C have a physical significance, it is usually impossible to determine their values with sufficient accuracy to allow a direct accurate calculation of C. However, this constant can be evaluated empirically as follows. The material balance equation is used to calculate the cumulative water influx into the pool at any date for which pressure and cumulative production are known. Since for a given reservoir, the summation term $\Sigma \Delta p\, Q_{tD}$ is a function of pressure, dimensionless time, and r_D, it can be calculated for any date during the known history if r_D is known and time can be expressed as dimensionless time (t_D). The

*Since we are using equal time intervals of Δt, the time periods can be expressed as multiples of Δt.

water influx at the corresponding time is known from material balance calculations, so equation (3) can be solved for the aquifer constant, C:

$$C = \frac{W_e}{\Sigma \Delta p \, Q_{tD}}.$$

If this calculation is carried out for each date corresponding to the end of a predetermined time increment during the known history, it will usually be found that the apparent value of the aquifer constant is erratic in the early life of a pool. This variation is due largely to inaccuracies in early pressure data and to the previously discussed limitations of the material balance equation when reservoir pressure has declined only slightly below the original pressure. Ordinarily, however, the value of C will become fairly constant with time after two or three years of producing history.

A comparison of equations (9) and (10a) shows that $\overline{\varphi c_t}$, $c_f + w$, and r_R^2, which are related to the total aquifer expansibilities, are involved in the evaluation of both C and t_D. As pointed out previously, these factors are difficult to evaluate, but errors are compensated. Although the calculated value of t_D directly influences the magnitude of the Q_{tD} function, experience has shown that an error in t_D is largely absorbed in the empirically determined constant, C. This is particularly true when the aquifer is acting in an infinite manner.

If the aquifer size as measured by r_D is unknown, it may be possible to evaluate this parameter concurrently with C. This is done by assuming several values of r_D and preparing a plot of the apparent or calculated C versus time for each r_D value. The correct r_D will permit C to become constant with time. If the assumed r_D is too small, C will continue to increase, and if r_D is too large, C will continue to decrease. This technique is illustrated in the example problem of Section VIII.

4. REMARKS ON THE APPLICATION OF WATER INFLUX CALCULATIONS

If the values of C calculated from past performance do not become essentially constant with time, then the data should be carefully studied to determine if adjustments are justified. The aquifer characteristics may invalidate the assumption of radial flow through a homogenous formation on which the Q_{tD} functions are based. If this is judged to be the case, an extrapolation in the trend of C versus time or C versus total withdrawals should be used for predictions instead of a single value of C.

Failure to obtain a constant C value may result from errors in the reservoir data. Previous studies have shown that adjustments of the following data factors may be justified:

a. *Pressure.* Errors in reservoir pressure will cause C values to be erratic if C is plotted against time. A plot of $\Sigma \Delta p Q_{tD}$ versus cumulative water influx can smooth out the pressure errors to give a good average C value; or, pressure values can be adjusted to give a constant C if plotted against time.

b. *Oil In Place.* If the oil-in-place value is too large, W_e values will be too small and will cause C values to be too small. C may increase or decrease with time from its true value depending upon the character of the aquifer and the hydrocarbons in the reservoir.

c. *Withdrawals.* Frequently, an inability to obtain a constant value of C may be the result of erroneous reservoir withdrawal data. For example, communication between zones may exist through a casing leak. An unaccounted loss of fluid would cause the volumetric-balance water influx to be too low, and thus C would tend to decrease with time. Similarly, an unaccounted entry of fluid would cause the material balance water influx to be too high and C would tend to increase.

d. *Ratio of Aquifer Radius to Reservoir Radius.* If the value of the ratio r_D used in the evaluation of dimensionless flow for the unsteady-state equation is too large, then the values of C determined for the latter life of the reservoir will decrease with time. This is illustrated in Fig. 7, which compares the C value trends to

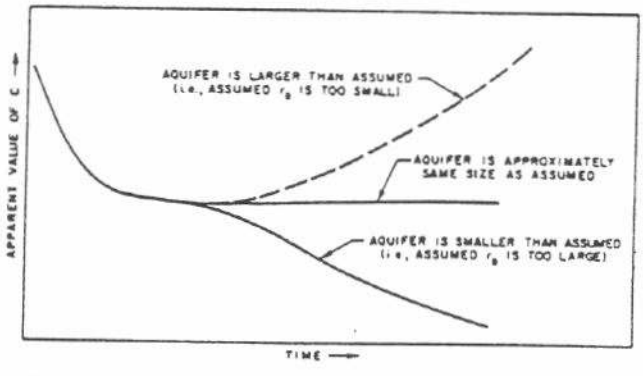

FIG. 7. Example determination of C values by assuming various aquifer sizes.

be expected for a field with a limited aquifer when the assumed r_D is correct, too small, or too large. Any aquifer will behave in the same manner as an infinite aquifer for some period of time as can be seen from the Q_{tD} vs t_D curves (Chapter 5-5, Appendix B). Thus any aquifer curve will coincide with the infinite

aquifer curve for low values of dimensionless time. The estimate of r_D used to solve the unsteady-state equation should be substantiated by geological data whenever possible.

e. *Permeability of the Aquifer.* Although permeability does not enter directly into the C value, dimensionless time, t_D, is proportional to permeability. Since Q_{tD} and thus $\Sigma\Delta p\ Q_{tD}$ is a function of t_D, the value of C for any time and the trend of C with time depend on the permeability value used. If C does not become constant with time, a different value of aquifer permeability can be tried.

When proper adjustments have been made and C has been determined satisfactorily, then past-history water influx calculated by the material balance and unsteady-state equations will agree. The validity of basic data adjustments and of the selected value of C can be checked by solving the material balance and unsteady-state equations simultaneously for pressure and water influx, to obtain a calculated pressure versus time for comparison with the observed pressures.

C. Recovery Efficiency of the Water Drive

The next step in matching the field production history is to calculate the water influx and compare it with the observed water-oil contact advance to obtain reservoir recovery efficiency, E_R. This section describes a simplified method for performing this calculation in a flank or bottom-water-drive reservoir. In using the method, we will assume that the water front advances as a level plane along structural contours and that an average reservoir recovery efficiency can be used for the water-invaded region. If the water-oil contact has advanced unevenly throughout the field, the invaded hydrocarbon volume can be determined by planimetering an isopach map of water advance at individual wells.

If the field has produced long enough for the water-oil contact to have risen noticeably, the reservoir recovery efficiency can be determined from field performance. From the hydrocarbon volume-depth curve, such as that shown in Fig. 4, the water-invaded hydrocarbon volume can be determined at any date for which the average level of the water-oil contact is known. Net water-influx values for the same dates are calculated from the material balance equation. For near constant-pressure operation, the average reservoir recovery efficiency up to any date may then be calculated from the following relationship:

$$E_R = \frac{W_e - W_p B_w}{HCV_e}, \qquad (13)$$

where $W_e - W_p B_w$ is the net water influx in barrels measured at reservoir condition, and HCV_e is the cumulative water-invaded hydrocarbon volume, also in barrels. For predictive calculations, the average value of efficiency for the entire reservoir history can be used. Or, if the calculated values of reservoir recovery efficiency show a definite trend with time, it may be desirable to extrapolate this trend as a basis for predictions.

If there are insufficient data to determine the reservoir recovery efficiency of the water drive from field history, it can be estimated by theoretical means. Welge's[12] method of calculating water saturation behind the advancing water front is a convenient means for making such a calculation (see Chapter 5-6 for a more complete description of this method). Welge's method uses graphical and calculational methods to solve the equation for the fraction of water in the flowing stream (f_w) as a function of water saturation. The equation for f_w is as follows:

$$f_w = \frac{\mu_o/\mu_w}{(\mu_o/\mu_w) + (k_{ro}/k_{rw})} - \frac{0.488\ (10^{-3})\ Akk_{ro}\,|\Delta\gamma|\ \sin\alpha_d}{q_t\,\mu_w\,[(\mu_o/\mu_w) + (k_{ro}/k_{rw})]}. \qquad (14)$$

Equation (14) is used to predict oil recovery as a function of the volume of water that has passed through the reservoir. Theoretically this constitutes only the displacement efficiency and does not include the volumetric sweep efficiency.* However, for most water-drive fields, the recovery at water breakthrough as predicted by the Welge method corresponds with the recovery in the water-invaded portion of the reservoir.

Equation (14) predicts the displacement efficiency as a function of water throughput in the portion of the reservoir swept by water. Generally, the oil displaced at water breakthrough is used as the basis for determining recovery efficiency. The displacement efficiency, E_D, must be multiplied by the volumetric sweep efficiency, E_V, to get the recovery efficiency on a reservoir volume basis, E_R. To get *recovery efficiency on a stock-tank-barrel basis*, $E_{N,WD}$, the change in the oil formation volume factor must be considered. This recovery efficiency can be predicted by the following equation *provided no gas saturation* is present:

$$E_{N,WD} = (E_D)(E_V)\left(\frac{B_{oi}}{B_o}\right), \qquad (13a)$$

where E_D is the displacement efficiency at water breakthrough from equation (14).

*See Chapter 3-3 for exact definitions of displacement, recovery, and volumetric sweep efficiencies.

In order to isolate the terms in equation (14) that ow the gravity effect on f_w, multiply the numerators d denominators of the right-hand term by μ_w/μ_o and rrange to obtain:

$$f_w = \left[\frac{1}{1+\frac{\mu_w k_{ro}}{\mu_o k_{rw}}}\right]\left[1-\frac{0.488(10^{-3})\,Akk_{ro}\,|\Delta\gamma|\,\sin\alpha_d}{q_t\,\mu_o}\right]. \quad (15)$$

The minus term on the right-hand side of equation 5) represents the effect of gravity on f_w at a given turation. For a level reservoir without vertical rmeability, this gravity group is zero.

For reservoirs where gravity is not important, oil ecovery efficiency is primarily a function of the ater-oil relative permeability characteristics and ne water-oil viscosity ratio.

For reservoirs where gravity is important, the oil ecovery will increase as the dip angle increases, as eservoir permeability increases, and as the rate of ter advance along the bedding plane decreases. 8 shows how the gravity term in equation (15)

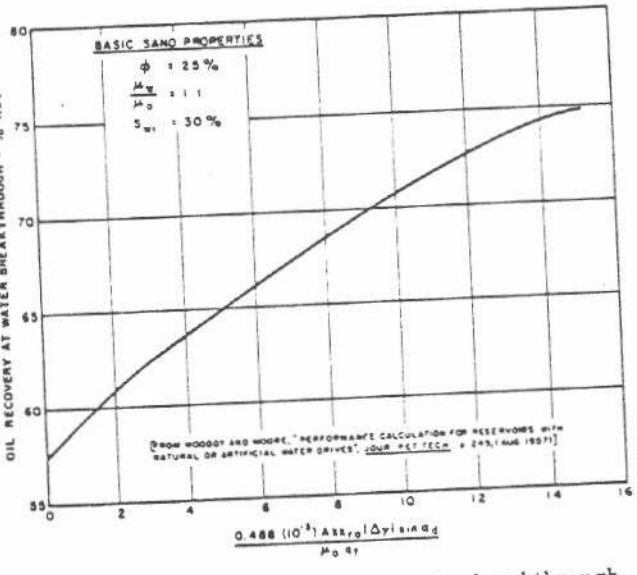

FIG. 8. Relation of oil recovery at water breakthrough to gravity term.

affects oil recovery at water breakthrough in a typical reservoir.[13] Basic data used in the preparation of this figure included relative permeability data d reservoir fluid data from a Southwest Texas Frio formation reservoir. Some specific examples of how reservoir permeability and the rate of water advance influence recovery are as follows. A reservoir having a five-degree dip to the bedding planes, a permeability of 100 md, and a water-advance rate of one foot per day would recover 58 percent of the original oil at breakthrough. If the permeability were one darcy and the other factors remain unchanged, breakthrough recovery would increase to 61.5 percent. If the rate in the high-permeability reservoir were reduced to 0.2 feet per day, recovery would be 70.5 percent.

For a study involving different production schedules and varying rates of water advance, Welge's method provides a technique for adjusting the recovery efficiency in reservoirs where gravity segregation is important. An example calculation of the recovery efficiency for such a reservoir is presented in Chapter 3-6.

D. Fluid Production Capacity

The past history of a field can provide important data on individual well productivity for use in future predictions. The productivity index of a well can be determined for any point in history where the producing rate (q_o), and the drawdown (reservoir pressure, p_e, minus wellbore flowing pressure, p_{wf}) are known. Thus, as shown in Chapter 2-1:

$$J = \frac{q_o}{p_e - p_{wf}}. \quad (16)$$

The change in the productivity index due to pressure and saturation changes can be predicted for a water-drive reservoir by the following equation (also from Chapter 2-1):

$$J = \frac{0.00708k\,k_{ro}\,h_n}{B_o\mu_o\,ln\,(r_e/r_w)}. \quad (17)$$

If reservoir pressure remains above the bubble point, the permeability to oil will not change until water invades a well. Then, for wells ahead of the water front,* only oil is produced and the productivity index becomes:

$$J = \frac{0.00708k_{o(w)}h_n}{B_o\mu_o\,ln\,(r_e/r_w)}. \quad (17a)$$

Equation (17a) can be used to predict future productivity indexes up to the time the water front reaches a well. The value of J will change only as B_o and μ_o change with pressure as long as the pressure stays above the bubble point. If the pressure falls below the bubble point the oil permeability must be adjusted for the existence of a gas saturation in evaluating J. The future oil production rate for a well at a given drawdown can be determined from equation (16) solved for q_o as follows:

$$q_o = J(p_e - p_{wf}). \quad (16a)$$

*If coning is important, the effective position of the water front may be several feet higher than the water-front position in the reservoir.

Equation (17) is theoretically applicable for wells behind the water front, but other methods are generally used to predict their future producing rates. Equation (17) requires an evaluation of k_{ro}, which is a function of water saturation. Generally, the water saturation cannot be determined with sufficient accuracy to calculate the oil production rate for a well producing oil and water. Decline-curve analysis may be used to estimate production trends for wells producing oil and water (see Chapter 5-8). Another technique that is sometimes effective is to establish trends of producing water-oil ratios for individual wells as a function of their structural position. This method automatically accounts for coning since all the completion *WOC's** are based on production tests. Fig. 9 illustrates how this method is used. The

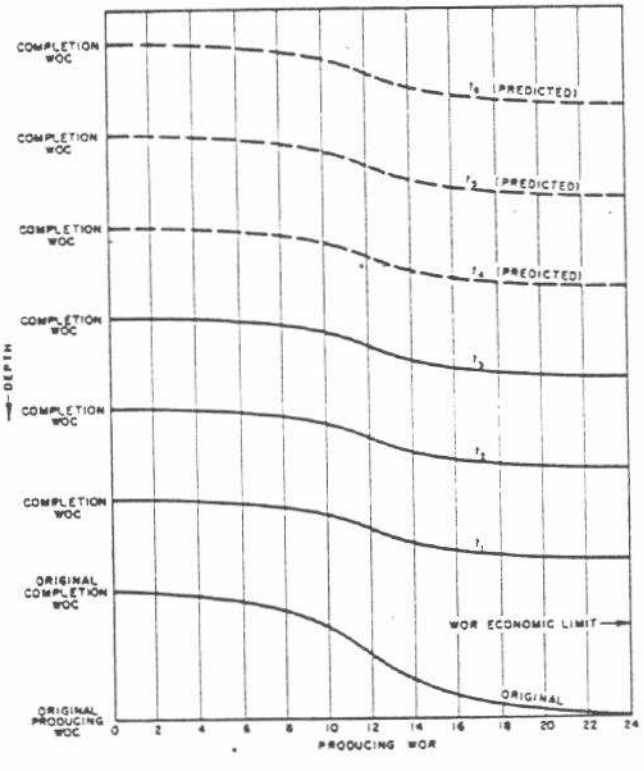

FIG. 9. Producing water-oil ratio vs depth.

solid curves, labeled t_1, t_2, and t_3, represent actual performance at three different times in the field history. For a given curve, the zero water-oil ratio is plotted at the completion *WOC* at the time depicted by the curve. Other points on the curve represent the producing water-oil ratios (at that same time), for wells producing from the interval between the original producing *WOC*** and current completion *WOC*. The dashed curves, labeled t_4, t_5, and t_6, in Fig. 9, represent predicted water-oil ratio trends for future times. The predicted water-oil ratio curves are drawn parallel to the curves derived from field history. The time corresponding to a curve is the time when the completion *WOC* will reach the level represented by the zero water-oil ratio on the curve. The curves are terminated at an economic limit such as the water-oil ratio of 24:1 shown in Fig. 9.

Using the methods of this section, we can predict the field oil producing capacity versus the subsea depth of the completion *WOC* if the initial pressure is maintained. An example of such a relationship is shown in Fig. 10. These basic capacities can then be

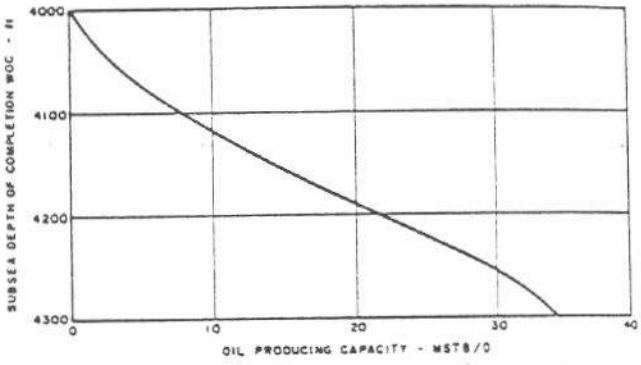

FIG. 10. Example of relationship between completion WOC depth and oil producing capacity of a water-drive reservoir.

modified to account for reservoir pressure and saturation changes. Thus we can predict the production capacity for any completion *WOC*, reservoir pressure, and reservoir saturation.

V. RESERVOIR PERFORMANCE PREDICTIONS

In the prediction method to be described in this section, the material balance equations, unsteady-state-flow equations, water advance equations, and fluid production equations are solved simultaneously to calculate future behavior. The calculations are illustrated with an example problem in Section VIII. The first step in predicting reservoir performance is to select a time interval for predictions. It is generally most convenient to use the same time interval for future predictions that was used to evaluate past reservoir behavior.

After the interval is chosen, the average field withdrawal rates of oil, water, and gas over the first interval are estimated. Part IV.D describes procedures for predicting oil production rates from produc-

*The completion *WOC* is defined in Chapter 1-9 as "the depth in the reservoir where water first appears in the produced oil".

**The producing *WOC* is defined in Chapter 1-9 as "the depth in the reservoir below which essentially no mobile oil is found".

'ty indexes or from the performance of the water-... ratio. In some cases, it is easier to predict production rates on a field basis rather than by individual wells. For example, in many foreign fields, wells are shut in or worked over when water is first produced, to keep the salt content of the crude within market specifications. Under these conditions, field producing capacity is simply related to the position of the *WOC*, and a curve can be calculated relating the field producing capacity to the *WOC* level such as illustrated in Fig. 10. To estimate the producing rate for an interval, we must first estimate the average position of the *WOC* for the interval. Then the average producing rate can be read from a plot such as Fig. 10. Adjustments to the rate derived from the curve may be required if the reservoir pressure has fallen below the bubble point.

When the withdrawal volumes have been estimated, the material balance and unsteady-state equations can be solved simultaneously for pressure and water influx at the end of the period using the value of C determined from past performance. This simultaneous solution is most readily obtained by assuming the pressure at the end of the period and calculating the water influx independently by the material bal-e and unsteady-state equations. If the two values of W_e agree within a predetermined limit, the assumed pressure is correct. If they do not agree, reestimate the pressure and recalculate water influx by both methods until the two values of W_e agree.

If, for the first estimated pressure, the influx calculated by material balance, $(W_e)_{mb}$, is greater than the unsteady-state influx, $(W_e)_{us}$, a lower pressure should be assumed. On the other hand, if the first estimated pressure results in $(W_e)_{mb}$ less than $(W_e)_{us}$, a higher pressure should be assumed. It is usually possible to obtain the correct pressure for the end of a time step in not more than three trials. If the difference between $(W_e)_{mb}$ and $(W_e)_{us}$ is plotted versus the estimated pressure for the first two trials, the correct pressure can be approximated by linear interpolation or extrapolation as illustrated in Fig. 11. The second trial pressure will often be sufficiently accurate if it is based on the assumption that the true W_e is the average of $(W_e)_{mb}$ and $(W_e)_{us}$. The desired pressure is then obtained from $\Sigma \Delta p Q_{iD}$, which is calculated by dividing the average W_e by the constant C.

After the correct pressure and water influx have ' -en determined, the assumed production rate based an assumed average *WOC* position must be checked. The reservoir hydrocarbon volume invaded is found by dividing W_e by the reservoir recovery efficiency. This then defines the level of the *WOC*, and

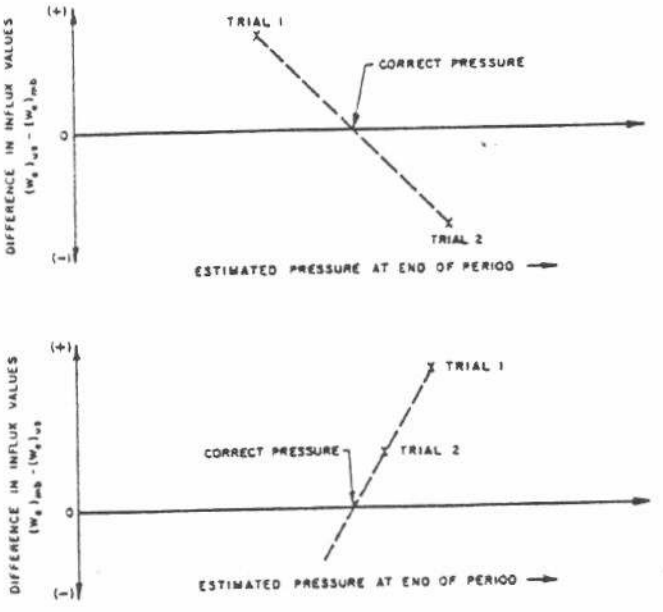

FIG. 11. Graphical estimation of pressures in performance prediction.

the average capacity producing rate is indicated from the plot of rate versus *WOC* position. If the rate that was used is grossly different than this indicated capacity, another rate must be assumed and the entire pressure calculation must be repeated.

After the producing rate, pressure, and W_e for the first period have been reconciled, rates are estimated for the second prediction period based on an assumed *WOC* advance; the same procedure is carried out for the second prediction period, and for succeeding periods until the reservoir reaches abandonment as a result of uneconomical production. A stepwise outline of this method is presented in Section VI.

VI. SUMMARY OF ANALYTICAL PROCEDURE

This section summarizes Sections III, IV, and V in a step-by-step procedure for performance analyses. By combining this basic procedure with the alternative methods presented in Section VII, individual procedures can be developed to fit most water-drive reservoir studies.

A. Analyze Past Performance

Evaluating the past reservoir behavior consists of the following steps:

1. Assemble available geologic, pressure, production, rock, and fluid-characteristics data (see Section II).
2. Determine the original oil in place.
   a. Construct a hydrocarbon volume distribution

curve based on available isopach maps, porosity data, and fluid-distribution data.

b. Calculate the original oil in place from the preceding hydrocarbon volume curve.

c. Check the calculated oil in place by using the material balance methods described in Part IV.A.

3. Evaluate aquifer constants r_D and C.

a. Use material balance to calculate cumulative gross water influx at the end of each time interval.

b. Use the unsteady-state equation to calculate the summation term, $\Sigma \Delta p Q_{tD}$, at the end of each time interval for two or three estimated values of r_D (frequently $r_D = \infty$ is a good first assumption).

c. Divide the gross water influx from step 3.a by the corresponding summation terms from the unsteady-state equation to determine an apparent value of C at the end of each time increment for each value of r_D.

d. Prepare a curve of apparent C versus time for each r_D value and choose the most probable value of r_D and C.

4. Evaluate the reservoir recovery efficiency of the water drive.

a. At the end of each time interval, calculate the recovery efficiency by using net water influx calculated from the material balance combined with observed waterfront positions at the corresponding times.

b. Determine an average reservoir recovery efficiency for the past history.

c. If the reservoir recovery efficiencies at different times vary significantly, plot the efficiencies versus cumulative influx to determine any significant trends. If no trend is shown, use the average efficiency.

d. If the history of *WOC* advance is insufficient to determine the recovery efficiencies from field performance, use the Welge method.

5. Evaluate the trend in production capacity. Plot the reservoir production capacity versus cumulative water encroachment or *WOC* level for use in predicting future production capacity.

The analysis of history for a water-drive field is shown in simplified flow diagram form in Fig. 12. This diagram is analogous to steps 1 through 4 above.

B. Predict Future Performance

After the observed reservoir performance has been analyzed, the future reservoir behavior can be calculated as follows:

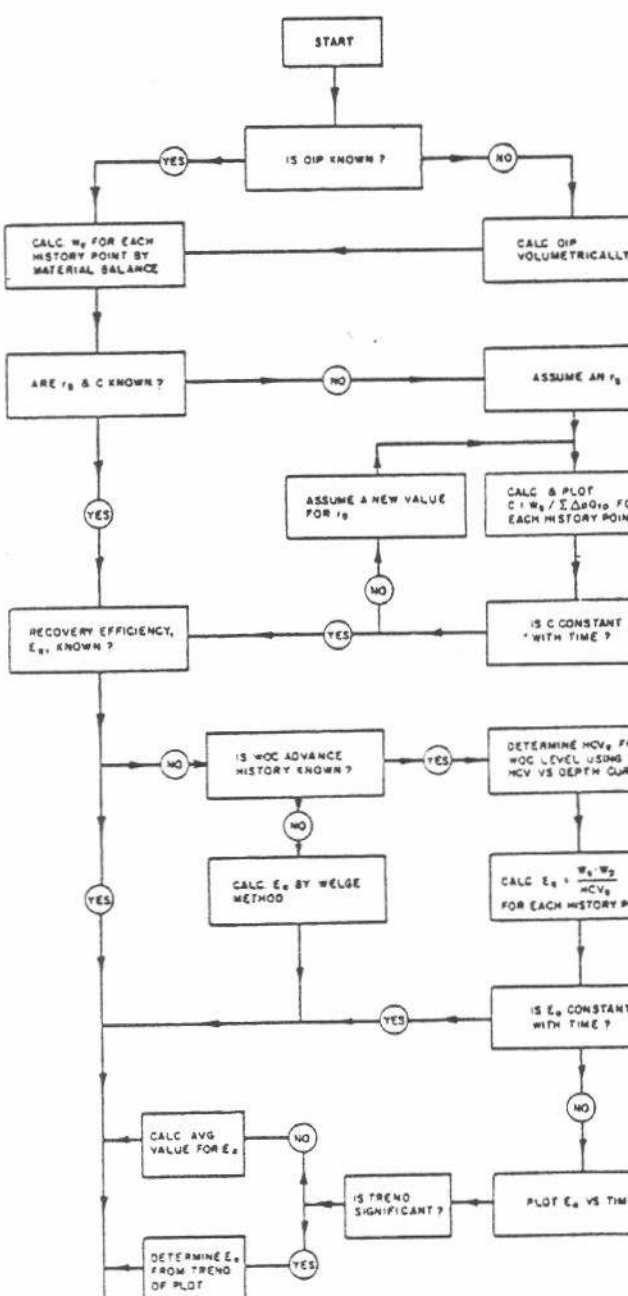

Fig. 12. Simplified flow diagram — analysis of history of water-drive reservoirs.

1. Determine production schedules to be used in the prediction by extrapolating the capacity production trend determined in step A. Such factors as local proration laws, plans for further well development and pipeline capacity

ity should also be considered in estimating producing rates.

2. Assume a time interval for the prediction periods.
3. Estimate total withdrawals for the first prediction period.
4. Estimate reservoir pressure at the end of the period.
5. Calculate gross water influx at the end of the period by the material balance equation. Use the estimated pressure and withdrawals.
6. Calculate the gross water influx to the end of the period using the unsteady-state equation and the aquifer constants already determined in step A.3.d.
7. Compare the water influx values from the two preceding steps.
8. If the water influx calculated by the material balance is equal to the water influx calculated by the unsteady-state equation, the estimated pressure is correct. If the two values of water influx do not agree, repeat steps B.4 through B.7 until the estimated pressure results in the same water influx by the two methods.
9. Using the net water influx from step B.5 and the recovery efficiency from steps A.4.b or c above, determine the position of the water-oil contact at the end of the prediction period.
10. From the new water-oil contact position, check the producing rate used in the period. If the rate used is unreasonable, repeat the calculation with a new rate.
11. Repeat steps B.3 through B.9 for subsequent periods up to the time of reservoir abandonment.

Fig. 13 presents steps 1 through 11 in simplified flow-diagram form. Figs. 12 and 13 may serve as rough guides for setting up problem solutions for specific water-drive fields.

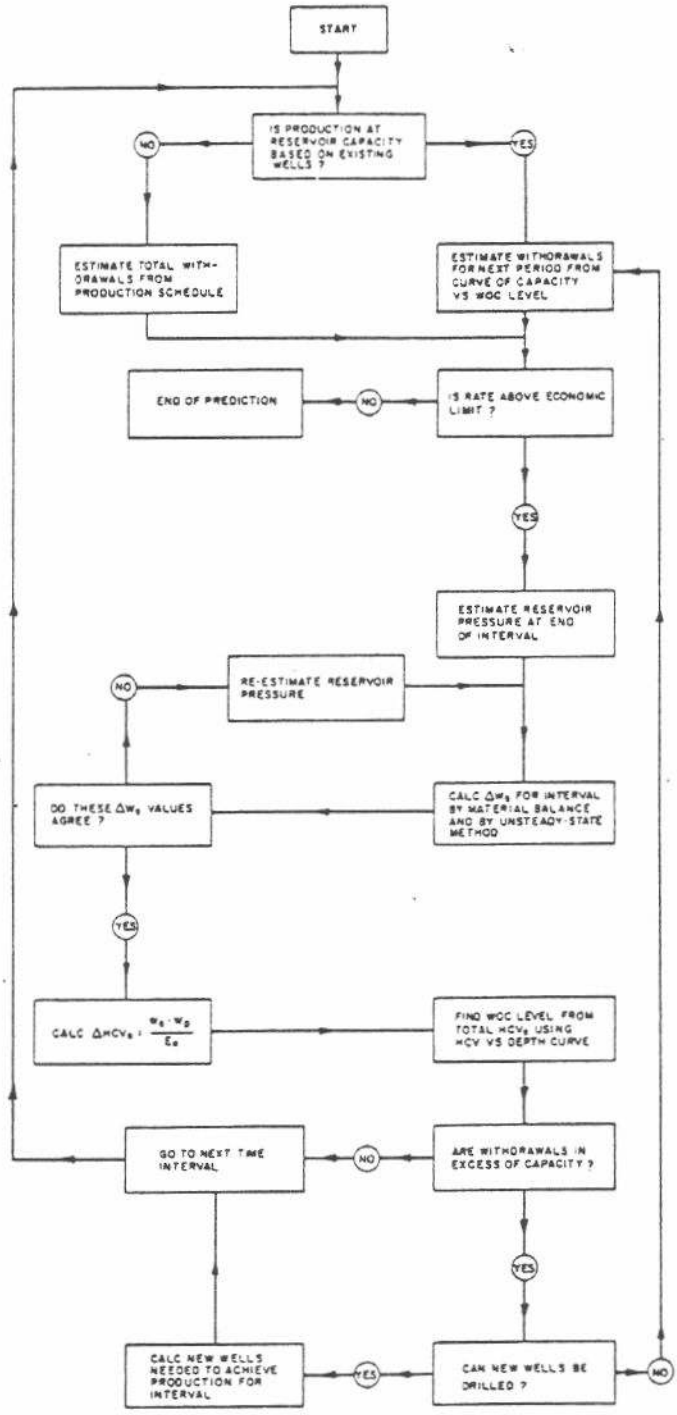

FIG. 13. Simplified flow diagram — predicting performance of water-drive reservoirs.

VII. ALTERNATIVE METHODS

The preceding sections presented a basic calculation procedure for analyzing water-drive reservoirs. There are many alternative methods for handling certain phases of the analysis, and, while it would be impossible to describe all of these methods, this section discusses the most important or best known of the alternative techniques. Some of these methods are more complex than the recommended method and were designed to overcome some of the inherent limitations in the basic technique. Other alternative approaches provide simplified calculations and are included because of their frequent use in the industry. In particular, the simplified water influx calculations (Part F below) have been widely used in the industry, but the method based on Q_{tD} functions as described in Section IV is more accurate and requires

no more work. Note that decline-curve analysis and the Welge method might also be treated as alternative methods; however these methods have been noted previously in this chapter and are discussed in detail elsewhere in this Manual.

The method to be used for a particular reservoir depends on the quality of reservoir data and the limits of accuracy required in the results. The best method of analysis may also be dictated by the amount of time available in which to get the required answers.

A. Computer Programs for Water-Drive Studies

1. TWO-DIMENSIONAL MATHEMATICAL MODELS

High-speed digital computers have made possible more precise calculations of reservoir performance with two-dimensional mathematical models. The use of advanced computer methods is discussed more fully in Chapter 5-10. In water-drive analyses, these methods can calculate pressures, saturations, and waterfront advance in the reservoir, including the effects of heterogeneities, capillarity, and gravity segregation. In contrast with other methods discussed in this chapter, which deal with the performance of the pool as a whole, the two-dimensional techniques make it possible to study the interaction of individual wells and different pool areas. These methods are particularly applicable to larger pools where reservoir characteristics and performance behavior may vary considerably within the field. A vertical two-dimensional model can be used for evaluating gravity effects, while a horizontal model will account for areal variations within a reservoir. Three-dimensional mathematical models are also available.

2. ONE-DIMENSIONAL MODELS

Although the basic procedures described in this chapter are amenable to hand calculation, many phases of the analysis can be expedited by computers. For example, Exxon's Computer Program Library includes a program entitled "One-Dimensional, Three-Phase, Unsteady-State Combination-Drive Calculations." This program makes one-dimensional analyses of reservoirs producing under any or all of the natural drive mechanisms. The method is based on the solution of the differential equations describing nearly all processes occurring in the reservoir. It allows for point-by-point variations in reservoir permeability, elevation, porosity, and cross-sectional area along a selected axis of the reservoir. Fluid flow is calculated considering three-phase relative permeability (developed by the program from conventional gas-oil and water-oil relative permeabilities), capillary pressures, and the gravity component of flow. The effects of pressure on fluid compressibilities, densities, and viscosity are also treated. The only restrictions on this technique are that gas-oil phase equilibrium must be adequately described by laboratory data, and the one dimension model must adequately describe the reservoir.

3. NONDIMENSIONAL OR TANK-TYPE ANALYSES

Several other computer programs are available for making water-drive calculations. These programs assume uniform pressures, saturations, and rock and fluid properties throughout the reservoir, and thus are classified as nondimensional or tank-type analyses. Exxon's computer program entitled "Volumetric Balance, Unsteady-State Program," follows the basic procedures of this chapter with a few exceptions. The program does not contain displacement equations; therefore, recovery efficiencies for the water drive must be precalculated and entered as data. Also, the program does not iterate on rate to assure its compatibility with the reservoir's production capacity. A significant feature of this program is its ability to automatically adjust various parameters affecting the computed aquifer behavior and thereby match observed field performance. This feature affords considerable time saving when several trials are needed to determine the aquifer parameters that give the best approximation of observed performance. Once determined, these parameters can be used as data for the one-dimensional technique noted above to obtain a rigorous projection of future reservoir performance. Other programs of assistance in water-drive studies are readily available from Exxon USA. For example, the "Computer Program Library" includes a program entitled "Constant Pressure Displacement" which calculates the recovery efficiency and an f_w versus S_w curve for a water displacement using the Buckley-Leverett equation and the Welge method.

B. Dietz[2] Method for Water-Advance Calculations

In some reservoirs where the flow rate is high, water tends to flow updip along the base of the formation, causing the water-oil contact to assume a tilted position. This behavior is exaggerated in water-drive reservoirs that contain viscous oils. Dietz[2] has proposed a method for predicting the movement of the water-oil contact for reservoirs in which the waterfront underruns the oil zone.

For rates of water advance below the "critical rate," the water-oil contact assumes a tilted, equilibrium state and remains at this constant slope* as it

*Calculation of the water-oil contact slope below the critical rate is illustrated in Chapter 5-6.

moves updip through the formation (see Fig. 14A). In many reservoirs, the water-oil contact remains essentially horizontal, as was assumed in the basic prediction technique described in Part VI.B of this chapter.

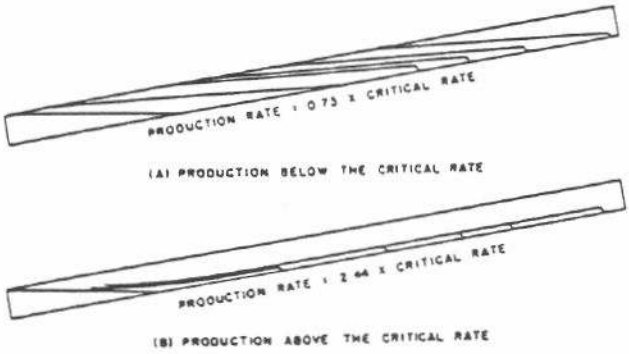

FIG. 14. Small-scale model experiment on water encroachment (by Dietz).

A marked change in the behavior of the water-oil contact occurs when the water influx rate is increased above the "critical rate," defined by the following equation:

$$\left(\frac{\Delta W_e}{\Delta t}\right)_c = \frac{(0.488\times10^{-3})\,kA\,(\gamma_w-\gamma_o)\sin\alpha_d}{(\mu_o/k_{ro})-(\mu_w/k_{rw})}. \quad (18)$$

This is equivalent to the critical rate equation derived in Chapter 5-6. When the water influx rate exceeds this critical value, an equilibrium state is not possible, and a growing water tongue will underrun the oil zone, eventually reaching the updip producing limit of the reservoir. This behavior is illustrated in Fig. 14B. If the water influx rate in a given reservoir appreciably exceeds the critical rate for an extended time, only a small percentage of the original oil in place will be recovered before the water tongue invades the lower producing intervals of most of the producing wells. If water coning is severe, the ultimate recovery efficiency may be extremely low. In some cases, it may be desirable to keep water-influx rates below the critical rate in order to achieve a higher ultimate recovery. In other cases, the critical rate will be too low for economic operation, and it must be exceeded.

If the water-influx rate is several times the calculated critical rate, then the following equation (derived by Dietz[2]) can be used to predict the shape and position of the water-oil contact at various stages of depletion:

$$x = \frac{-y}{\tan\alpha_d} + \frac{5.61\,W_e h^2}{M\bar{\varphi}A\left[\frac{h-y}{M}+y\right]^2(S_{oi}-S_{or})}, \quad (19)$$

where

x = distance from reference point (see Fig. 15) along the bedding plane, ft,

y = distance from reference point perpendicular to the bedding plane, ft (never larger than h),

α_d = dip angle of the reservoir, degrees,

$\bar{\varphi}$ = average effective porosity, fraction,

h = reservoir thickness, ft,

A = cross-sectional area to flow, sq ft,

S_{oi} = initial oil saturation in reservoir,

S_{or} = residual oil saturation in water-invaded portion,

W_e = cumulative water influx, bbl, and

M = water-to-oil mobility ratio.

Equation (19) is based on the assumption that vertical segregation of the oil and water phases is maintained in the y-direction but that gravity forces in the x-direction are negligible. This condition is met if the water-influx rate is considerably higher than the calculated critical rate.

To use the Dietz method, prepare a scaled cross-sectional drawing of the reservoir. For a specific time in the future at which W_e is known, solve equation (19) by putting in various values of y and obtain the corresponding values of x. Then plot these x, y points on the cross section to define the water-oil contact position for that time.

A calculated water-oil contact position is shown in Fig. 15. Repeat this procedure for several different times until the water tongue reaches the updip producing limit of the reservoir.

After the water tongue reaches the updip limit,

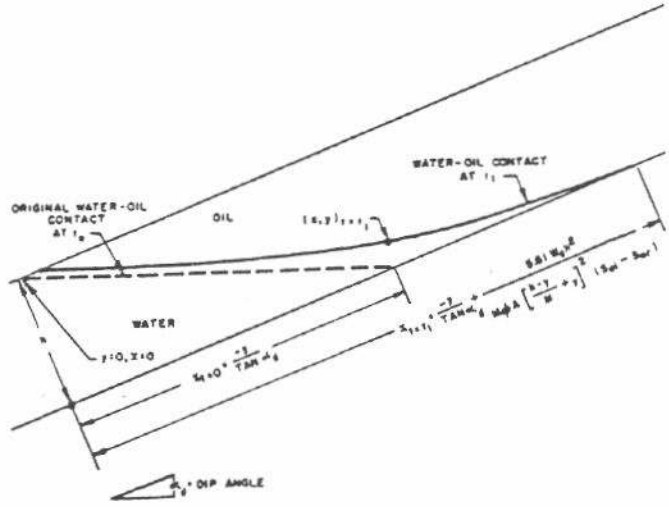

FIG. 15. An illustration of Dietz's calculation of water-oil contact movement.

equation (18) can no longer be used to compute movements of the water-oil contact. To permit further predictions, Joslin suggested a method which was used with good results in two reservoir studies. He reasoned that once the water-oil contact reached the updip limit of the reservoir, the future movement would be a function of oil withdrawals above the contact and the magnitude of the vertical potential gradient between the oil and water phases. Both of these factors decrease in the updip direction. Joslin's calculations, based on the assumption that the water-oil contact would rise vertically at any point in proportion to the reservoir withdrawals updip from this point agreed with observed field performance. Since the producing wells were evenly spaced in both reservoirs, a second assumption was made that the reservoir withdrawals would be proportional to the sand volume not yet watered out.

For example, at the start of a prediction with this method, the volume in acre-feet of remaining net oil sand (V_{Rt}) is determined by planimetering a scaled cross section. Then a vertical rise of the water-oil contact of z_t feet is assumed at the downdip limit of the oil zone; the vertical rise at a given x position, z_x, is assumed to be proportional to the remaining net oil sand updip from that point, V_{Rx}, divided by the total acre-feet of remaining net oil sand, V_{Rt}.

$$z_x = z_t \frac{V_{Rx}}{V_{Rt}}.$$

This equation is solved for different x-positions, thus defining the position of the water-oil contact. The area below the new water-oil contact is then planimetered, and the total volume (acre-feet) of sand watered-out during the period is determined. By using the average displacement efficiency in the reservoir, the net water influx required to invade this known sand volume is calculated. Finally, the above results are put on a time basis by correlating with independent calculations of net water influx versus time from the material balance and unsteady-state equations. By repeating this procedure, the position of the water-oil contact can be predicted for later times up to the time the reservoir is abandoned.

For viscous-oil reservoirs where the water-oil contact rise is not level, the Dietz calculation of water-front advance may be needed in addition to the procedure outlined in Part VI.B of this chapter. None of the methods presented considers the effect of water coning. In a reservoir with continuous vertical permeability and high well drawdowns, coning may result in a very low volumetric sweep efficiency. The prediction of water coning is covered in Chapter 2-4, Water and Gas Coning.

C. Water Influx Determination by Use of th Oil Pool Analyzer

The oil pool analyzer is an electric analog simulates the pressure behavior of a pool and aquifer. The use of analog models is described fully in Chapter 5-11, Physical Reservoir Mo The analyzer should be considered for cases w ideal radial flow through a homogeneous aquifer not apply. It is well suited for large basin studie which several water-drive pools produce from same formation and cause mutual interference effe It can also be used to study aquifers with unu heterogeneity or geometrical complexity.

D. Water Influx Analysis Based on Influence Functions

Influence functions derived from past reserv history are sometimes used to predict future wa influx, when Q_{tD} functions are not available fo reservoir of a particular shape or when an elect analyzer is unavailable. This is an application of constant rate solution to the unsteady-state fl problem, while the Q_{tD} functions are based on t constant pressure solution. (Both solutions are d cussed more in Chapter 5-5.) The influence functi for a reservoir varies with time and can be calculat from past performance using the following equati (this equation is presented in Section IV, Chapt 5-5):

$$p_i - p_n = \sum_{j=1}^{j=n} (\Delta q_e)_j F_{t_{(n-j+1)}} \quad , \quad (2$$

where the mathematical counters identify *equal* tin steps and Δq_e is the average increase in influx ra during a time step. For example, the influence fun tion for the first time step is:

$$F_{t,1} = \frac{p_i - p_1}{(\Delta q_e)_1}.$$

Similarly, the influence function for the second tim step is:

$$F_{t,2} = \frac{p_i - p_2 - (\Delta q_e)_2 F_{t,1}}{(\Delta q_e)_1},$$

and for the third time step:

$$F_{t,3} = \frac{p_i - p_3 - (\Delta q_e)_2 F_{t,2} - (\Delta q_e)_3 F_{t,1}}{(\Delta q_e)_1}.$$

Similarly, one can solve for:

$F_{t,4}$, $F_{t,5}$, $F_{t,6}$, to $F_{t,n}$.

After the influence functions have been calculated

from the past history, they are plotted versus time and the trend is extrapolated. Radial flow in an infinite-acting aquifer will give a straight-line relationship between the influence function, F_t, and the log of time, t. For a finite aquifer, the F_t vs t relationship will be linear after the pressure drop has reached the outer limit of the aquifer. Frick[3] gives other bases for extrapolating the F_t vs t relationship.

Results of the influence function method are often inaccurate because errors in early pressure measurements result in errors in F_t values for the early time periods. The stepwise nature of the F_t calculation requires that these early F_t values be used to calculate F_t values for later times. Thus the early pressure measurements, which are ordinarily inaccurate, influence F_t values for the entire history. Hutchison and Sikora[7] proposed a method for correcting the pressure data to minimize this source of error. Coats[1] presents some examples where field-derived influence functions have been successfully used to predict future performance.

E. Marsal Method

The Marsal method[9] is a mathematical means of applying the Buckley-Leverett type analysis to a stratified reservoir. Field-measured water cuts (fraction of water in total fluid) are used in place of relative permeability data. The Marsal method is based on the Buckley-Leverett equation of linear flow derived in Section IV, Chapter 5-6:

$$\left(\frac{df_w}{dS_w}\right)_{S_w} = \frac{\Delta V_p}{\Delta W_e}, \qquad (21)$$

where $(df_w/dS_w)_{S_w}$ is the change in fraction of water flow with respect to water saturation at a given saturation; ΔV_p is the pore volume of the portion of the reservoir traversed by S_w during a given time interval; and ΔW_e is the total water influx during the same time interval. Observe the time required for a given water cut (f_w) to move from one row of wells to the next row in a field. Since f_w is a unique function of S_w, this observation will also establish the velocity of the S_w corresponding to the observed f_w. If the reservoir pore volume between the two rows of wells (ΔV_p) is known together with the total water influx during the time of travel (ΔW_e), we can evaluate $(df_w/dS_w)_{S_w}$ from equation (21). The evaluation can be used to predict the movement (Δx) of the same S_w (or f_w) during any future time period (Δt) if the average water influx rate (q) is known. The following form of the Buckley-Leverett equation is used:

$$\Delta x = \frac{q\Delta t}{\varphi A}\left(\frac{df_w}{dS_w}\right)_{S_w} \qquad (22)$$

If $(df_w/dS_w)_{S_w}$ is evaluated for a range of saturations as denoted by a range of water cuts, a profile of f_w versus distance in the reservoir can be predicted for any future time. Producing water cuts from existing wells can be forecast from such a profile.

Marsal showed that this technique can be used to predict the overall or total characteristics of a stratified reservoir if no flow occurs between the strata.

F. Simplified Water Influx Calculations

The Schilthuis method[11] for computing water influx represents the rate of water flow from aquifer to a reservoir as a series of steady-state steps. The method assumes that the rate of water influx is always proportional to the pressure difference between the aquifer and the reservoir, $p_b - p_R$. The cumulative water encroachment, W_e, at the end of the nth time period may be calculated by

$$W_e = C_S \sum_{j=1}^{j=n} (p_a - p_R)_j \, \Delta t_j, \qquad (23)$$

where C_S is an aquifer constant (similar to C) which must be evaluated from field performance. The time steps used are not necessarily of equal duration. The pressure difference, $(p_a - p_R)_j$, is the average differential pressure over the time period, Δt_j, between the pressure at the aquifer's outer limit and the prevailing reservoir pressure. It is usually assumed that the aquifer pressure p_a is equivalent to the initial reservoir pressure. This assumption is valid for an infinite-acting aquifer.

Another method for calculating the cumulative water influx, known as the modified Hurst method,[5] involves the following equation:

$$W_e = C_H \sum_{j=1}^{j=n} \frac{(p_a - p_R)_j}{\log t_j} \Delta t_j, \qquad (24)$$

where C_H is a constant related to the aquifer effectiveness and must be evaluated from influx history. This formula is similar to the previous one, except for the logarithm of time introduced in the denominator. This equation accounts approximately for the gradually expanding radius of drainage in the aquifer throughout the reservoir's history.

Both of these simplified formulas and the more complex unsteady-state equation [equation (3)] have the same general form. Therefore, either of the simplified formulas can be used to calculate water influx in the same way that the unsteady-state method is used in Part VI.B of this chapter.

VIII. EXAMPLE RESERVOIR STUDY: PREDICTED PERFORMANCE OF A WATER-DRIVE FIELD

Problem: Predict the future performance of a water-drive reservoir with the characteristics listed below if water injection is used to maintain the reservoir pressure at approximately 2000 psia. Available information includes the reservoir data, fluid characteristics data, and aquifer data summarized in Table II; curves relating B_o, R_s, and $1/B_g$ to reservoir pressure as shown in Fig. 16; and pressure production and water-invasion data for various times in history as shown in Table III. A separate study of the field production capacity has indicated the relationship with water influx shown in Fig. 17. Producing wells will be shut in or recompleted whenever they begin producing water. (That is, assume zero water production throughout.)

Solution: This problem consists of two parts: (1) prediction of future pressure behavior to 2000 psi, and (2) prediction of subsequent injection rates needed to maintain this pressure level. The steps involved in analyzing past performance and predicting future behavior, listed in Section VI, will be followed in these examples. The numbers used here coincide with the step numbers of Section VI.

A. Past Performance

1. Assemble available geologic, pressure, production, rock characteristics, and fluid characteristics data. These data are given in the problem statement.

2. Evaluate the original oil in place by a volumetric calculation, using data in Table II and Fig. 16. Studies which preceded this problem gave average values for pay thickness, porosity, and connate water as shown in Table II. Note especially that the connate water represents a volumetrically weighted average value because the connate water saturation would be very high near the original water-oil contact, but would decline to near the irreducible saturation near the top of the structure.

$$\begin{bmatrix}\text{Original Oil}\\ \text{in Place (STB)}\end{bmatrix} = \frac{7758\,Ah\bar{\varphi}\,(1-S_{wi})}{B_{oi}}$$

$$= \frac{7758(9977)(43)(0.165)(1-0.22)}{1.467}$$

$$= 292\ (10^6)\ \text{bbl.}$$

If solution-gas drive contributed appreciably to the recovery, a material-balance calculation could be used to check this value. However, for this reservoir, calculations would reveal that inherent errors are too great to accurately determine the original oil in place by material balance. Thus, the volumetric value of N will be used in this example.

TABLE II — Reservoir, Fluid, and Aquifer Data for Example Problem

Reservoir Data	
Area, acres	9977
Water-Oil Contact, ft. subsea	4339
Average Pay Thickness, ft.	43
Average Porosity, %	16.5
Average Connate Water, S_{wi}, %	22.0
Fluid Data	
Initial Pressure at 4200 ft. subsea datum, psia	2157
Reservoir Temperature, °F	174
Oil Saturation Pressure, psia	2080
Initial Oil Formation Volume Factor, res B/STB	1.467
Solution GOR, scf/STB	785
Oil Viscosity, cp	0.55
Oil Gravity, °API	39.5
Oil Compressibility, vol/vol/psi	26.6×10^{-6}
Aquifer Data	
Permeability to Water, md	1750
Porosity, %	16.5
Rock Compressibility, vol/vol/psi	4.0×10^{-6}
Water Compressibility, vol/vol/psi	3.0×10^{-6}
Water Viscosity, cp	0.3
Reservoir Periphery Open to Water Influx, degrees	360
Est. Avg. Gross Thickness, ft.	50

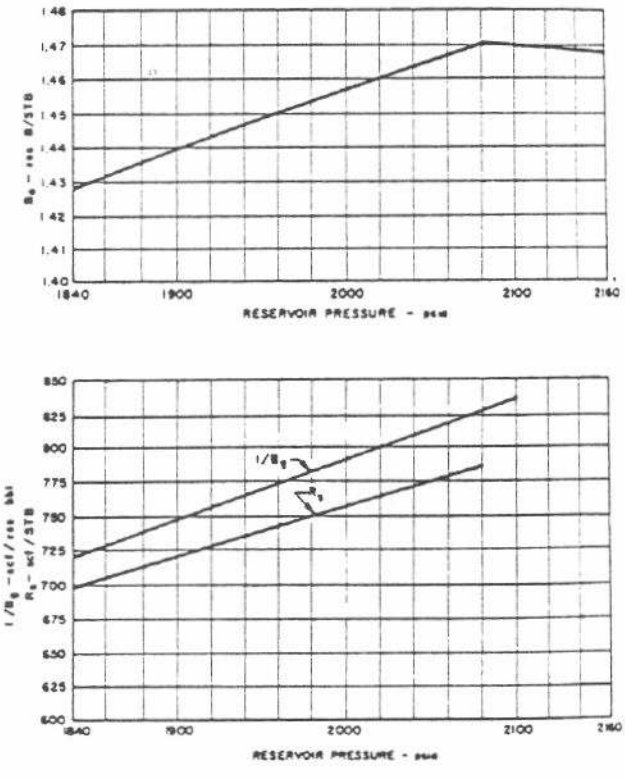

FIG. 16. PVT data for example problem.

3. Evaluate aquifer constants r_D and C.
   a. The first step in analyzing past history for

TABLE III — Past Production Data for Example Problem

Date	Oil Production, STB		Gas Production, Mcf		Average Reservoir Pressure, psia	Hydrocarbon Volume Invaded by Water, bbl
	Period	Cumulative (N_p)	Period	Cumulative		
9/1/61	0	0	0	0	2157	0
3/1/62	850,000	850,000	667,250	667,250	2151	2,010,000
9/1/62	2,600,000	3,450,000	2,041,000	2,708,250	2137	9,490,000
3/1/63	3,350,000	6,800,000	2,629,750	5,338,000	2129	19,900,000
9/1/63	3,500,000	10,300,000	2,747,500	8,085,500	2116	28,540,000
3/1/64	6,200,000	16,500,000	4,867,000	12,952,500	2086	47,470,000

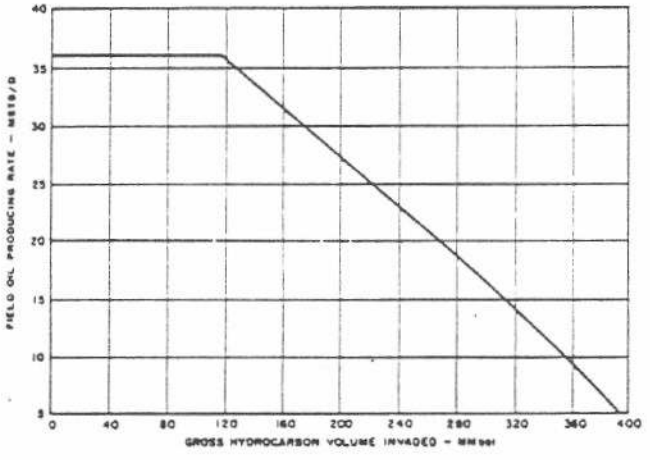

FIG. 17. Maximum oil production rate vs gross hydrocarbon volume invaded.

aquifer evaluation is to calculate the cumulative water influx by material balance at each of several dates at which the pressure and production are known. All measured pressures in this example are above the bubble point, so equation (1), solved for W_e, becomes

$$W_e = N(B_{oi} - B_o) - N B_{oi} \bar{c}_{f+w} (p_i - p) + N_p B_o + W_p B_w. \quad (1a)$$

For best accuracy, B_o is calculated rather than read from the curve of B_o versus pressure. The following equation is valid for B_o from the initial pressure to the bubble point:

$$B_o = B_{oi} [1 + c_o (p_i - p)]$$
$$= 1.467 [1 + 26.6 \times 10^{-6} (p_i - p)].$$

The value of $\bar{c}_{f+w}$ for the oil zone is determined from the following equation (Chapter 5-4):

$$\bar{c}_{f+w} = \frac{c_f + c_w S_{wi}}{1 - S_{wi}}.$$

Table II shows: $c_f = 4 \times 10^{-6}$; $c_w = 3 \times 10^{-6}$; and $S_{wi} = 22$ percent.

Thus:

$$\bar{c}_{f+w} = \frac{(4 \times 10^{-6}) + (3 \times 10^{-6})(0.22)}{(1 - 0.22)}$$
$$= 6 \times 10^{-6}/\text{psia}.$$

With this information we can now calculate W_e using equation (1a). For example, on March 1, 1964,

TABLE IV — Calculation of Past Water Influx by Material Balance

(1) Date	(2) Reservoir Pressure p, psia	(3) $(p_i - p)$, psia	(4) B_o	(5) Calculation of W_e (All values are bbl.) $N(B_{oi} - B_o)$	(6) $NB_{oi}\bar{c}_{f+w}(p_i - p)$	(7) $N_p B_o$	(8) W_e
9/1/61	2157	0	1.46700	0	0	0	0
3/1/62	2151	6	1.46723	— 67,200	15,400	1,247,100	1,164,500
9/1/62	2137	20	1.46778	—227,800	51,400	5,063,800	4,784,600
3/1/63	2129	28	1.46809	—318,300	72,000	9,983,000	9,592,700
9/1/63	2116	41	1.46860	—467,200	105,400	15,126,600	14,554,000
3/1/64	2086	71	1.46977	—808,800	182,500	24,251,200	23,259,900

Columns:

(1) and (2) from Table III.
(3) $p_i = 2157$ psia.
(4) $B_o = B_{oi}[1 + c_o(p_i - p)] = 1.46700[1 + 26.6 \times 10^{-6}(p_i - p)]$.
(5) $N(B_{oi} - B_o) = 292(10^6)(1.46700 - B_o)$.
(6) $NB_{oi}\bar{c}_{f+w}(p_i - p) = 292(10^6)\ 1.46700\ (6)\ 10^{-6}\ (p_i - p)$
$= 2570.2(p_i - p)$.
(7) N_p(from Table III) times B_o (Column 4).
(8) $W_e = N(B_{oi} - B_o) - NB_{oi}\bar{c}_{f+w}(p_i - p) + N_p B_o$.

when the pressure had declined to 2086 psia, and 16,500,000 stock-tank barrels of oil had been produced, the cumulative influx was:

$$W_e = 292(10^6)\,(1.467 - 1.46977)$$
$$- 292(10^6)\,(1.46700)\,(6)\,(10^{-6})\,(2157 - 2086)$$
$$+ 16{,}500{,}000\,(1.46977) + 0$$
$$= 23{,}259{,}900 \text{ barrels.}$$

Table IV shows the water influx calculation for all data points.

b. Column (8), Table V, shows in detail the calculation of $\Sigma \Delta p Q_{tD}$ at the end of each time interval for assumed r_D values of 5, 10, and ∞. The choice of r_D values is somewhat arbitrary, but logs from wells drilled near the field should give an idea of the extent of the aquifer. The first trial should probably be for $r_D = \infty$ and the next estimate can be based on the trend of C values (see Fig. 7).

c. The values of the apparent aquifer constant, C, determined at each history point for each of the aquifer ratio values are tabulated in Column (9) of Table V.

d. The C values for each r_D ratio are plotted against time in Fig. 18. The curves in Fig. 18 suggest that the actual aquifer-field ratio is between 5 and 10. For $r_D = 5$, the calculated C values are erratic but tend to increase with time, indicating r_D is too small. For

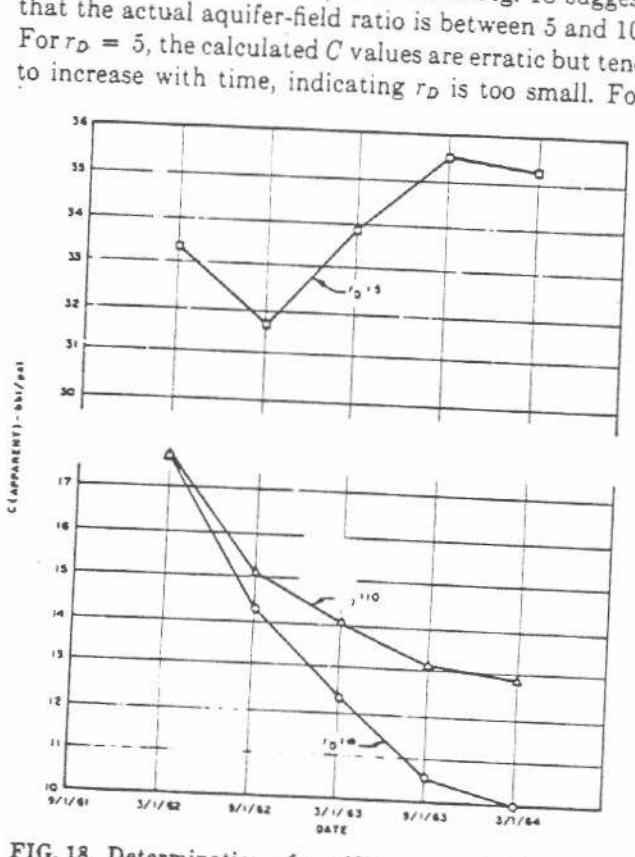

FIG. 18. Determination of aquifer constants (for example problem).

$r_D = 10$ and ∞, the C values continue to decli suggesting the aquifer is limited in size. Later pred tions will use Q_{tD} values for an r_D value of 10* and estimated C value of 12,500 (Fig. 18). However, t C value and r_D value should be checked periodica as more field history becomes available. As a rule thumb, a future prediction should cover a time spa not greater than the recorded history of the field.

The value of C should be calculated from th aquifer properties for comparison with the value dete mined from history. Using the aquifer propertie shown in Table II:

$$C = 1.12\, h\bar{\varphi}_a\, c_{f+w}\, r_R^2\, f_R$$
$$= (1.12)(50)(0.165)(7 \times 10^{-6})$$
$$(138.34 \times 10^{-6})(360/360)$$
$$= 8948,$$

where c_{f+w} for the aquifer is the sum of the rock and water compressibilities shown in Table II.

The C value of 8948 determined from aquifer properties is in good agreement with the value of 12,500 indicated by past history when we consider that aquifer factors such as h, c_{f+w}, and $\bar{\varphi}_a$ are generally known only approximately. The C value based on history should always be used, but the C value based on aquifer properties should be of the same order of magnitude (possibly no more than 50 percent in error) unless data for the aquifer are extremely meager. The above calculated C value (8948) supports the choice of $r_D = 10$ rather than $r_D = 5$, since the field history C value for $r_D = 5$ is about 35,000.

4. Evaluate the reservoir recovery efficiency, E_R.

a. To obtain this recovery efficiency, the cumulative net water influx calculated by material balance is divided by the observed hydrocarbon volume invaded by water (as observed in the field). E_R is given in Table VI.

b. The calculated average recovery efficiency for the five history points is 51.3 percent as shown in Table VI. However, the inherent inaccuracy of material balance for small pressure drops suggests that the efficiency for the earliest date (3-1-62) be deleted from the average. Under these circumstances, the average becomes 49.7 percent. We will use 50 percent in future calculations.

c. The last four calculated displacement efficiencies

* The Q_{tD} curves (Appendix B to Chapter 5-5) do not show a curve for r_D between 5 and 10, so $r_D = 10$ will be used. As more history becomes available, the choice between $r_D = 5$ and $r_D = 10$ should become more clear-cut.

TABLE V — Evaluation of Aquifer Constants

Date	(1) Reservoir Pressure, psia	(2) W_e, Mbbl	(3) t, days	(4) t_D	(5) Q_{tD} $r_D=5$	(5) Q_{tD} $r_D=10$	(5) Q_{tD} $r_D=\infty$	(6) $\bar{p}$, psia	(7) Δp_{avg}, psi	(8) $\Sigma\Delta pQ_{tD}$ $r_D=5$	(8) $\Sigma\Delta pQ_{tD}$ $r_D=10$	(8) $\Sigma\Delta pQ_{tD}$ $r_D=\infty$	(9) Aquifer Constant, C $r_D=5$	(9) Aquifer Constant, C $r_D=10$	(9) Aquifer Constant, C $r_D=\infty$
9/1/61	2157	0.0	0.0	0.0	0	0	0	2157	0	0	0	0	—	—	—
3/1/62	2151	1,164.5	182.5	42.2	11.5	22	22	2154	3	35	66	66	33,271	17,644	17,644
9/1/62	2137	4,784.6	365	84.5	12	32	38	2144	10	151	316	334	31,686	15,141	14,325
3/1/63	2129	9,592.7	547.5	126.5	12	39	52	2133	11	283	679	778	33,896	14,128	12,330
9/1/63	2116	14,554.0	730	169.0	12	43	66	2122.5	10.5	409	1102	1367	35,584	13,207	10,647
3/1/64	2086	23,259.9	912.5	211.0	12	45	82	2101	21.5	661	1806	2350	35,189	12,880	9,898

Columns

(1) Given in Table III.

(2) Calculated in Table IV.

(3) Cumulative time from start of production—days.

(4) Dimensionless time, $t_D = \dfrac{0.00633\,k_w}{\mu_w \overline{\varphi_a} c_{f+w} r_R^2} t = \dfrac{(0.00633)(1750)\,t}{(0.3)(0.165)(7\times10^{-6})(9977\times43{,}560)/\pi} = 0.231\,t$.

(5) Q_{tD} read at t_D from curve of r_D in Graphs I and II, Appendix B, Chapter 5-5. The r_D values are assumed.

(6) Average reservoir pressure during interval t_n to t_{n-1}: $\bar{p}_n = \dfrac{p_{n-1}+p_n}{2}$.

(7) Change in average pressure since previous interval: $\Delta p_{avg} = \bar{p}_{n-1} - \bar{p}_n$.

(8) $\Sigma\Delta pQ_{tD}$. Multiply each value of Δp by the Q_{tD} corresponding to the time over which the Δp has existed and sum the products, or use equation (3) of the text. For example, $\Sigma\Delta pQ_{tD}$ at 3/1/64 for $r_D = \infty$ is determined as follows:

$$(\Delta p \times Q_{tD})_n = \sum_{j=1}^{j=n} \Delta p_j Q_{(tD_n - tD_{j-1})}$$

$3 \times 82 = 246$
$10 \times 66 = 660$
$11 \times 52 = 572$ $\quad \Sigma\Delta pQ_{tD} = 2350$
$10.5 \times 38 = 399$
$21.5 \times 22 = 473$

(9) W_e divided by $\Sigma\Delta pQ_{tD}$ (Column 8) for each value of r_D.

TABLE VI — Calculation of Recovery Efficiency

Date	(1) Hydrocarbon Volume Invaded by Water, bbl	(2) Net Water Influx, bbl	(3) Recovery Efficiency Percent (Reservoir Basis)
3/1/62	2,010,000	1,164,500	57.9
9/1/62	9,490,000	4,784,600	50.4
3/1/63	19,900,000	9,592,700	48.2
9/1/63	28,540,000	14,554,000	51.0
3/1/64	47,470,000	23,259,900	49.0
		Average	51.3

Columns:

(1) Given in Table III.

(2) W_e calculated by material balance in Table IV.

(3) Recovery efficiency percent = (net water influx/water invaded hydrocarbon volume) 100.

in Table VI are substantially the same. Thus, no extrapolation of a trend into the future is indicated.

5. Evaluate the production capacity trends.

It is not necessary to evaluate the production capacity trends in this problem, since this has already been done. The results are given in Fig. 17.

B. Predicting Performance

Pressure predictions will be made to the time when the reservoir pressure drops to 2000 psia. Thereafter (as required by the problem) water will be injected to maintain this pressure constant and we will predict the amount of water to be injected during each time period.

1. Determine the production schedules to be employed in the prediction.

The production schedule, production rate versus cumulative influx (Fig. 17), will be used to predict capacity rates.

2. Assume a time interval for the prediction periods.

A time interval of six months is readily handled mathematically. We will use a time interval of six months (the same as that used in the analysis of the past history) for the first few years in the future, but at later times, the time interval will be enlarged to reduce the amount of calculation.

3. Estimate total withdrawals for a period.

Total production for each period is estimated from the capacity rate curve of Fig. 17. The capacity rate at the mid-point of a period is read at the estimated value of the HCV invaded at that time. The value of W_e to the start of the period will already be known from material balance calculation for the previous period (see Table VII). We must estimate influx for the next period, divide it by two, and add the result to W_e to the period start. Influx rates can be estimated from the preceding trend. Table VIII shows the estimation of oil production rates.

4. Estimate reservoir pressure at the end of the period.

To make the first estimate of a pressure at the end of an interval, the simplest approach is to make a straight-line extrapolation of the last few points of a plot of reservoir pressure versus time. For example, extrapolation of the history portion of the pressure plot of Fig. 19 gives an estimated pressure on September 1, 1964, of 2076 psia, which is very close to the calculated value of 2077 psia.

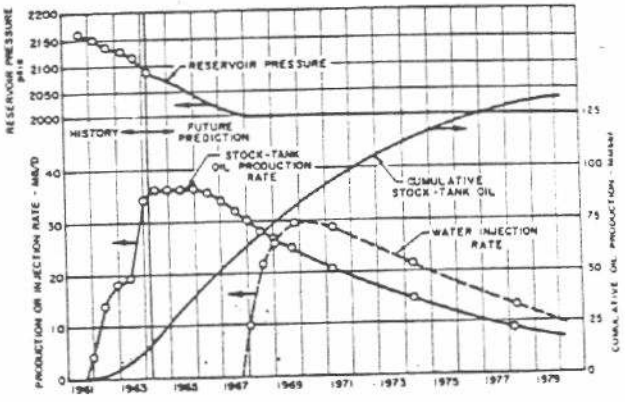

FIG. 19. Reservoir performance.

5. Calculate gross water influx at the end of the period by material balance.

The gross water influx on September 1, 1964, can now be calculated using the previously estimated oil production and pressure in the basic material balance equation:

$$W_e = N_p B_o - N_p R_s B_g + G_p B_g - N (B_o - B_{oi}) - N (R_{si} - R_s) B_g - N B_{oi} \bar{c}_{f+w} (p_i - p) + W_p B_w.$$

Note that above the bubble point, the second, third, and fifth terms of the right-hand side fall out since $N_p R_s B_g$ equals $G_p B_g$ and R_{si} equals R_s. The calculations are performed in Table VII.

6. Calculate gross water influx by the unsteady-state equation.

The gross water influx for the same date (September 1, 1964) is calculated by the unsteady-state equation. Influx values shown in Table IX are calculated from the following equation:

$$W_e = C \Sigma \Delta p \, Q_{tD}.$$

The calculation is carried out by using the same pressure as the one assumed for calculating W_e b

TABLE VII — Calculation of Future Water Influx by Material Balance

	(1)	(2)	(3)		(4)	(5)		(6) Fluid Properties at End of Interval			(7) W_e, M res B							
			Oil Production, MSTB		R_s, scf/ STB	Gas Production, MMscf		R_s, scf / STB	B_o, res B/ STB	$1/B_g$, scf/ res B								
Date	p, psia	$\bar{p}$, psia	ΔN_p	N_p	at $\bar{p}$	ΔG_p	G_p				N_pB_o	$N_pR_sB_g$	G_pB_g	$N(R_{si}-R_s)B_g$	$N(B_o-B_{oi})$	$NB_{oi}\bar{c}_{f+w}(p_i-p)^*$	W_p	$(W_e)_{mb}$
3/1/64**	2086	2101	6,200	16,500	785	4867	12,953	785	1.46977	831	24,251	15,587	15,587	—	809	182	0	23,260
9/1/64	2076	2081	6,570	23,070	785	5157	18,110	784	1.46933	827.8	33,897	21,877	21,877	533	681	208	0	32,475
	2077	2081.5			785	5157	18,110	784	1.4695	828.2	33,901	21,866	21,866	399	730	206	0	32,566
3/1/65	2056	2066.5	6,570	29,640	781	5125	23,149	777	1.4658	818.6	43,446	28,134	28,278	2,854	— 350	260	0	40,826
	2061	2069			782	5131	23,178	779	1.4667	820.9	43,473	28,127	28,235	2,134	— 88	247	0	41,288
	2062	2069.5			782	5131	23,178	779.5	1.4668	821.3	43,476	28,131	28,221	1,955	— 59	245	0	41,425
9/1/65	2050	2056	6,570	36,210	777	5105	28,283	775	1.4648	815.9	53,040	34,395	34,665	3,579	— 642	275	0	50,098
	2051	2056.5			777	5105	28,283	775	1.4650	816.3	53,048	34,378	34,648	3,577	— 584	272	0	50,053
3/1/66	2040	2045.5	6,570	42,780	773.4	5081	33,364	771.3	1.4630	812.4	62,587	40,616	41,068	4,924	—1168	301	0	58,982
	2037	2044			772.8	5077	33,360	770.2	1.4625	810	62,566	40,678	41,185	5,335	—1314	308	0	58,744
	2036	2043.5			772.6	5076	33,359	769.9	1.4623	809.5	62,557	40,687	41,209	5,447	—1372	311	0	58,693
9/1/66	2024	2030	6,400	49,180	767.7	4913	38,272	765.5	1.4603	804.1	71,818	46,819	47,596	7,081	—1956	342	0	67,128
	2023	2029.5			767.5	4912	38,271	765.1	1.4601	803.6	71,808	46,824	47,626	7,159	—2015	344	0	67,123
3/1/67	2010	2016.5	6,000	55,180	762.7	4576	42,847	760.4	1.4578	797.7	80,441	52,600	53,713	9,005	—2686	378	0	74,857
	2013	2018			763.3	4580	42,851	761.5	1.4583	799.1	80,469	52,584	53,624	8,587	—2540	370	0	75,092
9/1/67	2000	2006.5	5,800	60,980	759.1	4403	47,254	756.7	1.4561	793.2	88,793	58,174	59,574	10,418	—3183	403	0	82,555
3/1/68	2000	2000	5,550	66,530	756.7	4200	51,454	756.7	1.4561	793.2	96,874	63,468	64,869	10,418	—3183	403	0	90,637
9/1/68	2000	2000	5,200	71,730														98,209
3/1/69	2000	2000	4,900	76,630														105,344
3/1/70	2000	2000	8,900	85,530														118,303
3/1/72	2000	2000	15,200	100,730														140,435
3/1/76	2000	2000	23,500	124,230														174,653
			22,000	122,730														172,469
3/1/80	2000	2000	13,100	135,830														191,544

These data are not required for calculating $(W_e)_{mb}$ as long as reservoir pressure remains constant at 2000 psia. At constant pressure,

$$\Delta W_e = B_e(\Delta N_p) = 1.4561\ \Delta N_p$$
$$W_e = 90{,}637 + \Sigma\Delta W_e$$

*Rock and water compressibility in the oil zone is included, but generally this term can be omitted at pressures below the bubble point.

**Known from past history analysis—see Table IV.

Columns:

(1) Reservoir pressures at end of interval—guess from plot of pressure versus time of history and previously calculated points, Fig. 19, until it reaches 2000 psia, at which value it is fixed by the problem.

(2) Arithmetic average reservoir pressure for interval $\frac{p_{n-1} - p_n}{2}$.

(3) ΔN_p is from Table VIII, Column (6): $N_p = \Sigma\Delta N_p$.

(4) From Fig. 16 at $\bar{p}$. [For increased accuracy, the following equation was derived from Fig. 16: $R_s = 775 - 0.366(2050 - \bar{p})$.]

(5) $\Delta G_p = \Delta N_p(R_s \text{ at } \bar{p})$; $G_p = \Sigma\Delta G_p$.

(6) From Fig. 16 at p: $R_s = 775 - 0.366(2050 - p)$; $B_o = 1.470 - 0.000174(2080 - p)$; and $1/B_g = 825 - 0.4545(2070 - p)$.

(7) $W_e = N_pB_o - N_pR_sB_g + G_pB_g - N(R_{si} - R_s)B_g - N(B_o - B_{oi}) - NB_{oi}\bar{c}_{f+w}(p_i - p) + W_p$
$= N_pB_o - N_pR_sB_g + G_pB_g - 292(10^4)(785 - R_s)B_g - 292(10^4)(B_o - 1.467) - 2570(2157 - p)$.

TABLE VIII — Evaluation of ΔN_p

Date	(1) $\left(\frac{\Delta W_e}{2}\right)_{n-1}$, MMB	(2) $(W_e)_{avg}$, MMB	(3) Est. Avg. HCV Invaded, MMB	(4) Est. Avg. q_o, MSTB/D	(5) Δt, days	(6) Est. ΔN_p, MSTB	(7) $(W_e)_{mb}$, MMB	(8) $(W_e)_{avg}$, MMB	(9) Avg. HCV Invaded, MMB	(10) Avg. Capacity q_o, MSTB/D	(11) ΔN_p, MSTB
9/1/63	—	—	—	—	—	—	14.6	—	—	—	—
3/1/64	—	—	—	—	—	—	23.3	—	—	—	—
9/1/64	4.35	27.65	55.30	36.0	182.5	6,570	32.6	27.95	55.90	36.0	6,570
3/1/65	4.65	37.25	74.50	36.0	182.5	6,570	41.4	37.00	74.00	36.0	6,570
9/1/65	4.40	45.80	91.60	36.0	182.5	6,570	50.1	45.75	91.50	36.0	6,570
3/1/66	4.35	54.45	108.90	36.0	182.5	6,570	58.7	54.40	108.80	36.0	6,570
9/1/66	4.30	63.00	126.00	35.0	182.5	6,400	67.1	62.90	125.80	35.0	6,400
3/1/67	4.20	71.30	142.60	32.9	182.5	6,000	75.1	71.10	142.20	32.9	6,000
9/1/67	4.00	79.10	158.20	31.8	182.5	5,800	82.6	78.85	157.70	31.8	5,800
3/1/68	3.75	86.35	172.70	30.4	182.5	5,550	90.6	86.60	173.20	30.4	5,550
9/1/68	4.00	94.60	189.20	28.5	182.5	5,200	98.2	94.40	188.80	28.5	5,200
3/1/69	3.80	102.00	204.00	26.8	182.5	4,900	105.3	101.75	203.50	26.8	4,900
3/1/70	7.10*	109.10	218.20	24.4	365	8,900	118.3	111.80	223.60	24.5	8,943
3/1/72	13.00*	124.80	249.60	20.8	730	15,200	140.4	129.35	258.70	21.0	15,330
3/1/76	22.10*	151.45	302.90	16.1	1460	23,500	174.7	157.55	315.10	14.2	20,732
3/1/76	—	—	—	15.1**	1460	22,000	172.5	156.45	312.90	15.0	21,750
3/1/80	15.75	188.25	376.50	9.0	1460	13,100	191.5	182.00	364.00	9.0	13,100

*$(\Delta W_e)_{n-1}$ is used when the time interval is double the preceding interval.

**Average of Columns 4 and 10 for the previous trial for this time period.

Columns:

(1) $(\Delta W_e/2)_{n-1} = [(W_e)_{n-1} - (W_e)_{n-2}]/2$ where W_e is read from Col. 7.

(2) Est. $(W_e)_{avg} = (\Delta W_e/2)_{n-1} + (W_e)_{n-1}$.

(3) Estimated Average Hydrocarbon Volume Encroached = Est. $(W_e)_{avg}/E_R$ = Est. $(W_e)_{avg}/0.5$.

(4) Read from Fig. 17 at Est. Avg. HCV Encroached.

(5) Length of period between successive dates.

(6) Estimated ΔN_p = (Avg. q_o)(Δt).

(7) From (7) of Table VII.

(8) $(W_e)_{avg} = [(W_e)_n + (W_e)_{n-1}]/2$.

(9) Average HCV Encroached = $(W_e)_{avg}/E_R = (W_e)_{avg}/0.5$.

(10) Read from Fig. 17 at Avg. HCV Encroached.

(11) ΔN_p = (Avg. Cap. q_o)(Δt). This must be within 10 percent of Est. ΔN_p (Col. 6); otherwise, reestimate ΔN_p in Col. 6.

TABLE IX — Calculation of Unsteady-State Water Influx and Water Injection

Date	(1) t, days	(2) t_D	(3) Q_{tD}	(4) p, psia	(5) $\bar{p}$, psia	(6) Δp_{avg}, psia	(7) $\Sigma\Delta pQ_{tD}$ ($r_D = 10$)	(8) $(W_e)_{us}$, Mbbl	(9) $(W_e)_{mb}$, Mbbl	(10) W_i, Mbbl	(11) ΔW_i, Mbbl	(12) i_w, B/D
9/1/64	1095	254	47	2076	2081.0	20	2622.5	32,781	32,475			
				2077	2081.5	19.5	2611.5	32,644	32,566	0	0	0
3/1/65	1277.5	296	48.5	2056	2066.5	15.0	3376.0	42,200	40,392			
				2061	2069	12.5	3321.0	41,513	40,841	0	0	0
				2062	2069.5	12	3310.0	41,375	41,425	0	0	0
9/1/65	1460	338	49	2050	2056	13.5	4019.5	50,244	50,098			
				2051	2056.5	13	4008.5	50,106	50,053	0	0	0
3/1/66	1642.5	380	49.5	2040	2045.5	11.0	4638.5	57,981	58,982			
				2037	2044	12.5	4671.5	58,394	58,744			
				2036	2043.5	13	4682.5	58,531	58,693	0	0	0
9/1/66	1825	423	50	2024	2030	13.5	5348.8	66,860	67,143			
				2023	2029.5	14	5359.8	66,998	67,123	0	0	0
3/1/67	2007.5	467.7	50	2010	2016.5	13	6033.3	75,416	74,857			
				2013	2018	11.5	6000.3	75,004	75,092	0	0	0
9/1/67	2190	510.3	50	2000	2006.5	11.5	6620.0	82,750	82,555	0	0	0
3/1/68	2372.5			2000	2000	6.5	7111.3	88,891	90,637	1,746	1,746	9,567
9/1/68	2555			2000	2000	0	7401.3	92,516	98,209	5,693	3,947	21,627
3/1/69	2737.5			2000	2000	0	7583.5	94,794	105,344	10,550	4,857	26,614
3/1/70	3202.5			2000	2000	0	7751.8	96,898	118,303	21,405	10,855	29,740
3/1/72	3932.5			2000	2000	0	7846.8	98,085	140,435	42,350	20,945	28,692
3/1/76	5392.5			2000	2000	0	7850.0	98,125	172,469	74,371	32,021	21,932
3/1/80	6752.5			2000	2000	0	7850.0	98,125	191,544	93,419	19,048	13,047

Columns:

(1) Cumulative time from production start, days.

(2) Dimensionless time = 0.544 t (where t is in days); see Table V, footnote (4).

(3) Read at t_D from curve for $r_D = 10$ in Graph II, Appendix B, Chapter 5-5.

(4) Estimated pressure at end of interval — from Table VII, Col. 1; 2000 psia is to be maintained by water injection.

(5) Average reservoir pressure for interval $= \dfrac{p_{n-1} + p_n}{2}$.

(6) Change in average pressure from preceding interval $= (\bar{p})_{n-1} - (\bar{p})_n$.

(7) $\Sigma\Delta pQ_{tD}$. Multiply each value of Δp (including the past history) by the Q_{tD} value corresponding to the time over which Δp has existed. From equation (3) in text,

$(\Sigma\Delta pQ_{tD})_n = \sum_{j=1}^{j=n} \Delta p_j Q_{(t_{D_n} - t_{D_{j-1}})}$. See Table V, footnote (8) for example step-wise calculation.

(8) Unsteady state water influx = 12,500 $\Sigma\Delta pQ_{tD}$.

(9) Material balance water influx from Col. 7 of Table VII, and Col. 8 of Table IV.

(10) For pressures down to 2000 psia, $W_i = 0$; difference between Col. 8 and Col. 9 is water injected to maintain $p = 2000$ psia.

(11) ΔW_i = water injected during the period $= (W_i)_n - (W_i)_{n-1}$.

(12) $\Delta W_i/(t_n - t_{n-1})$.

material balance and by using Q_{tD} functions as evaluated from the past history.

7, 8. Compare the two values of water influx.

If the correct pressure was assumed, the water influx by material balance (Table VII) will equal the water encroachment by unsteady state (Table IX). If the difference between the two values is greater than 200,000 barrels,* a new pressure is assumed and the water influx calculations are repeated.

To illustrate the iteration on pressure, consider the calculation for September 1, 1964, when pressure is estimated as 2076 psia. W_e by material balance is 32,475 Mbbl (Table VII) and W_e by unsteady state is 32,781 Mbbl (Table IX). Although the difference is very small, it is not within our established error limit of 200 Mbbl. Therefore, pressure is reestimated one psi higher (2077 psia), and the calculations are repeated. The latter pressure gives $(W_e)_{mb} = 32{,}566$ Mbbl, and $(W_e)_{us} = 32{,}644$ Mbbl. Since the difference is within acceptable limits, 2077 psia is accepted as the correct prediction of pressure for September 1, 1964, and 32,566 Mbbl (the material balance W_e) is taken as the correct water influx.

9. Determine the position of the water-oil contact at the end of the period.

As noted previously in step B.3, the net water influx to any time is used to determine the gross hydrocarbon volume invaded at that time by using the recovery efficiency (50 percent) indicated by past history. For example, on September 1, 1964, the cumulative water influx is 32,566 Mbbl. Thus:

Gross Hydrocarbon

$$\text{Volume Invaded} = W_e/E_R$$
$$= 32{,}566 \text{ Mbbl}/0.5$$
$$= 65{,}132 \text{ Mbbl.}$$

10. Check the producing rate used for the period.

The average producing rate used for the period should be checked on Fig. 17 using the invaded hydrocarbon volume determined in the preceding step. On Fig. 17, read the average producing rate at the mid-point of the period using the average of the HCV's invaded at the start and at the end of the period. An exact check of the average rate is not required. Predicted producing rates are not precise, so if the rate checks within 10 percent, it is acceptable. Table VIII describes a procedure for estimating the producing rate for a period and for checking this rate based on the HCV invaded during the period.

11. Steps B.3 through B.9 are repeated for each future time period with little difference in the procedure except that once the pressure reaches 2000 psia, the pressure is fixed. After that time, W_e by material balance represents the total water encroachment necessary to maintain the pressure at 2000 psia, and W_e by unsteady state is the natural water influx. The effective injection necessary to maintain the 2000 psi pressure is the difference between W_e by material balance and W_e by unsteady state. Total water encroachment, natural influx, and injection are calculated and shown in Table IX. Actual injection will probably have to exceed the injection volumes shown because part of the injected water will not effectively enter the oil zone. Generally, 10 to 30 percent of the injected water is not effective. The predicted reservoir performance is shown graphically in Fig. 19.

*The permissible error is governed by the nature of the problem. Often the acceptable error is taken as 0.5 to 1.0 percent. The error limit of 200 Mbbl in this problem is based on the accuracy of the pressure measurements. A pressure error of one psia may introduce an error of 200 Mbbl.

REFERENCES

1. Coats, K. H., et al.: "Determination of Aquifer Influence Functions from Field Data," *Jour. Pet. Tech.*, December 1964, p 1417.

2. Dietz, D. N.: "A Theoretical Approach to the Problem of Encroaching and By-Passing Edge Water," *Proc. Konikl. Ned.-Akad. Weienschap*, Series B, v. 56, 1953, pp 83ff.

3. Frick, T. C., Editor-in-Chief: *Petroleum Production Handbook*, McGraw-Hill, New York, 1962.

4. Guthrie, R. K., and Greenberger, M. H.: "The Use of Multiple-Correlation Analysis for Interpreting Petroleum-Engineering Data," *API Drlg. & Prod. Pract.*, 1955.

5. Hurst, W.: "Water Influx Into a Reservoir and Its Application to the Equation of Volumetric Balance," *Trans. AIME*, v. 151, 1943, p 57.

6. Hurst, W., and Van Everdingen, A. F.: "The Application of the LaPlace Transformation to Flow Problems in Reservoirs," *Trans. AIME*, v. 186, 1949, p 305.

7. Hutchison, T. S., and Sikora, V. J.: "A Generalized Water-Drive Analysis," *Jour. Pet. Tech.*, July 1959, p 169.

8. Joslin, W. J.: "Applying the Frontal-Advance Equation to Vertical Segregation Reservoirs," *Jour. Pet. Tech.*, January 1957, p 87.

9. Marsal, D.: "Mathematical Treatment of Water Invasion of Oil-Bearing Formations," Paper, DGM Annual Meeting Berlin, Oct. 11, 1957, *Erd. Kohle*, v. 10, Dec. 1957, pp 825-6.

10. "Predicting Residual Oil," *Humble Production Research Bulletin*, Oct.-Dec. 1962, pp 6-10.

11. Schilthuis, R. J.: "Active Oil and Reservoir Energy," *Trans. AIME*, v. 118, 1936, p 33.

12. Welge, H. J.: "A Simplified Method for Computing Oil Recovery by Gas or Water Drive," *Trans. AIME*, v. 95, 1952, p 91.

13. Wooddy, L. D., Jr., and Moore, W. D.: "Performance Calculations for Reservoirs with Natural or Artificial Water Drives," *Jour. Pet. Tech.*, August 1957, p 245.

CHAPTER 3-6

Gas-Cap and Combination-Drive Reservoirs

CONTENTS

I. INTRODUCTION

ıe three basic producing mechanisms for conven-
ıl oil recovery are solution-gas drive, water drive,
gas-cap drive. Most reservoirs produce by a
bination of two or more of these drives and are
gnated "combination-drive reservoirs." This
ıter discusses the engineering techniques used to
uate combination-drive reservoirs and to make
ormance predictions for them. It also discusses
ial techniques applicable to gas-cap-drive reser-
s. Since gravity forces may be effective in increas-
the efficiency of the basic drive mechanisms, the
culation methods also include a treatment of
vitational segregation. The techniques discussed in
s chapter are applicable to any combination of
tural water drive, flank water injection, gas-cap
ve, crestal gas injection, and solution-gas drive.

The main steps in performing a combination-drive
servoir study are as follows:

1. Assemble basic reservoir, production, and pressure data required for the analysis.
2. Determine the original oil in place, the original gas in place, and the distribution of reservoir fluids.
3. From laboratory tests and field data, determine the recovery efficiencies for the water and gas-cap displacements. The data may include residual oil saturation after water displacement, residual oil saturation after gas displacement, water-oil relative permeability curves, gas-oil relative permeability curves, water-oil and gas-oil capillary pressure curves, and the factors affecting the volumetric efficiency of the gas-cap and water displacements.
4. Analyze the reservoir performance for the known history to obtain or verify the data of steps 2 and 3.
5. Predict future performance for several possible operating plans.
6. Apply economic analyses based on predicted reservoir performance and determine the most economically attractive depletion program.

In this chapter, steps 1 through 5 above will be discussed in detail. The final step is covered in pter 5-1, Economic Analyses.

A basic, detailed stepwise technique for predicting pool-wide behavior is summarized in Section VI and illustrated with an example in Section VIII of this chapter. Although this basic method is not intended to handle all possible situations, it illustrates the principles of combination-drive reservoir analysis and provides a foundation for modifications to meet particular problems. In this chapter, we will also discuss alternative methods for handling certain phases of combination-drive studies. In selecting the particular techniques to be used, the engineer should be guided by the quality of data available, the time and money allotted to complete the study, and the availability of a high-speed computer.

II. GAS-CAP AND COMBINATION-DRIVE RESERVOIR CHARACTERISTICS

This section summarizes some of the main features of gas-cap and combination-drive reservoirs. Gas-cap drive is the producing mechanism under which a volume of free gas in the upper part of the structure expands into the oil zone to displace oil downdip toward producing wells. The gas-cap-drive reservoir is usually characterized by a slow but fairly constant rate of decline of reservoir pressure with cumulative production. It may also be characterized by the production of substantial and increasing quantities of gas from wells that produce from the part of the reservoir invaded by the encroaching gas. In most cases, however, these wells are shut in or worked over to reduce free-gas production and conserve reservoir energy. The uniformity and effectiveness of oil displacement during the initial phase of gas-cap encroachment depend on the rate of gas advance. Therefore, it may sometimes be feasible to restrict the production rate to receive maximum benefit from gas-cap drive. Reservoir pressure maintenance by gas or water injection is often advisable to maintain well productivity and increase ultimate recovery.

In a reservoir with a gas cap but no water drive, reservoir pressure must drop to permit the gas cap to expand. Since the oil is initially at its saturation pressure, this drop in pressure will permit gas to come out of solution. Therefore, solution-gas drive will always be associated with the gas-cap drive mechanism. The larger the volume of gas-cap gas in relation to the volume of oil in place, the less will be the pressure drop in the oil zone per unit of oil produced. Therefore, the larger the relative size of the gas cap, the less will be the significance of solution-gas drive in the reservoir. A gas-cap drive is most effective if high vertical permeability allows gas released in the oil zone to rise into the cap.

In a reservoir with water drive but with no gas cap, the reservoir pressure must drop for the water to enter the reservoir. Thus, there is also a possibility of solution-gas drive in combination with a water drive. Dissolved gas will be liberated from solution in the oil if the initial reservoir pressure equals the bubble-

point pressure. If the initial pressure is greater than the bubble-point pressure, the reservoir will initially produce only by expansion of the oil, rock, and water; and gas will remain in solution until reservoir pressure declines to the bubble point. The more effective the water drive, the less dominant will be the solution-gas or expansion drive because the less will be the decline in reservoir pressure. In reservoirs with efficient gravity segregation, the gas released from solution in the oil migrates to the upper part of the formation where it forms a secondary gas cap. As reservoir pressure declines, this gas expands to produce oil by secondary gas-cap drive.

Oil displacement by a combination of water, gas-cap, and solution-gas drives involves movement into the oil zone of water from the aquifer and gas from the gas cap at the same time that gas is liberated from solution in the oil. The degree to which reservoir pressure is maintained as the reservoir is produced depends upon many factors. Among these are: (1) the strength of the water drive as determined by the size and permeability of the aquifer; (2) the volume of the gas cap compared with the volume of the oil zone; (3) the rate of production; and (4) the amount of reservoir energy lost through producing large quantities of free gas and water.

The efficiencies of oil recovery by solution-gas drive and by water drive are discussed in Chapters 3-4 and 3-5, respectively. The efficiency of oil recovery by gas displacement is influenced by the residual oil saturation, flow velocities, and the volumetric sweep efficiency. In reservoirs where conditions favor gravity segregation (i.e., high permeability, low oil viscosity, vertical flow, low flow velocity, etc.), gas-cap-drive recovery may be 70 to 80 percent of the original oil in place. In thin, horizontal reservoirs, where gravity segregation has little chance to aid recovery, gas-cap drive will normally yield only 30 to 40 percent of the initial oil. Under such circumstances, the adverse mobility ratio of gas to oil results in low volumetric sweep efficiency, and thus in low recovery. A gas cap can overrun the oil along the reservoir flank if the gas-oil interface advances too fast. If the rate of advance is below the critical rate, the Deitz method (see Chapter 3-5) can be used to predict the tilt of the gas-oil contact. Table I summarizes the oil content and recovery data for 15 large combination-drive reservoirs in Exxon's worldwide operations. As shown in Table I, recoveries from typical gas-cap and combination-drive reservoirs range from 30 to 68 percent. The average recovery efficiency for the 15 fields shown is about 52 percent.

Gas-cap shrinkage and the subsequent migration of oil into this originally oil-free region of the reservoir should be avoided. When the gas cap shrin portion of the migrating oil will be perman trapped in the gas cap as residual oil, the reducing the total oil recoverable from the reser Gas-cap shrinkage can result from excess fre withdrawals in a combination-drive reservoir, pa ularly where an active water drive is present. M rial balance calculations of gas-cap volume ve time will indicate whether the gas cap is shrinkin expanding. It is also wise to periodically check gas-cap shrinkage directly by neutron log or by o direct measurements of the gas-oil contact position

III. BASIC RESERVOIR AND AQUIFER DATA NEEDED FOR STUDIE

This section discusses the data ordinarily nee for a combination-drive reservoir study. Much of t information can be estimated empirically or analogy. Also, many sound engineering decisions be reached without complete data.

In using the basic analysis technique described this chapter, the oil reservoir is generally consider to be a unit having average values of porosit permeability, and other reservoir properties. Howe er, if core analysis data show significant differenc in sand quality between the gas cap and aquife these differences must be considered. Usually, a average value of pressure is assumed to apply for a entire field at a given time. If there is pronounce structural relief in the reservoir or if for any othe reason there is a significant difference between gas cap pressure and the average oil-zone pressure, thi difference should be taken into account in materia balance calculations. When the pressure difference are significant, the volumetric behavior of the gas cap and the oil zone should be computed on the basis of their respective average pressures.

A structural map and cross section of a typical combination-drive reservoir are shown in Fig. 1. The figure also illustrates some of the data requirements for the field. A complete listing of desirable data follows:

A. Hydrocarbon Reservoir Characteristics

1. Average porosity, $\bar{\varphi}_R$, (see Chapters 1-2, Rock Properties, and 1-3, Reservoir Stratification and Volume).
2. Connate water distribution (see Chapter 1-9, Fluid Distributions).
3. Average absolute permeability, $\bar{k}$, md (see Chapters 1-2 and 1-3).
4. Depth of water-oil contact (see Chapter 1-9).
5. Depth of gas-oil contact (see Chapter 1-9).

TABLE I. — Data from Selected Gas-Cap and Combination-Drive Reservoirs

Type of Reservoir	Date of Initial Production	Principal Producing Mechanisms	Oil Characteristics		Formation Characteristics			Original Oil in Place, MMSTB	Recovery Factor, % OIP	Cum. Prod. to 3/1/64, MMSTB	1964 Prod. Rate, STB/D	Avg. Depletion Rate to 3/1/64, % OIP/yr.
			Gravity, °API	Viscosity, cp	Avg. Perm., md	Avg. Porosity, %	Avg. Connate Water, %PV					
A. Sandstone	1926	Secondary gas cap and gas inj.	36	1.1	1000	22.0	15.0	661	60	328	25,000	2.2
B. Sandstone	1938	Secondary gas cap, flank water, and gas and water injection	24	3.5	1700	31.5	19.0	4,208	62	1300	220,000	1.9
C. Sandstone	1939	Secondary gas cap and gas inj.	25-31	0.8-2.0	975	20.4	12.4	2,102	53	510	100,000	1.8
D. Sandstone	1942	Secondary gas cap and gas inj.	29	2-6	108	10.5	9.0	675	65	200	45,000	2.0
E. Sandstone	1945	Secondary gas cap and gas inj.	22-34	0.7-2.8	750	22.0	15.0	2,524	59	627	186,000	2.2
F. Sandstone	1945	Secondary gas cap	26	2.1	158	14.7	17.3	1,192	35	105	11,000	1.4
G. Sandstone	1945	Secondary gas cap	22	4.5	174	16.0	19.0	787	30	44	7,000	1.0
H. Sandstone	1951	Secondary gas cap and gas inj.	23	3	786	21.4	15.0	507	50	47	15,000	1.4
I. Sandstone	1954	Secondary gas cap and flank water	24	8	1900	31.8	24.0	1,102	37	62	21,000	1.5
J. Sandstone	1954	Secondary gas cap and flank water	28	0.6	1245	24.0	20.0	121	55	25	10,000	3.8
K. Sandstone	1954	Secondary gas cap	26	2	148	18.0	22.0	145	51	2	1,000	0.3
L. Sandstone & Limestone	1962	Gas cap and flank water	38	0.4	150	14.5	12.0	1,440	50	22	55,000	1.5
M. Limestone	1946	Secondary gas cap, flank water, and gas and water injection	37	0.4	410*	21.0	7.0	16,000	55	2000	380,000	1.3
N. Limestone	1947	Gas cap, bottom water, and gas and water injection	39	0.8	3-3000*	15.7	10.0	296	68	143	19,700	4.2
O. Limestone	1951	Secondary gas cap and flank water	37	0.7	308*	15.5	10.0	30,000	55	1550	380,000	0.7

*Actual permeability is much higher than the core analysis values shown.

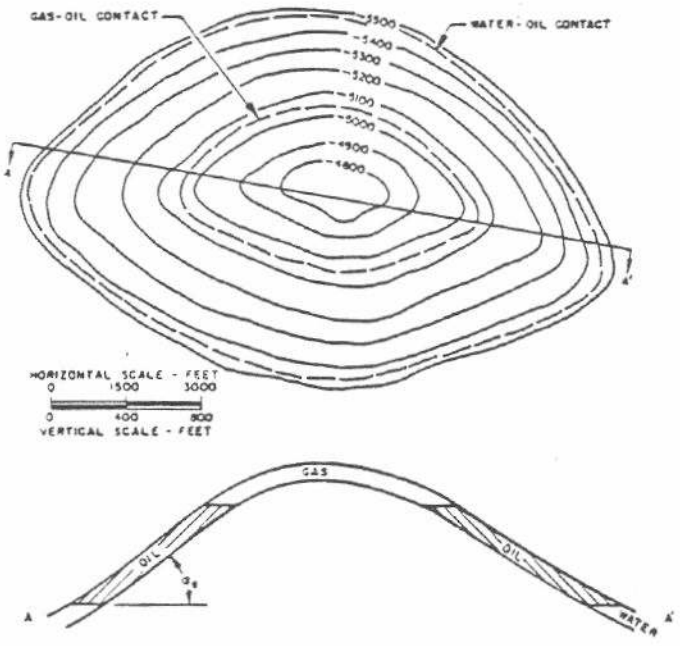

FIG. 1. Typical combination-drive reservoir.

6. Hydrocarbon volume vs depth curve (see Chapter 1-3).
7. Average angle of dip of the formation, α_d, degrees (see Fig. 1).
8. Original oil in place, N, stock-tank barrels (see Section IV of this chapter).
9. Original gas in place, G, scf (see Section IV).
10. Average radius of the hydrocarbon-bearing reservoir, r_R, ft.
11. Reservoir periphery open to water influx, θ, degrees.
12. Average area exposed to influx of water, A, sq. ft.

B. Aquifer Characteristics

1. Effective permeability to water, k_w, md (see Chapter 1-2).
2. Net formation thickness, h_a, ft (see Chapter 1-3).
3. Average radius of the aquifer, r_a, ft.
4. Average porosity, $\overline{\varphi}_a$ (see Chapters 1-2 and 1-3).

C. General Reservoir Rock Properties

1. Relative permeability to oil and water vs water saturation.
2. Water-oil relative permeability ratio vs water saturation.
3. Relative permeability to gas and oil vs oil saturation.
4. Gas-oil relative permeability ratio vs oil sa tion.
5. Drainage capillary pressure vs water satura
6. Imbibition capillary pressure vs water sa tion.
7. Rock compressibility, c_f, vol/vol/psi.

D. Reservoir Fluid Properties (see Chapter 1

1. Flash liberation data.
2. Differential liberation data.
3. Gas volume factor vs pressure, B_g vs p.
4. Oil viscosity vs pressure, μ_o vs p.
5. Gas viscosity vs pressure, μ_g vs p.
6. Water viscosity, μ_w.
7. Specific gravity of the oil at reservoir condi with respect to fresh water, γ_o.
8. Specific gravity of the water at reservoir ditions with respect to fresh water, γ_w.
9. Specific gravity of the gas at reservoir condi with respect to fresh water, γ_g.
10. Compressibility of undersaturated oil, c_o, vol/psi.
11. Water compressibility, c_w, vol/vol/psi.

E. Reservoir Production Data (Oil, Water, Gas) by Wells

F. Reservoir Pressure Data for Preparing baric Maps at Various Dates to Ob Average Reservoir Pressures (see Cha 1-6)

G. Maps Showing the Water-Oil Ratio Statu the Wells at Various Times in the His of the Reservoir

H. Water Influx Rates for Neighboring P Producing from the Same Formation (will permit accounting for possible in ference effects between reservoirs.)

IV. ANALYSIS OF PAST PERFORMAN

The known history of combination-drive reser can be analyzed to determine many of the rese parameters listed above and to determine the e tiveness of the different producing mechanisms. basic types of calculations are employed: (1) d mining original fluids in place; (2) evaluating aquifer constants; (3) calculating the efficiencie the gas-cap and water displacements; (4) deter ing the reservoir production capacity; and (5) uating individual drive indexes. When making n

l balance calculations on a field with a very thick zone, use the material balance technique for rtially undersaturated reservoirs (see Chapter 5-4, aterial Balance).

. Original Fluids in Place

The most reliable method for the early determiation of the volumes of fluids originally in place is e volumetric method, which is discussed in detail in hapter 1-3. By the time the reservoir has expericed a sizable pressure drop (say 200 psi or more), aterial balance calculations should be used to check ese volumetric calculations. As an aid in reservoir erformance calculations, it is often convenient to lot the original oil-zone and gas-cap hydrocarbon olumes as a function of subsea depth. An example of uch a hydrocarbon volume versus depth curve is

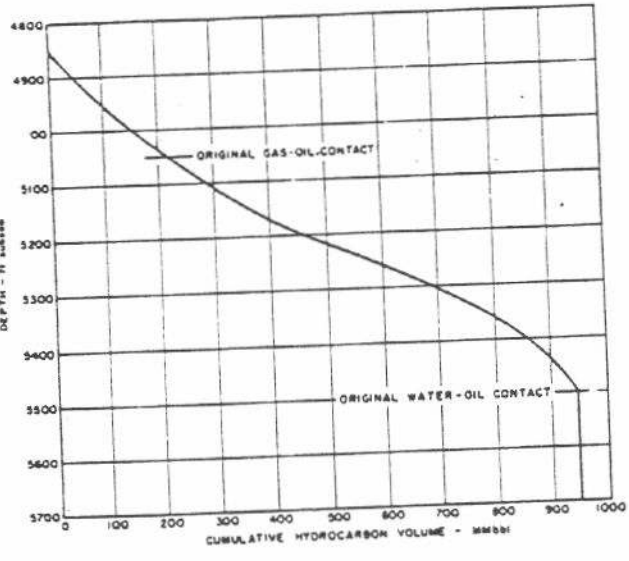

FIG. 2. Example hydrocarbon volume-depth curve.

shown in Fig. 2. The hydrocarbon volume-depth curve accounts for both water-saturation distribution and reservoir pore volume distribution above the water-oil contact.

Whenever volumetric data are unavailable or of doubtful value, the material balance method may be used to estimate the original oil and gas in place. Material balance requires accurate pressure, production, and fluid property data. Extreme caution should used with this method, since the results are very sensitive to the accuracy of fluid property and pressure data. In applying this method to a combination-drive reservoir, the accuracy is greatly improved if the ratio of the initial reservoir gas-cap volume to the initial reservoir oil-zone volume is used. This ratio, m, can usually be established from isopach maps based on production tests and well logs. If porosity and connate water saturation do not differ greatly between the gas cap and oil zone, the ratio, m, can be determined more accurately than the actual gas-cap or oil-zone hydrocarbon volumes.

If no water drive exists, and if m is known, the following form of the material balance equation (see Section III, Chapter 5-4) is recommended for determining the original oil in place:

$$N = \frac{N_p [B_t + (R_p - R_{si}) B_g]}{B_t - B_{ti} + (m B_{ti}/B_{gi})(B_g - B_{gi})}, \qquad (1)$$

where

$B_t = B_o + (R_{si} - R_s) B_g$, and

$m = GB_{gi}/NB_{ti}$.

After solving for N from equation (1), the original gas in place, G, may be determined from the known ratio, m:

$$G = \frac{m N B_{ti}}{B_{gi}}. \qquad (2)$$

Equations (1) and (2) can also be used to evaluate N if G is known. Also, if data are available for several stages of depletion, it is sometimes possible to evaluate m, G, and N by iterating on m until the same N and G are calculated for each set of data.

If there is a water drive, a water influx term must be introduced into the numerator of equation (1) and handled in the manner described in Chapter 3-5 for water-drive reservoirs (i.e., the water influx is calculated by an unsteady-state-flow analysis). Although it is theoretically possible to solve simultaneously for original oil in place, original gas in place, and water influx, there are many uncertainties in the results, and this practice is not normally recommended for a combination-drive reservoir.

B. Determining Aquifer Constants

The procedure for making water-influx calculations for combination-drive reservoirs is identical to that employed for water-drive reservoirs. The material-balance and unsteady-state equations are solved simultaneously for various dates in the producing history to evaluate the aquifer constant (C) and aquifer extent as measured by the ratio r_a/r_R (also known as r_D). After the best values of C and r_D are established, predictions of future behavior can be made using these values. This procedure is discussed and illustrated by example in Chapter 3-5.

The material balance equation used for this purpose is the same as the basic material balance equation of Chapter 5-4:

Gross Water Influx
= [(Original Oil Volume − Current Oil Volume)]
− [(Solution Gas Liberated − Solution Gas Produced)]
− (Gas Cap Expansion) + (Produced Water)

$$W_e = [N B_{oi} - (N - N_p) B_o] - \{[N R_{si} - (N - N_p) R_s] B_g - G_p B_g\} - [(G - G_{pc}) B_g - G B_{gi}] + W_p B_w. \quad (3)$$

Equation (3) can be modified to account for flank or bottom water injection or crestal gas injection. For flank or bottom water injection, the water influx is natural influx plus the injected water entering the original hydrocarbon volume, $W_e + f_i W_i$, where f_i is the fraction of injected water that drives water into the hydrocarbon volume. For crestal gas injection, the reservoir volume of the cumulative gas injected ($G_i B_g$) is subtracted from the right-hand side of equation (3).

Section VI summarizes the steps to be followed in evaluating the aquifer constants of a combination-drive reservoir.

C. Calculating Recovery Efficiencies

If the reservoir produced long enough for the gas-oil or water-oil contacts to advance measurably, an average recovery efficiency can be determined for each invaded region. From definitions given in Chapter 3-3, the overall recovery efficiency, expressed as the fractional recovery of stock-tank oil originally in place, can be calculated from the following equation if p_r is above the bubble-point:

$$E_N = (E_D)(E_V)\frac{B_{oi}}{B_o}, \quad (4)$$

where E_N is the overall recovery efficiency (stock-tank barrel basis), E_D is the fractional displacement efficiency, and E_V is the volumetric sweep efficiency [E_A (areal efficiency) × E_I (vertical invasion efficiency)].

The net gas-cap expansion and water influx can be determined by material balance and unsteady-state flow calculations for various dates in the history. If the positions of the gas-oil and water-oil contacts are known, the hydrocarbon volume invaded by gas or water can be determined from a hydrocarbon volume-depth curve, such as the one shown in Fig. 2.

Generally, it is assumed that the water-oil and gas-oil contacts will advance approximately on structure, so that whenever the water-oil or gas-oil contact levels are known the invaded hydrocarbon volume can be determined from the hydrocarbon volume-depth curve. If the contacts advance irregularly, the invaded hydrocarbon volume must be determined in another manner. For example, if the gas cap has reached several wells at different structural position an isopach map (see Chapter 1-3) of the gas-invade reservoir can be prepared and planimetered. A simila determination can be made for the water-invade sand.

The volume of displacing fluid in the invade region divided by the invaded hydrocarbon volum equals the displacement efficiency (E_D) times th volumetric sweep efficiency (E_V). The average gas o water reservoir recovery efficiency ($E_{R,GD}$ or $E_{R,WD}$ respectively) for any time period can then be calcu lated from the following relationships:

$$E_{R,GD} = (E_V E_D)_{GD} = \frac{\text{Total Gas-Cap Expansion}}{\text{Gas-Invaded } HCV} = \frac{(G - G_{pc}) B_g - G B_{gi}}{(HCV_e)_{GD}}; \quad (4a)$$

$$E_{R,WD} = (E_V E_D)_{WD} = \frac{\text{Effective Net Water Influx}}{\text{Water-Invaded } HCV} = \frac{W_e - W_p}{(HCV_e)_{WD}}. \quad (4b)$$

For predictions, the average value of reservoir recovery efficiency determined from production history may be used. Or, if the calculated values of reservoir recovery efficiency show a definite trend with time, it may be desirable to extrapolate this trend as a basis for predictions.

If there is insufficient information to determine the gas or water reservoir recovery efficiencies from field history, they may be estimated theoretically. The Welge method of calculating average displacement efficiency behind the advancing gas or water front is convenient for this purpose. The volumetric sweep efficiency must be estimated independently. The Welge method is discussed in Section VII and illustrated by an example in Section VIII of this chapter (also, see Chapter 5-6). In a study involving different production schedules and varying producing rates, the Welge method will account for the effect of rate on displacement efficiency.

D. Determining Reservoir Production Capacity

Production rate calculations are needed to determine the number and location of producing wells required to meet a given production schedule. Also, these calculations help us to forecast the production schedule that could be obtained from a fully developed field, taking into account the loss of wells and gradual depletion of the reservoir as the gas-oil and water-oil contacts advance. This section describes formulas and techniques which may aid in such predictions of oil producing rate. A complete chapter, 2-1, is devoted to the oil productivities of individual wells.

To calculate a well's oil production rate in STB/D, the radial steady-state flow equation given in Chapter 5-5, Fluid Flow, can be used, provided well-test data are used to establish the relationship between production rate and pressure drawdown. The steady-state equation is used for combination-drive reservoirs, because most of the fluid produced by a well is replaced by the flow of fluid across the well's external drainage radius. The flow equation is given by:

$$q_o = \frac{0.00708\, k\, k_{ro}\, h(p_e - p_{wf})}{B_o\, \mu_o\, ln\, (r_e/r_w)}. \qquad (5)$$

In a combination-drive reservoir, equation (5) is most readily applied to wells producing from that part of the reservoir uninvaded by the gas cap or water. For these wells, k_{ro} depends on the average gas or water saturation in the oil zone. A method for calculating this gas saturation at any pressure level is included in an example in a later section of this chapter. The combination of terms $kh/ln\,(r_e/r_w)$ can be determined from the initial productivity index or other well-test information; p_e, the pressure at the radius of drainage, can be considered to be the average reservoir pressure at any stage of depletion and can be calculated by material balance and unsteady-state equations; p_{wf}, the bottom-hole flowing pressure, can be specified; and the oil viscosity, μ_o, and formation volume factor, B_o, are evaluated at the weighted average pressure in the drainage area. This pressure is usually close to p_e.

The gas-oil ratio of a well in the oil zone can be calculated from equation (6), which is also developed in Chapter 5-5:

$$R = \frac{k_{rg}\, B_o\, \mu_o}{k_{ro}\, B_g\, \mu_g} + R_s. \qquad (6)$$

The gas-oil relative permeability ratio, k_{rg}/k_{ro}, is usually determined from laboratory data; however, it can be determined from the field producing history if sufficient history is available. This calculation is illustrated for a solution-gas-drive field in Chapter 3-4.

For wells producing from the parts of the reservoir invaded by gas or water, it is difficult to apply theoretical equations for fluid production. This is because saturation conditions are uncertain, and consequently, there are uncertainties in determining the relative-permeability values to use. Decline curves may be used to estimate production trends for such wells (see Chapter 5-8, Decline Curve Analyses). Plots of producing water-oil or gas-oil ratios versus depths can be used as illustrated for water-oil ratios in Chapter 3-5.* Ideally, wells invaded by gas or water are shut in or recompleted to prevent the waste of reservoir energy associated with excess gas and water production.

E. Evaluating Individual Drive Indexes

The relative importance of each drive mechanism in a combination-drive reservoir can be determined from the material balance equation. This can be demonstrated by solving equation (3) for the total oil produced from the reservoir:

[Reduction in Oil Volume in Reservoir]
= [Net Water Influx] + [Gas-Cap Expansion]
+ [Liberated Gas in the Reservoir].

$$[N\, B_{oi} - (N - N_p)\, B_o] = [W_e - W_p B_w] + [(G - G_{pc})\, B_{gc} - G\, B_{gci}] + [N\, R_{si} - (N - N_p)\, R_s - G_{ps}]\, B_{gs}. \qquad (7)$$

Equation (7) shows that the total reservoir oil voidage is replaced by water influx, gas-cap expansion, or gas released from solution. The drive index for a given mechanism is defined as the fractional replacement of oil by that mechanism. The following equations give the drive index for each individual mechanism:

Water Drive:

$$I_w = \frac{W_e - W_p B_w}{N\, B_{oi} - (N - N_p)\, B_o}. \qquad (8a)$$

Gas-Cap Expansion:

$$I_{gc} = \frac{(G - G_{pc})\, B_{gc} - G\, B_{gci}}{N\, B_{oi} - (N - N_p)\, B_o}. \qquad (8b)$$

Solution-Gas Drive:

$$I_{sg} = \frac{[N\, R_{si} - (N - N_p)\, R_s - G_{ps}]\, B_{gs}}{N\, B_{oi} - (N - N_p)\, B_o}. \qquad (8c)$$

The drive indexes determined from equations (8a), (8b), or (8c) are averages for the entire producing history to the time corresponding to N_p. The relative strengths of the individual drive mechanisms will change with time. The drive indexes can be evaluated for a particular time increment by comparing the incremental values of net water influx, gas-cap expansion, and net released solution gas with the corresponding value of total reservoir oil voidage for that time period.

V. PREDICTING FUTURE PERFORMANCE

Predicting the future performance of a combination-drive reservoir involves the simultaneous solution of material balance and unsteady-state equa-

*Also, consult computer program libraries for programs that permit calculating WOR and GOR after breakthrough.

tions. In addition, the effects of reservoir depletion on the field's producing capacity must be considered. This is the same general problem as that outlined in Chapter 3-5 for predicting the performance of a water-drive reservoir. However, the prediction of a combination-drive reservoir with all three drives effective is more difficult because changes in the produced gas-oil ratio must be predicted.

In a reservoir with an active water drive, the reservoir pressure will not drop much, so that gas saturations will be near or below the equilibrium saturations. Generally, then, no free gas flows in the reservoir and the produced gas-oil ratio equals the solution gas-oil ratio. Similarly, the effect of gas released from oil trapped behind the advancing water front is small and can be neglected.

By contrast, the producing gas-oil ratio is more difficult to predict if solution-gas drive is effective together with a water drive or a gas-cap drive. The producing gas-oil ratio will vary with the gas saturation in the producing zone; therefore, a trial-and-error solution must be used to find a gas-oil ratio compatible with the average gas saturation for a prediction period. For a combination-drive field where solution-gas drive is not important, the oil-zone gas saturation might reach a peak value early in the producing life, then decline to near the equilibrium value. The procedure for calculating the gas saturation in the oil zone must consider that some of the released gas comes from oil that is trapped in the zones invaded by the gas cap and by water. To account for the gas released from this trapped oil in an exact manner requires a calculating procedure that iterates on several different parameters. This problem is not suitable for hand calculation.

An approximate method for hand-calculating the oil-zone gas saturation is described in the following paragraphs. The method assumes that all of the evolved gas originally associated with the trapped oil remains in the gas-cap or water-invaded zones and supplements the volume of the original gas-cap expansion or of the water influx. The method further assumes that the average oil saturations remain constant in the gas-cap-invaded zone and water-invaded zone. The equation for calculating the total gas-cap expansion, including gas released from trapped oil at any pressure level, is:

Total Gas-Cap Expansion

$$= \frac{G\,(B_g - B_{gi})}{1 - \left[\left(\frac{S_o}{1 - S_o}\right)\left(\frac{1}{B_o}\right)(R_{si} - R_s)\,B_g\right]}, \qquad (9a)$$

where

S_o = average oil saturation in gas-cap-invaded zone, fraction of HCV.

Equation (9a) accounts for the reservoir volume of gas liberated from the oil and trapped in the gas cap, further expanding the original gas cap. A similar equation is used to determine the effective water influx (water influx plus the reservoir volume of gas released from the trapped oil) as follows:

Effective Net Water Influx

$$= \frac{W_e}{1 - \left[\left(\frac{S_o}{1 - S_o}\right)\left(\frac{1}{B_o}\right)(R_{si} - R_s)\,B_g\right]}, \qquad (9b)$$

where

S_o = average oil saturation in water-invaded zone, fraction of HCV.

To illustrate this concept, consider Fig. 3, a schematic diagram of a reservoir with a gas-cap and

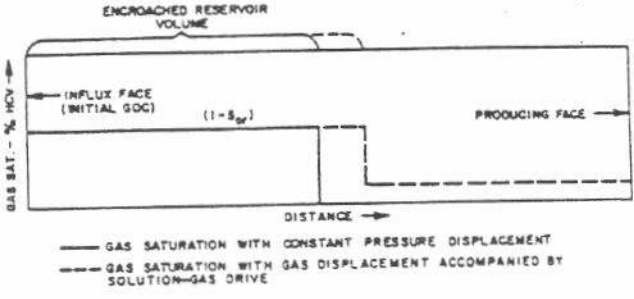

FIG. 3. Schematic diagram illustrating calculation of gas saturation.

solution-gas drive. The solid line shows the saturation that would exist after displacement at a constant pressure. The broken line shows the gas saturation if the displacement is accompanied by a pressure drop that releases gas from the trapped oil with no further reduction of the residual oil in the encroached area. This diagram could also be used to represent the water displacement by replacing "gas saturation" with "water plus gas saturation".

Thus, the prediction of reservoir performance for a time period involves estimating the reservoir pressure at the end of the period and the oil and gas produced during the period. These pressure and production estimates must simultaneously satisfy the material balance equation, the unsteady-state water-encroachment equation, the reservoir productivity factors, and the gas-oil ratio equation. A stepwise prediction procedure is presented in the next section and is illustrated with an example later in the chapter.

VI. SUMMARY OF ANALYTICAL PROCEDURE

The procedure for predicting the performance of combination-drive reservoirs is similar to that described in Chapter 3-5. The following summarizes the steps involved in the overall analytical procedure.

A. Analyze Past Performance

1. Assemble available geologic, pressure, production, rock, and fluid characteristics data.

2. Calculate the original gas and oil in place by volumetric or material balance equations.

3. Evaluate the aquifer constants r_D and C.

a. Divide the history into a number of equal time intervals.

b. Using the material balance equation, calculate cumulative gross water influx at the end of each time interval.

c. Assume a value for r_D and use the unsteady-state equation to calculate the summation term $\Sigma \Delta p\, Q_{tD}$ at the end of each time interval.

d. Divide the gross water influx from step b by the corresponding summation term from step c to determine an apparent value of C for each date.

e. Plot apparent C against time. If C becomes approximately constant with time, the assumed value of r_D is correct and this C value should be used for future predictions. If C does not become constant rework steps c, d, and e using a different r_D.

4. Determine the reservoir recovery efficiency of the water drive.

a. Calculate reservoir recovery efficiency by equation (4b) at the end of each time interval. Net water influx is calculated from material balance and adjusted for released gas using equation (9b). The hydrocarbon volume invaded at the same time is determined from the water-oil contact level using the hydrocarbon volume-depth curve.

b. Plot the reservoir recovery efficiency versus time. If this shows a consistent trend, use it for future predictions; otherwise assume that the future recovery efficiency will equal the average recovery efficiency for the past history.

5. Determine the reservoir recovery efficiency of the gas-cap drive.

a. Calculate the reservoir recovery efficiency by equation (4a) at the end of each time interval. The expansion of the original gas cap is calculated by material balance and adjusted for gas released from trapped oil by equation (9a). The invaded hydrocarbon volume is determined from the hydrocarbon volume-depth curve based on the gas-oil contact position.

b. Plot the reservoir recovery efficiency versus time. If this shows a consistent trend, use it for future predictions; otherwise, assume that the future recovery efficiency will equal the average recovery efficiency for the past history.

Fig. 4 presents a simplified flow diagram for evaluating a combination-drive reservoir from its pressure-production history. The flow diagram contains essentially the same information presented in the above steps.

B. Predict Future Performance

After satisfactory agreement has been achieved between computed and observed reservoir performance for past periods of production, the future reservoir behavior can be calculated as follows:

1. Determine production schedules to be considered in future operations.

2. Assume a time interval for the prediction periods (usually the same interval as that used in analyzing history).

3. Estimate total oil and gas withdrawals for the first prediction period.

4. Estimate reservoir pressure, p, at the end of the first prediction period.

5. Calculate gross water influx at the end of the period by the material balance equation. Use the estimated pressure and withdrawals.

6. With the estimated pressure from step 4, calculate the gross water influx by the unsteady-state equation. Use the aquifer constant, C, determined from the study of reservoir history.

7. Compare the water influx values from the two preceding steps. If the water influx calculated by the material balance (step 5) is within a preset limit of the water influx calculated by the unsteady-state equation (step 6), the estimated pressure is correct. If values of water influx calculated by the two methods differ by more than the preset limit, assume a different pressure (step 4) and repeat steps 5, 6, and 7 until agreement is reached.

8. Calculate the total effective water influx from

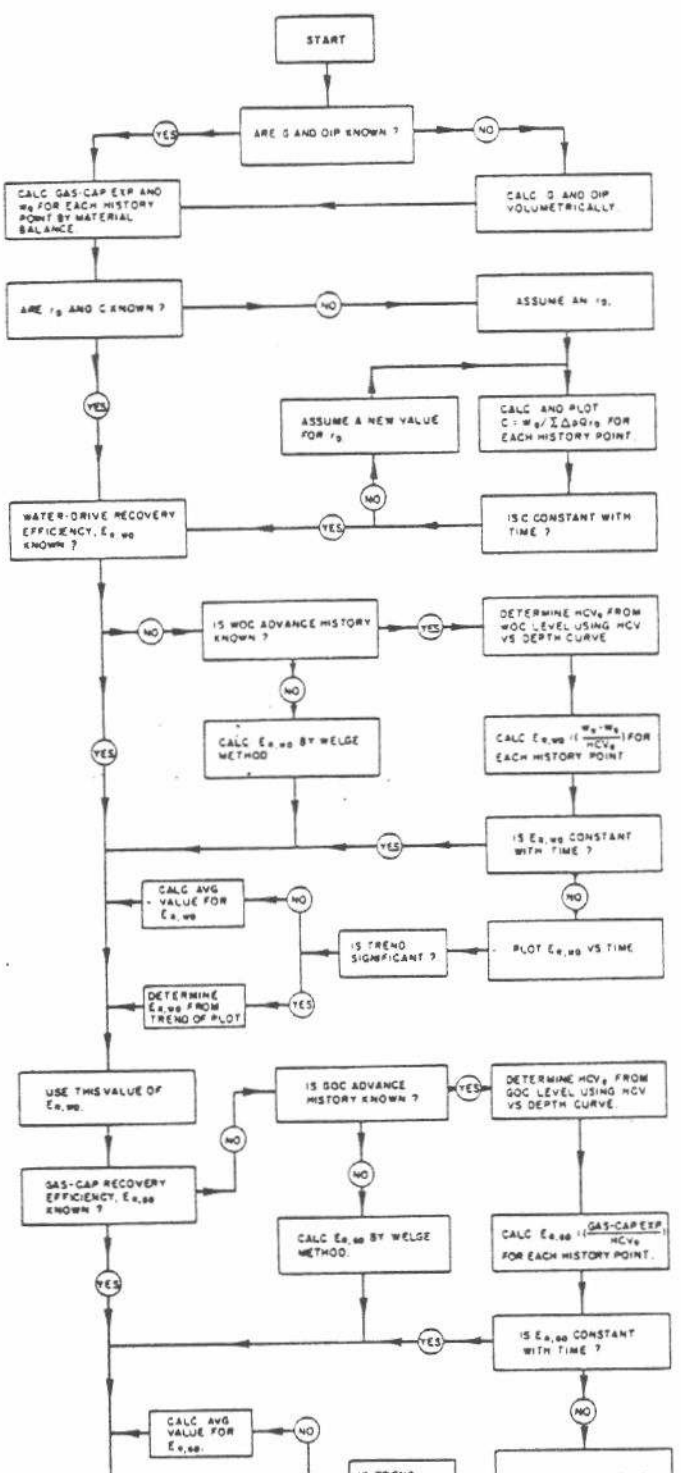

FIG. 4. Simplified flow diagram — analysis of history of combination-drive reservoirs.

equation (9b), using the material balance water influx from step 7.

9. On the basis of the material balance value for expansion of the original gas cap, calculate the total gas-cap expansion, including the volume of gas released from trapped oil by equation (9a).

10. On the basis of the total effective net water influx and the total gas-cap expansion, determine the hydrocarbon volume not yet invaded. Subtract from the original oil in place the produced oil and the trapped oil, and convert this volume to reservoir barrels. Find the oil-zone oil saturation by dividing the oil (reservoir bbl) in this zone by the uninvaded hydrocarbon volume. Check the assumed oil production rate in light of the productive hydrocarbon volume and its gas saturation. Also check the assumed GOR against the calculated gas saturation and reservoir pressure. If oil production rate and GOR are not reasonably near the values assumed initially, repeat steps through 10.

11. On the basis of the uninvaded hydrocarbon volume and the gas saturation at the end of the first period, estimate oil and gas production for the next prediction period and return to step 3. See Chapter 2-1 for the calculation of well productivities as a function of reservoir pressure, gas saturation, and invasion by gas or water. Continue calculations for each time period up to the time of reservoir abandonment.

Fig. 5 is a simplified flow diagram for predicting the performance of a combination-drive reservoir. This diagram, together with the above stepwise prediction procedure, may be helpful in setting up a prediction model for a specific reservoir.

VII. ALTERNATIVE METHODS

In the preceding sections, we described a method for analyzing and predicting the performance of a combination-drive reservoir. This recommended hand-calculation procedure can be utilized in many combination-drive reservoir studies. However, several alternative methods should be considered.

A. The Welge Method

In the foregoing discussion of combination-drive analysis, we largely ignored the theoretical prediction of gas or water recovery efficiencies. We assumed that the gas-cap and water-drive recovery efficiencies could be determined from field history, using equations (4a) and (4b). This approach is recommended

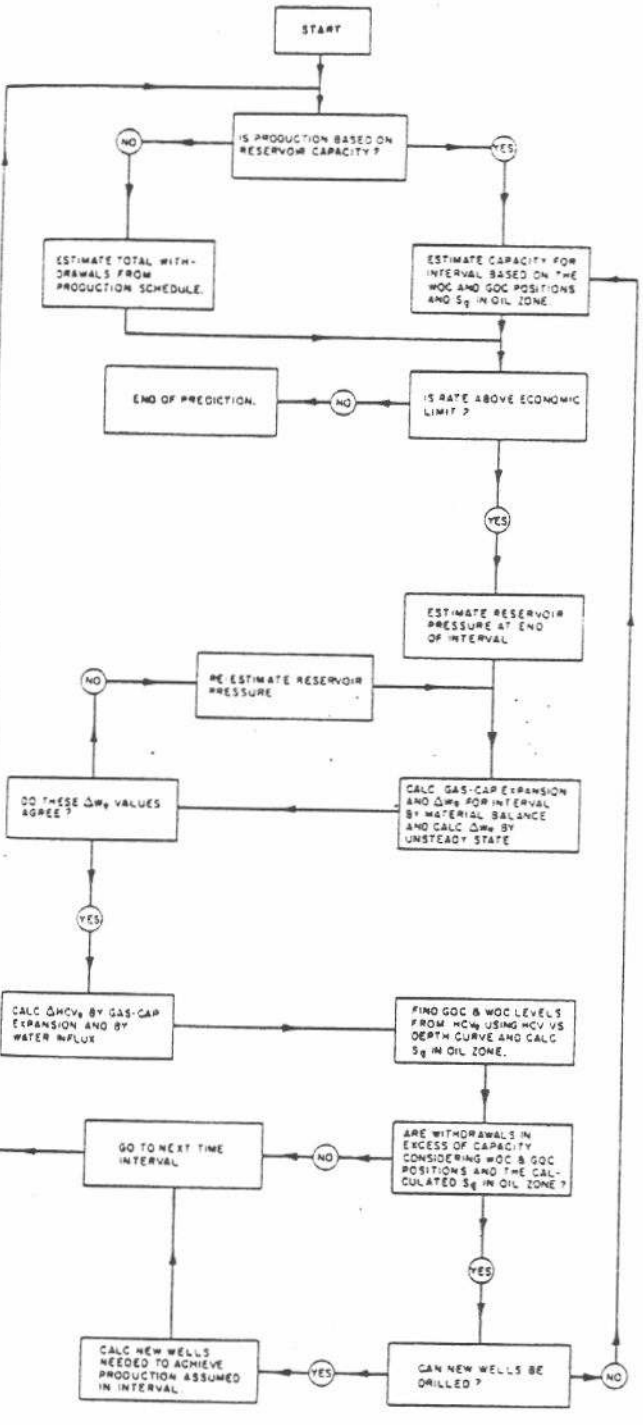

FIG. 5. Simplified flow diagram — predicting performance of combination-drive reservoirs.

ıficient history is available and if producing onditions will not change drastically in the future. lowever, theoretical predictions of recovery effiency are needed for new fields or for evaluating the ffect of producing-rate changes on efficiency.

The Welge method[5] based on the Buckley and Leverett[1] flow relationships for immiscible fluids is recommended for general use in calculating recovery efficiencies in combination-drive reservoirs. The reservoir's volumetric sweep efficiency must be estimated independently from coning calculations. The Welge method assumes that the reservoir can be described as a linear system and that the average reservoir pressure remains constant enough that fluid properties do not change. It also assumes that the reservoir flowing pressure drop is small, so that fluid properties can be properly evaluated at the average pressure. Capillary pressure gradients are neglected. Although the foregoing stipulations are seldom if ever exactly satisfied in the field, the method can be used in some cases without serious error.

The Welge method includes gravity effects in the fractional flow equation to account for the effect of gravity on displacement efficiency. For the displacement of oil by either gas or water, the fraction of displacing phase, f_d, in the flowing stream at a given displacing phase saturation is derived in Chapter 5-6, Fluid Displacement, as:

$$f_d = \frac{\mu_o/\mu_d}{(\mu_o/\mu_d) + (k_{ro}/k_{rd})} - \frac{0.488(10^{-3})\,A\,k\,k_{ro}\,|\,\Delta\gamma\,|\,\sin\alpha_d}{q_t\,\mu_d\,[(\mu_o/\mu_d) + (k_{ro}/k_{rd})]}, \qquad (10)$$

where

$|\Delta\gamma|$ = the absolute difference in specific gravities (water base) of the oil and displacing phase (always a positive value),

α_d = dip angle of the reservoir, degrees,

q_t = total fluid flow rate, B/D at reservoir conditions, and the subscripts o and d refer to the displaced (oil) and the displacing (gas or water) phases, respectively. Other terms in the equation use practical units of cp, md, and sq ft.

When the fraction of displacing phase flowing is plotted against saturation, the resulting curve can be used to estimate the efficiency of displacement by gas-cap expansion and by water drive. This procedure is illustrated by the example problem of the next section. In this example, a simple graphical analysis is used. However, when the cross-sectional area of the reservoir varies greatly, when there is a wide variation in the rate q_t, or when the initial saturation transition zones are extensive, it is necessary to make more complex evaluations by using the Buckley-Leverett equation. These methods are outlined in Chapter 5-6.

To calculate an f_d vs S_d curve from equation (10),

the rate q_t must be evaluated. For a gas-cap drive, q_t is calculated from the gas-cap expansion, while for a water drive, q_t is determined from the net water influx. Calculations of q_t are illustrated in the example problem of the following section. Because flow must be treated as linear, q_t must be based on an average cross-sectional area, A, perpendicular to flow. The horizontal hydrocarbon area can be found from the slope of the hydrocarbon volume-depth curve. This can be converted to A by dividing by the hydrocarbon porosity and multiplying by sin α_d The area, A, can also be evaluated directly from the sand thickness and reservoir width or perimeter.

The Welge method assumes that q_t (for either gas-cap expansion or water drive) remains constant for the period over which the f_d vs S_d curve is applicable. Generally, rates in the field do not remain constant. Hicks et al. [2] discuss handling variable rates. They conclude that for a period of declining rate, the average rate for the period can be used without error, but if rates are increasing, the frontal saturations decrease with time and the average rate is not suitable.

The Welge method is frequently used for predicting the recovery efficiency in crestal gas injection projects. For example, the method has been used to evaluate the effect of producing rate on recovery for the LL-370 reservoir[3] in Venezuela and for the Elk Basin Field[4] in Wyoming. For both of these fields, the predicted recovery efficiencies have been substantiated by field observations of the gas-cap advance. The optimum producing rate in both cases was determined with the aid of the Welge method.

B. The Wooddy-Moscrip Method

Wooddy and Moscrip[7] describe a method for analyzing a combination-drive reservoir wherein the displacement equations are solved simultaneously with the volumetric balance and unsteady-state equations. This method is similar to the analytical procedure described in Section VI, with the addition of displacement efficiency calculated by the Buckley-Leverett method. The effect of gravity on the gas and water f_d vs S_d curves is evaluated for each time interval. The rate term (q_t) in equation (10) is calculated from the gas-cap expansion and water influx values determined from the volumetric-balance and the unsteady-state equations.

Like most reservoir prediction methods, this method uses history as a basis for making reliable predictions of future reservoir behavior. The analysis of past history involves matching the gas-cap and water-drive displacement efficiencies as well as the pressure history.

The inclusion of displacement efficiency equations results in a complex calculation involving a number of trial-and-error factors for each time step. Therefore, the effective use of this method requires a high-speed computer. Generally, recovery efficiencies remain relatively constant so that the method outlined in Section VI and illustrated in the example problem of Section VIII can be used without serious loss of accuracy. If the rate, q_t, changes abruptly for future predictions, the assumed displacement efficiencies should be checked periodically by the Welge method. If the calculated displacement efficiencies become significantly different from the assumed values, the new values should be used in the predictions.

C. Computer-Oriented Methods

Analysis of reservoir performance is trending more and more toward the use of high-speed computers. Numerical techniques developed for the solution of reservoir performance equations require a computer. A numerical method for analyzing a gas-cap reservoir has been proposed by Stone and Garder.[5] Similar methods are being used by Exxon U.S.A. for two-dimensional studies of combination-drive reservoirs (see Chapter 5-10).

Although the method described in this chapter can be applied using a desk calculator, the work is facilitated by using a digital computer. Various one-dimensional reservoir fluid flow programs are available from Exxon U.S.A. For example, the Computer Program Library includes a program entitled "One-Dimensional, Three-Phase, Unsteady-State Combination-Drive Calculations." This program makes one-dimensional analyses of reservoirs producing under any or all of the natural drive mechanisms. The method of calculation is based on the solution of the differential equations describing nearly all processes occurring in the reservoir. It allows for point-by-point variations in the reservoir permeability, elevation, porosity, and cross-sectional area along a selected axis of the reservoir. Fluid flow is calculated considering three-phase relative permeability (developed by the program from conventional gas-oil and water-oil relative permeabilities), capillary pressures, and the gravity component of flow. The effects of pressure on fluid compressibilities, densities, and viscosity are also treated. The only restrictions on the completeness of this technique are that gas-oil phase equilibrium must be adequately described by laboratory data, and the one-dimension model must adequately describe the reservoir.

Several other computer programs are available for making combination-drive calculations. These programs assume uniform rock and fluid properties throughout

the reservoir and thus are classified as nondimensional or tank-type analyses. The computer program entitled "Volumetric-Balance, Unsteady-State Calculation" follows the same fundamental equations as those of this chapter with a few minor exceptions. The program does not contain displacement equations; therefore, recovery efficiencies for the gas-cap and water drives must be precalculated and entered as data. Also, the gas liberated from trapped oil is not added to the gas-cap volume in computing the volume of oil zone invaded. However, as the volume of gas liberated from the trapped oil is normally quite small in comparison to the volume of gas contained in the gas cap, its neglect introduces only a minor error. A significant feature of this program is its ability to automatically adjust various parameters affecting the computer aquifer behavior and thereby match observed field performance. This feature affords considerable time saving when several trials are needed to determine the aquifer parameters that give the best approximation of observed performance. Once determined, these parameters may then be used as data for the one-dimensional technique noted above to obtain a rigorous projection of future reservoir performance.

VIII. EXAMPLE RESERVOIR PROBLEM: PERFORMANCE PREDICTION FOR A COMBINATION-DRIVE FIELD

Problem: Predict the future pressure and gas-oil ratio versus time up to January 1, 1967, for a combination-drive reservoir whose pressure-production history is summarized in Table II. The production rate for future operation will be assumed constant at 60,000 STB/D.* Data are insufficient to permit the calculation of recovery efficiencies for the gas-cap drive and water drive from field observations.

Reservoir rock and fluid data are listed in Table III and Figs. 6, 7, 8, and 9.

Solution: The steps involved in analyzing the past performance and predicting future behavior are listed

TABLE II. — Pressure Production History — Example Problem

Date	Reservoir Pressure @ Datum, psia	Cumulative Production	
		Oil, MMSTB	Gas, MMMscf
1/1/1962 (discovery)	2400	0	0
7/1/1962	2380	2.10	2.11
1/1/1963	2320	9.70	9.60
7/1/1963	2260	19.00	18.62
1/1/1964	2180	30.00	30.55
7/1/1964	2100	42.00	47.12

No water has been produced. No gas-cap gas has been produced.

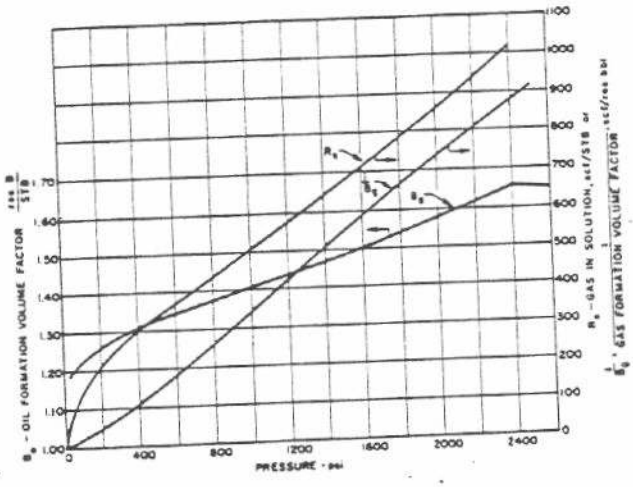

FIG. 6. PVT data for example problem.

TABLE III. Reservoir Rock and Fluid Data — Example Problem

Gas Cap	
Original Gas-Cap Volume, MMbbl	219.27
Original Gas in Place (G), MMMscf	191.17
Permeability, md	155
Specific Gravity (water base) of Gas @ 2260 psia	0.13
Dip Angle, degrees	6
Average Radius @ GOC, ft	4950
Average Thickness, ft	100
Oil Zone	
Original Oil-Zone Volume, MMbbl	725
Original Oil in Place (N), MMSTB	438.86
Connate Water, % PV	20
Specific Gravity of Oil	0.63
Dip Angle, degrees	6
Average Radius @ WOC (r_R), ft	10,700
Average Thickness, ft	100
Aquifer	
Dimensionless Radius, r_D = Aquifer Radius/ Field Radius, (r_a/r_R)	10
Aquifer Permeability, md	155
Average Porosity, %	20
Rock and Water Compressibility, c_{f+w}, psi^{-1}	6×10^{-6}
Water Viscosity, cp	0.37
Specific Gravity of Water	1.13

*This assumption of an average producing rate was made to simplify the problem. In an actual study, the field producing capacity should be checked at each time step as described in Part VI.B. This iteration on producing rate is illustrated in Chapter 3-5.

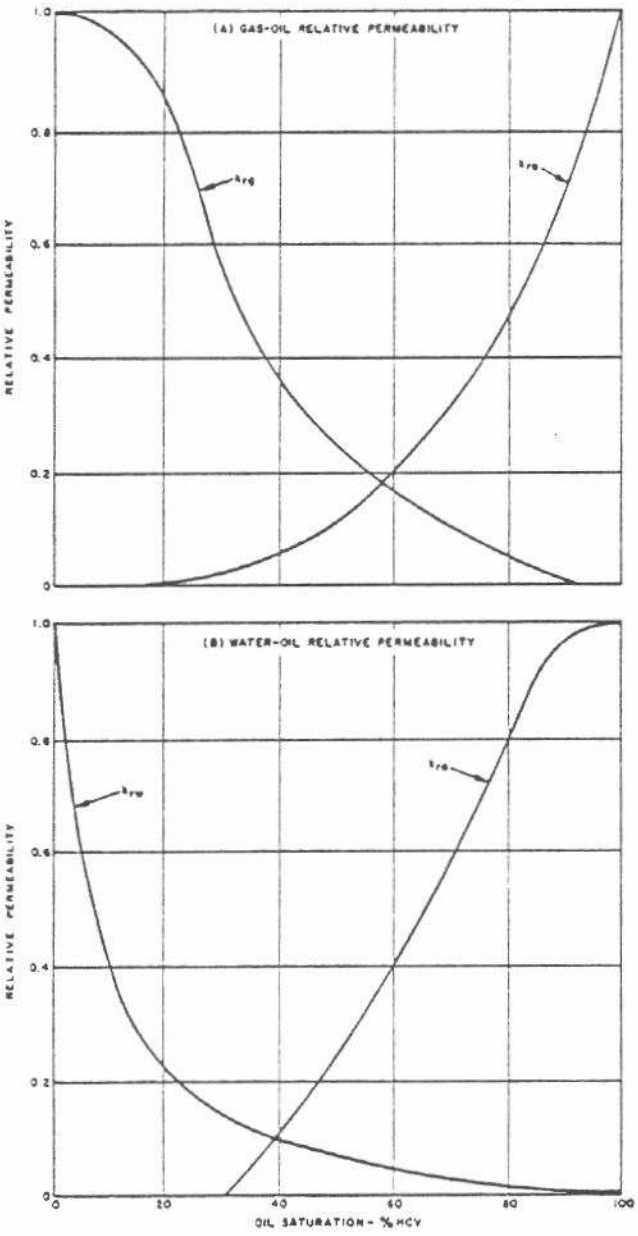

FIG. 7. Relative-permeability data — example problem.

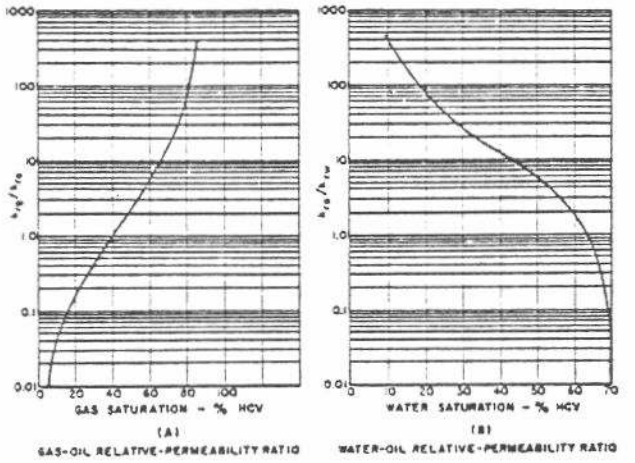

FIG. 8. Relative-permeability ratios — example problem.

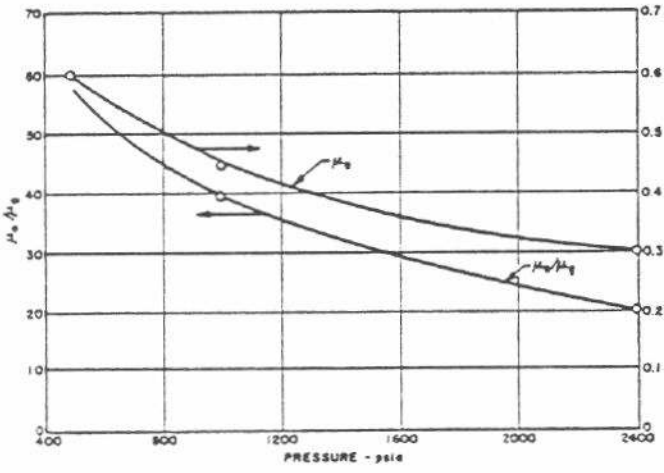

FIG. 9. Oil viscosity and oil-gas viscosity ratio vs pressure — example problem.

in Section VI and will be followed in the solution of this problem. The numbers used here coincide with the step numbering of Section VI.

A. Analyze Past Performance

1. All available geologic, pressure, production, rock, and fluid characteristics data have been assembled and are given in this problem.

2. The original gas-cap and oil-zone volumes are given in Table III. These figures are the result of volumetric calculations as illustrated by examples in Chapters 1-3 and 3-5.

3. Determine the aquifer constant, C, from the pressure-production history. The aquifer size is given as $r_D = 10$.

a. Use a time step of six months, the same as the interval over which production and pressure data are given (Table II).

b. Calculate water influx to the end of each history period by material balance in Table IV. Use equation (3), simplified by the fact that no gas-cap gas or water is produced ($G_{pc} = 0$, $W_p = 0$), and the same B_g curve applies to the gas-cap gas and solution gas. Thus, equation (3) can be written

$$W_e = [NB_{o_i} - (N - N_p)\,B_o] - [NR_{s_i} - (N - N_p)\,R_s]\,B_g + G_p\,B_g - G\,(B_g - B_{g_i}).$$

For example, on 7/1/64 W_e is:

$$W_e = [(438.86)\ (10^6)\ (1.652)$$
$$- (438.86 - 42.00)\ (10^6)\ (1.594)]$$
$$- [(438.86)\ (10^6)\ (1010)$$
$$- (438.86 - 42.00)\ (10^6)\ (898)]\ 1299$$
$$+ (47.12)\ (10^9)\ (1299)\ (10^{-6})$$
$$- (191.17)\ (10^9)\ (1299 - 1147)\ (10^{-6}).$$
$$W_e = [92.40 - 112.84 + 61.22 - 29.06] \times 10^6 \text{ res bbl}$$
$$= 11.72 \times 10^6 \text{ res bbl.}$$

The results of similar calculations for the end of each six-month period are given in Table IV. W_e is listed under Column 10.

c. The summation, $\Sigma\Delta pQ_{tD}$ is calculated as Column 7 of Table V. Q_{tD} is read from the $r_D = 10$ curve of Graph II, Appendix B, Chapter 5-5 at

$$t_D = \frac{0.00633\ k_w t}{\mu_w\ \bar{\phi}_a\ c_{f+w}\ r_R^2} = 0.0194\ t\ (t \text{ is in days}).$$

The products ΔpQ_{tD} are obtained by multiplying each Δp by the Q_{tD} corresponding to the time over which the Δp has existed and then summing up the individual products. The calculation of $\Sigma\Delta pQ_{tD}$ for 7/1/64 is illustrated in detail in footnote (7), Table V. At that time $\Sigma\Delta pQ_{tD} = 1674$.

d. The aquifer constant C is calculated in Column 12 of Table IV. For example, the calculation for 7/1/64 is

$$C = \frac{W_e}{\Sigma\Delta pQ_{tD}} = \frac{11.72 \times 10^6}{1674} = 7001.$$

e. The values of C versus time from Table IV are plotted in Fig. 10, from which the best value of C for predicting future water influx is found

FIG. 10. Aquifer constant from past history.

TABLE IV. — History — Material Balance Calculation of Water Influx

Date	(1) Reservoir Pressure, psia	(2) B_o, res B/STB	(3) R_s, scf/STB	(4) B_g, res bbl/10^6 scf	(5) N_p, 10^6 STB	(6) $NB_{oi}-(N-N_p)B_o$, 10^6 res bbl	(7) $[NR_{si}-(N-N_p)R_s]B_g$, 10^6 res bbl	(8) G_pB_g, 10^6 res bbl	(9) $G(B_g-B_{gi})$, 10^6 res bbl	(10) W_e, 10^6 res bbl	(11) $\Sigma\Delta pQ_{tD}$, psi	(12) C, res bbl/psi
1/1/62	2400	1.652	1010	1147	0	—	—	—	—	—	—	—
7/1/62	2380	1.647	1003	1156	2.1	5.65	5.99	2.44	1.72	0.38	37	10,270
1/1/63	2320	1.635	980	1180	9.7	23.32	26.74	11.33	6.31	1.60	207	7,729
7/1/63	2260	1.624	960	1215	19.0	43.14	48.82	22.62	13.00	3.94	536	7,351
1/1/64	2180	1.608	932	1255	30.0	67.55	78.05	38.34	20.65	7.19	1021	7,042
7/1/64	2100	1.594	898	1299	42.0	92.40	112.84	61.22	29.06	11.72	1674	7,001

(1) From Table II.
(2) From Fig. 6 at pressure in Column 1.
(3) From Fig. 6 at pressure in Column 1.
(4) From Fig. 6 at pressure in Column 1.
(5) From Table II.
(6) Reduction in reservoir oil volume.
(7) Reservoir volume of released gas.
(8) Reservoir volume of produced gas (G_p is given in Table II).
(9) Expansion of original gas cap.
(10) Material-balance water influx: Column 6 — Column 7 + Column 8 — Column 9.
(11) From unsteady-state calculations in Table V-A (Past History).
(12) Aquifer Constant: Column 10 divided by Column 11.

TABLE V. — Unsteady-State Calculation of $\Sigma\Delta pQ_{tD}$ and W.

Date	(1) t, days	(2) p, psia	(3) t_D	(4) Q_{tD}	(5) $\bar{p}$, psia	(6) Δp, psi	(7) $\Sigma\Delta pQ_{tD}$	(8) W_e, 10^6 bbl
				A. *Past History*				
		2400	0	0	—	—	—	—
1/1/62	0	2380	3.54	3.7	2390	10	37	—
7/1/62	182.5	2320	7.08	5.9	2350	40	207	—
1/1/63	365	2260	10.62	7.8	2290	60	536	—
7/1/63	547.5	2180	14.16	9.6	2220	70	1021	—
1/1/64	730.0	2100	17.70	11.3	2140	80	1674	—
7/1/64	912.5							
				B. *Future Prediction*				
		1980	21.24	13.0	2040	100	2546	17.82
1/1/65	1095.0	2000			2050	90	2509	17.56
		2015			2057.5	82.5	2481	17.37
		1930	24.78	14.2	1972.5	85	3472	24.30
7/1/65	1277.5	1840	28.32	16.0	1885	87.5	4535	31.75
1/1/66	1460.0	1850			1890	82.5	4517	31.62
		1845			1887.5	85	4526	31.68
		1775	31.86	17.2	1810	77.5	5721	40.05
7/1/66	1642.5	1770			1807.5	80	5730	40.11
		1690	35.40	18.2	1730	77.5	7034	49.23
1/1/67	1825	1700			1735	72.5	7016	49.11
		1710			1740	67.5	6997	48.98

(1) Time since start of production, days.

(2) Reservoir pressure at the time shown in Column 1. End-of-interval pressures for the "future predictions" are the same as those shown in Table IX.

(3) Dimensionless time, $t_D = \dfrac{0.00633\, k_w t}{\mu_w \bar{\phi}_a c_{f+w} r_R^2} = \dfrac{0.00633 \times 155\, t}{(0.37)(0.2)(6 \times 10^{-6})(114.14 \times 10^6)} = 0.0194\, t.$

(4) From Graph 1, Appendix B, Chapter 5-5. Read at t_D on curve for $r_D = 10$.

(5) Average pressure for interval = 1/2 (pressure at start plus pressure at end).

(6) Pressure drop from previous interval = $\bar{p}$ for previous interval minus $\bar{p}$ for this interval.

(7) Summation of pressure drops times the Q_{tD} for the time over which Δp has existed. This is calculated by listing the Δp values as shown above opposite the Q_{tD} value that corresponds to the time over which each Δp has existed (the Q_{tD} values as shown in Column 4 are listed in inverse order to accomplish this). For example, to calculate $\Sigma\Delta pQ_{tD}$ at 7/1/64, see below:

Date	Δp	Q_{tD} (inverse order)	ΔpQ_{tD}
7/1/62	10	11.3	113.0
1/1/63	40	9.6	384.0
7/1/63	60	7.8	468.0
1/1/64	70	5.9	413.0
7/1/64	80	3.7	296.0
			$\Sigma\Delta pQ_{tD} = 1674.0$

(8) Predicted unsteady-state water influx = 7000 $\Sigma\Delta pQ_{tD}$. This is used for future dates only.

to be 7000. If C did not approach a constant value, the correctness of $r_D = 10$ would be questioned. Then, steps c, d, and e would have to be repeated using a different r_D until C approached a constant value.

4. and 5. Field observations are not available for the calculation of water-drive and gas-cap-drive reservoir recovery efficiencies. Consequently, we will calculate displacement efficiencies by the Welge method. A fractional volumetric sweep efficiency of 1.0 will be assumed.

The first step in evaluating reservoir recovery efficiencies is to determine the cumulative gas-cap expansion and water influx as of 7/1/64 by material balance. The average rates, q_t, of gas-cap expansion and water influx can then be determined.

From equation (3), the gas-cap expansion is $[(G - G_{pc})B_{gc} - GB_{gci}]$. G_{pc} is zero, and from Fig. 6, 1 B_g (or $1/B_{gc}$) at 2100 psi is 770 scf/bbl, and $1/B_{gi}$ (at 2400 psi) is 872 scf/bbl.

$$\text{Gas-Cap Expansion} = G(B_g - B_{gi})$$
$$= 191.17\times10^9\left(\frac{1}{770} - \frac{1}{872}\right)$$
$$= 29.06\times10^6 \text{ bbl.}$$

$$q_i \text{ (avg. rate of gas-cap expansion)} = \frac{29.06\times10^6 \text{ bbl}}{(365\times2.5) \text{ days}}$$
$$= 31{,}847 \text{ B/D.}$$

Calculate water influx by equation (3). Table IV shows that water influx for the latest history date (7/1/64) is 11.72×10^6 bbl.

$$q_i \text{ (avg. water influx rate)} = \frac{11.72\times10^6}{(365\times2.5) \text{ days}}$$
$$= 12{,}844 \text{ B/D.}$$

The next step is to calculate the f_d vs S_d curves for the gas-cap and water-drive mechanisms using equation (10):

Gas Cap: Having determined q_i in the previous step, the only unknown in equation (10) is A, the reservoir cross section perpendicular to flow. This factor can be determined with the aid of a reservoir cross section. The average gas-cap radius is 4950 ft, so the cross section in the direction of flow is: $2\pi r_g h \cos\alpha_d = (2\pi)\ (4950)\ (100)\ (0.9945) = 3.093 \times 10^6$ sq ft. The oil-gas viscosity ratio is read from Fig. 9 at the average past history pressure (2250 psia). By substituting for everything that is not a function of gas saturation, equation (10) becomes:

$$f_g = \frac{\mu_o/\mu_g}{(\mu_o/\mu_g) + (k_{ro}/k_{rg})} - \frac{0.488(10^{-3})A\ k\ k_{ro}|\Delta\gamma|\sin\alpha_d}{q_i\ \mu_g\ [(\mu_o/\mu_g) + (k_{ro}/k_{rg})]}$$

$$= \frac{21.5}{21.5 + (k_{ro}/k_{rg})}$$
$$- \frac{0.488(10^{-3})\ [(3.093)(10^6)]}{(31{,}847)(0.015)\ [(21.5) + (k_{ro}/k_{rg})]}$$
$$- \frac{(155\ k_{ro})(0.63 - 0.13)(0.1045)}{(31{,}847)(0.015)\ [(21.5) + (k_{ro}/k_{rg})]}$$
$$= \frac{21.5 - 25.59\ k_{ro}}{21.5 + (k_{ro}/k_{rg})}.$$

The calculation of f_g versus S_g is shown in Table VI and the data are plotted in Fig. 11. The average gas saturation is determined by constructing a tangent to the f curve. The tangent line starts at the oil-zone gas saturation (at $f = 0$) and extends to the average gas saturation in the invaded zone (at $f = 1$). The tangent line in Fig. 11 starts at a gas saturation of 5 percent, which is about the average gas saturation in the oil zone during the producing history (see Table VIII). For future dates, the tangent line starting point may change as the oil-zone gas saturation increases. Fig. 11 indicates an average gas-cap displacement efficiency of about 50 percent *HCV* up to 7/1/64, and this value will be used in predicting future performance.

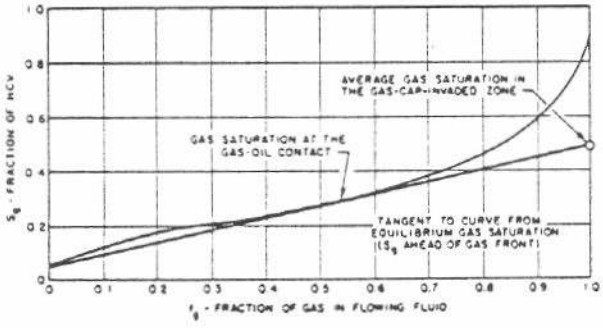

FIG. 11. Average gas saturation in gas cap from f_g vs S_g curve.

TABLE VI. — Calculation of f_g versus S_g

S_g, % HCV	k_{rg}/k_{ro} (Fig. 8A)	k_{ro} (Fig. 7A)	$21.5 - 25.59\ k_{ro}$	$21.5 + \frac{k_{ro}}{k_{rg}}$	f_g*
10	0.033	0.715	3.20	51.8	0.062
20	0.14	0.48	9.21	28.64	0.322
30	0.39	0.31	13.49	24.06	0.561
40	1.0	0.20	16.35	22.5	0.727
50	2.3	0.117	18.50	21.93	0.844
60	5.8	0.067	19.78	21.67	0.913
70	17.0	0.033	20.66	21.56	0.958
80	75.0	0.011	21.22	21.51	0.986
90	∞	0	21.50	21.50	1.000

$$*f_g = \frac{21.5 - 25.59\ k_{ro}}{21.5 + (k_{ro}/k_{rg})}$$

Water Drive: The cross-sectional area perpendicular to flow for the water-drive portion of the reservoir can be calculated from the reservoir radius: $A = 2\pi r_R h \cos \alpha_d = (2\pi)\ (10{,}700)\ (100)\ (0.9945) = 6.69 \times 10^6$ sq ft. Oil viscosity is read from Fig. 9 at the average pressure (2250 psig.). Substituting appropriate water-drive terms into equation (10) (as we did for the gas-drive case):

$$f_w = \frac{0.31/0.37}{(0.31/0.37) + (k_{ro}/k_{rw})} - \frac{(0.488)(10^{-3})\,[(6.69)(10^6)]}{(12{,}844)(0.37)\,[(0.84) + (k_{ro}/k_{rw})]} - \frac{(155\,k_{ro})(1.13 - 0.63)(0.1045)}{(12{,}844)(0.37)\,[(0.84) + (k_{ro}/k_{rw})]};$$

$$f_w = \frac{0.84 - 5.56\,k_{ro}}{0.84 + (k_{ro}/k_{rw})}.$$

The calculation of f_w versus S_w is summarized in Table VII and the curve is shown in Fig. 12. A tangent cannot be constructed to the curve; this implies that displacement is piston-like, and the water saturation behind the front is constant at 70 percent hydrocarbon volume. Under these conditions, displacement will not be rate-sensitive unless the rate is extremely high. A residual oil saturation of 30 percent hydrocarbon volume is assumed in the future predictions.

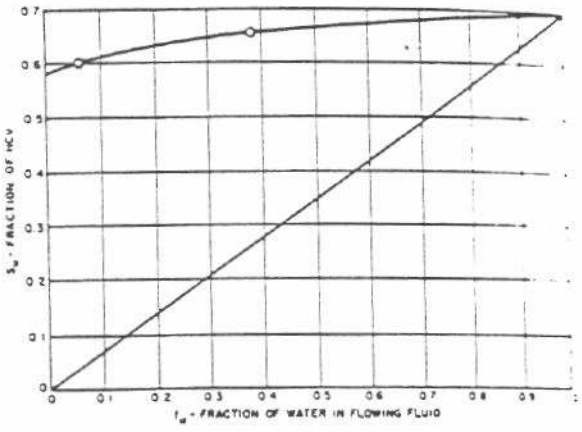

FIG. 12. Determination of water saturation from f_w vs S_w curve.

B. Predict Future Performance

1. Oil production rate is given for this problem.

2. Continue a time interval of six months as for the previous performance analysis.

3. Total withdrawal of stock-tank oil, ΔN_p, for an interval equals 182.5 days times 60,000 STB/D. Determine the gas production, ΔG_p, for an interval by estimating the producing GOR, using equation (6):

$$R = \frac{k_{rg}}{k_{ro}} \frac{B_o \mu_o}{B_g \mu_g} + R_s. \qquad (6$$

Both the average pressure and average gas saturation of the oil zone must be estimated in order to calculate R. Estimate the average pressure from the pressure trend shown in Table II, and the average gas saturation from the trend of gas saturation versus pressure calculated in Table VIII and plotted in Fig. 13. The estimation of producing GOR for a period and the procedure for checking the estimate are illustrated in Table VIII.

4. Estimate the reservoir pressure at the end of a time step by extrapolating the plot of reservoir pressure versus time.

5. and 6. The gross water influx calculated by the material balance equation (3) is shown in Table IX, and compared with water influx calculated by the unsteady-state flow equation (see Table V). For the material balance calculation, the value of ΔN_p is constant for each time step, while the pressure at the

TABLE VII. — Calculation of f_w versus S_w

S_W, %HCV	k_{ro}/k_{rw} (Fig. 8B)	k_{ro} (Fig. 7B)	$0.84\text{-}5.56\,k_{ro}$	$0.84 + k_{ro}/k_{rw}$	f_w
20	70	0.8	—	—	*
25	39	0.7	—	—	*
30	24	0.59	—	—	*
35	16	0.49	—	—	*
40	12	0.41	—	—	*
45	8.5	0.33	—	—	*
50	6	0.26	—	—	*
55	3.7	0.19	—	—	*
60	1.8	0.12	0.17	2.64	0.064
65	0.52	0.06	0.51	1.36	0.375
70	0	0	0.84	0.84	1.000

*For these water saturations, the calculated values of f_w are negative, which means that these saturations would result in counterflow of water; i.e., water would move downdip by gravity.

TABLE VIII

Calculation of Gas Saturation in the Oil Zone

Date	(1) p, psia	(2) R_s, scf/STB	(3) B_g, res bbl/10^6 scf	(4) B_o, res B/STB	(5) $G(B_g-B_{gi})$, 10^6 res bbl	(6) $1-\frac{B_g}{B_o}(R_{si}-R_s)$	(7) Total Gas-Cap Expansion, 10^6 res bbl	(8) W_e, 10^6 res bbl	(9) $1-\frac{0.3B_g}{0.7B_o}(R_{si}-R_s)$
7/1/62	2380	1003	1156	1.647	1.72	0.9951	1.73	0.38	0.9979
1/1/63	2320	980	1180	1.635	6.31	0.9783	6.45	1.60	0.9907
7/1/63	2260	960	1215	1.624	13.00	0.9626	13.51	3.94	0.9840
1/1/64	2180	932	1255	1.608	20.65	0.9391	21.99	7.19	0.9739
7/1/64	2100	898	1299	1.594	29.06	0.9087	31.98	11.72	0.9609
1/1/65	2015	865	1360	1.579	40.72	0.8751	46.53	16.52	0.9465
7/1/65	1930	834	1418	1.560	51.81	0.8400	61.68	24.51	0.9314
1/1/66	1845	802	1486	1.546	64.81	0.8000	81.01	31.34	0.9143
7/1/66	1770	774	1553	1.534	77.62	0.7611	101.98	39.78	0.8976
1/1/67	1700*	749	1623	1.521	91.00	0.7215	126.12	48.48	0.8806
	1710	752	1613	1.521	89.09	0.7264	122.64	48.34	0.8827

(1) Reservoir pressure at end of interval, from Table II (history) or IX (prediction).

(2) From Fig. 6 at pressure in Column 1.

(3) From $(1/B_g)$ curve (Fig. 6) at pressure in Column 1. F

(4) From Fig. 6 at pressure in Column 1.

(5) Original gas-cap gas in place (191.17 MMMscf) times change from original $B_g(B_{gi}$ = 1147 res bbl/MMscf).

(6) Calculated from preceding columns (R_{si} = 1010 scf/STB, $[S_o/(1-S_o)]$ = 1, since S_o = 0.50, see Fig. 11).

(7) Column 5 divided by Column 6 [see equation (9a)].

(8) Cumulative water influx by material balance (Table IX).

(9) Calculated from preceding columns (S_o in water-invaded region = 0.70, see Fig. 12).

* This pressure was not acceptable because of inaccurate GOR (see Table X).

Calculation of Gas Saturation in the Oil Zone

Date	(10) Effective Water Influx, 10^6 res bbl	(11) HCV Invaded by gas cap, 10^6 res bbl	(12) HCV Invaded by Water, 10^6 res bbl	(13) HCV not yet Invaded, 10^6 res bbl	(14) Oil Trapped by Gas Cap, 10^6 STB	(15) Oil Trapped by Water, 10^6 STB	(16) N_p, 10^6 STB	(17) Oil in Uninvaded HCV, 10^6 res bbl	(18) S_g, fraction of HCV
7/1/62	0.38	3.46	0.54	721.00	1.05	0.10	2.10	717.45	0.005
1/1/63	1.62	12.90	2.31	709.79	3.94	0.42	9.70	694.55	0.021
7/1/63	4.00	27.02	5.71	692.27	8.32	1.05	19.00	666.64	0.037
1/1/64	7.38	43.98	10.54	670.48	13.68	1.97	30.00	32.28	0.057
7/1/64	12.20	63.96	17.43	643.61	20.06	3.28	42.00	595.39	0.075
1/1/65	17.45	93.06	24.93	607.01	29.47	4.74	52.95	555.33	0.085
7/1/65	26.32	123.36	37.60	564.04	39.54	7.23	63.90	511.98	0.092
1/1/66	34.28	162.02	48.97	514.01	52.40	9.50	74.85	467.06	0.091
7/1/66	44.32	203.96	63.31	457.73	66.47	12.39	85.80	420.62	0.081
1/1/67	55.05	252.24	78.64	394.12	82.91	15.51	96.75	370.65	0.060
	54.76	245.28	78.22	401.50	80.63	15.43	96.75	374.24	0.068

(10) Column 8 divided by Column 9 [see equation (9b)].

(11) Column 7 divided by gas-cap displacement efficiency. (Efficiency = 0.5.)

(12) Column 10 divided by water displacement efficiency. (Efficiency = 0.7.)

(13) Original oil-filled HCV minus the sum of Columns 11 and 12. (Original oil-filled volume = 725 MMres bbl.)

(14) Column 7 times $\left(\frac{0.50}{1-0.50}\right)$ divided by B_o.

(15) Column 10 times $\left(\frac{0.30}{1-0.30}\right)$ divided by B_o.

(16) Cumulative oil production from Table II or Table IX.

(17) Original stock-tank oil in place minus the sum of Columns 14 through 16 times B_o. (Original OIP = 438.86 MMSTB.)

(18) 1.000 minus the oil saturation (S_o). S_o equals Column 17 divided by Column 13.

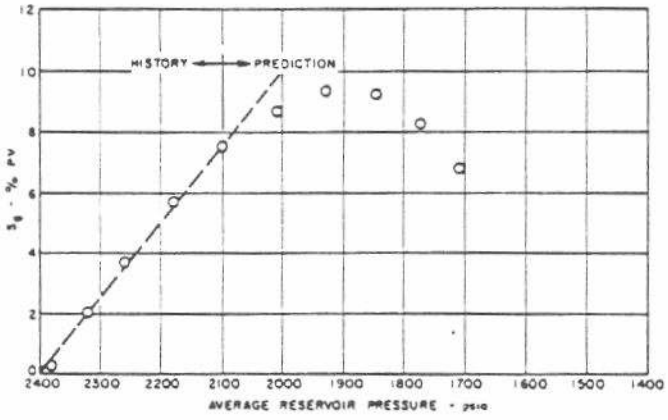

FIG. 13. Oil-zone gas saturation vs pressure.

end of the interval and ΔG_p are estimated as described in steps 3 and 4.

7. When the W_e values by material balance and unsteady-state flow agree within a preset limit (one million barrels for the example problem), we can go n to step 8. However, if W_e by material balance and unsteady-state flow differ by more than one million barrels, a new pressure estimate must be made and steps 5 and 6 repeated. This is illustrated in Table IX.

8. Calculate the effective net water influx (W_e plus gas released from trapped oil) using equation (9b). The effective net water influx for each future time step is shown in Column 10, Table VIII.

9. The total gas-cap expansion (expansion of original gas cap plus volume of gas released from trapped oil) calculated from equation (9a) is shown in Column 7, Table VIII.

10. The calculated gas saturation of the oil zone at the end of each increment is shown in Column 18, Table VIII. The procedure for calculating the gas saturation is described in Columns 13 through 18.

The oil production is given, so no check is necessary. However, the estimated producing GOR must be checked by calculating the GOR based on the correct pressure and gas saturation at the end of the interval. If the estimated GOR differs too much from the calculated GOR (10 percent limit was used in this example), go back to step 3, use a better estimate for the GOR, and repeat all subsequent steps. This procedure is illustrated in Table X.

11. Estimate the pressure and GOR for the next period based on the calculated pressure and gas

TABLE IX. — Prediction of Future Pressure Versus Time.

Date	Estimated End-of-Interval Pressure, psia	B_o, res B/STB	R_s, scf/STB	B_g, res bbl/10^6 scf	ΔN_p, 10^6 STB	N_p, 10^6 STB	ΔG_p, 10^9 scf [ΔN_p times Col. 9, Table X]	G_p, 10^9scf	$NB_{oi} - (N-N_p)B_o$, 10^6 res bbl	$[NR_{si} - (N-N_p)R_s]B_g$, 10^6 res bbl	G_pB_g, 10^6 res bbl	$G(B_gB_i)$, 10^6 res bbl	Material-Balance W_e, 10^6 res bbl	Unsteady-State W_e, 10^6 res bbl	ΔW_e, 10^6 res bbl
1/1/65	1980	1.572	853	1385	10.95	52.95	19.37	66.49	118.35	157.98	92.06	45.50	6.93	17.82	10.89
	2000	1.577	861	1370					116.42	152.04	91.09	42.63	12.84	17.56	4.72
	2015	1.579	865	1360					115.64	148.83	90.43	40.72	16.52	17.37	0.85
7/1/65	1930	1.560	834	1418	10.95	63.90	19.09	85.58	140.06	185.09	121.35	51.81	24.51	24.30	0.21
1/1/66	1840	1.545	800	1492	10.95	74.85	21.26	106.84	162.60	226.84	159.41	65.95	29.22	31.75	2.53
	1850	1.548	805	1481					161.51	222.48	158.23	63.85	33.41	31.62	1.79
	1845	1.546	802	1486					162.21	224.85	158.76	64.81	31.34	31.68	0.34
7/1/66	1775	1.535	776	1550	10.95	85.80	20.74	127.58	183.05	262.37	197.75	77.04	41.39	40.05	1.34
	1770	1.534	774	1553					183.40	263.98	197.98	77.62	39.78	40.11	0.33
1/1/67	1690	1.520	745	1634	10.95	96.75	19.28	146.86	204.99	307.81	239.97	93.10	44.05	49.23	5.18
	1700*	1.521	749	1623					204.65	303.52	238.35	91.00	48.48	49.11	0.63*
	1710	1.521	752	1613	10.95		16.73	144.31	204.65	299.99	232.77	89.09	48.34	48.98	0.64

*Despite the water influx agreement, this pressure was rejected because the assumed GOR was too high (see Table X).

TABLE X. — Evaluation of Producing Gas-Oil Ratios

	Estimated Gas-Oil Ratio for Next Increment									Calculated Gas-Oil Ratio for Last Increment											
	(1)	(2)	(3)	(4)	(5)	(6)	(7)	(8)	(9)	(10)	(11)	(12)	(13)	(14)	(15)	(16)	(17)	(18)	(19)	(20)	(21)
Date	Est. Avg. Pres. for Inter., psia	Est. Avg. S_g, Frac. HCV	k_g/k_o	B_o, res B/ STB	$1/B_g$, scf/ res bbl	μ_o/μ_g	Free GOR, scf/ STB	R_s, scf/ STB	Prod. GOR, scf/ STB	Avg. Pres., psia	S_g For Interval, Fraction HCV: At Start	At End	Avg.	k_g/k_o	B_o, res B/ STB	$1/B_g$, scf/ res bbl	μ_o/μ_g	Free GOR, scf/ STB	R_s, scf/ STB	Prod. GOR, scf/ STB	% Error
1/1/65	2040	0.084	0.032	1.584	744	23.7	894	875	1769	2057.5	0.075	0.085	0.080	0.029	1.585	750	23.5	810	878	1688	4.6
7/1/65	1970	0.084	0.032	1.571	712	25.0	895	848	1743	1972.5	0.085	0.092	0.088	0.036	1.571	712	25.0	1007	848	1855	6.4
1/1/66	1885	0.100	0.041	1.555	690	25.5	1122	820	1942	1887.5	0.092	0.091	0.092	0.038	1.554	689	25.5	1038	818	1856	4.4
7/1/66	1810	0.100	0.041	1.540	660	26.5	1104	790	1894	1807.5	0.091	0.081	0.086	0.035	1.539	659	26.6	944	789	1733	8.5
1/1/67	1730	0.093	0.038	1.525	628	27.5	1001	760	1761	1735	0.081	0.060	0.071	0.027	1.526	629	27.5	713	761	1474	16.3
	1740	0.080	0.029	1.527	631	27.3	763	765	1528	1740	0.081	0.068	0.075	0.028	1.527	631	27.3	737	765	1502	1.7

(1) Average of pressure at start of interval and *estimated pressure* at end of interval.

(2) S_g estimated from Fig. 13 at pressure in Column 1.

(3) k_g/k_o from Fig. 8A at S_g in Column 2.

(4) From Fig. 6 at pressure in Column 1.

(5) From Fig. 6 at pressure in Column 1.

(6) From Fig. 9 at pressure in Column 1.

(7) Column 3 times Column 4 times Column 5 times Column 6.

(8) From Fig. 6 at pressure in Column 1.

(9) Column 7 plus Column 8.

(10) Average of pressure at start of interval and *correct pressure* at end of interval (from Table IX).

(11) S_g at end of previous interval (from Table VIII).

(12) S_g at end of this interval (from Table VIII).

(13) Average of Columns 11 and 12.

(14) From Fig. 8A at S_g in Column 13.

(15) From Fig. 6 at pressure in Column 10.

(16) From Fig. 6 at pressure in Column 10.

(17) From Fig. 9 at pressure in Column 10.

(18) Column 14 times Column 15 times Column 16 times Column 17.

(19) From Fig. 6 at pressure in Column 10.

(20) Column 18 plus Column 19.

(21) 100 (absolute difference between Column 20 and Column 9)/(Column 9). If this error is more than 10 percent, estimate a new GOR based on the calculated S_g for the interval, and repeat the entire calculation.

saturation for the previous period, and repeat the production procedure for all future intervals. In this example, the average gas-oil ratio for an interval is calculated from the average gas saturation for the interval. An alternate procedure is to calculate the gas-oil ratios for the start and for the end of the interval. The average of these two gas-oil ratios is used as the average for the interval.

The final predicted performance for the reservoir is shown along with the past history in Fig. 14.

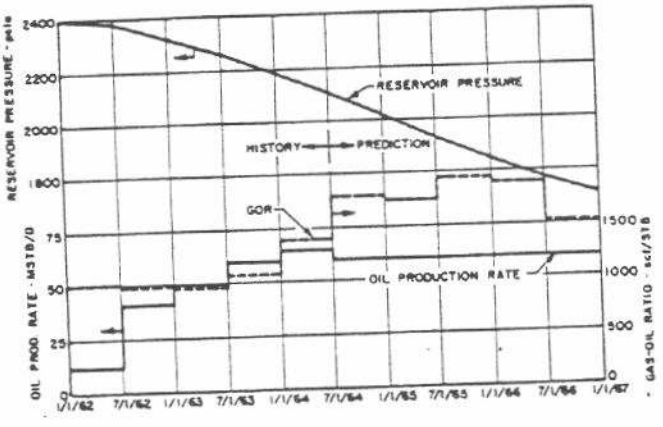

FIG. 14. Production history and predicted future behavior — example problem.

In the calculation procedure used in this example, we assumed that the gas cap would contain all of the gas ever released from the trapped oil. This procedure merely approximates the amount of gas available from three sources: (1) gas released from residual oil in the gas cap, (2) gas liberated in the oil zone but incorporated into the advancing gas cap, and (3) liberated gas migrating to the gas cap by gravity segregation. An analysis of these processes indicates that this assumption is reasonable if reservoir pressure drops slowly (less than 5 percent per year), because the volume of released gas will generally be small compared to the total gas-cap volume. However, if reservoir pressure drops rapidly, a significant error could result from assuming that all released gas is contained in the gas cap. Where pressure drops rapidly, a more complex analysis of released gas in the gas cap may be needed for better accuracy, but high-speed computers would probably be required. The previously described Wooddy-Moscrip method or a two-dimensional computer program could be used.

The same assumption (that all gas released from the residual oil is contained in the invaded zone) was used to estimate the amount of released gas remaining in the water-invaded zone. At gas saturations below the equilibrium value, more than the assumed amount of gas would be trapped, but the difference between the assumed and actual values would generally cause only a small error in the analysis. As gas saturation increases, some of the gas might be pushed ahead of the water front. This would improve the validity of the assumption except in cases of very high gas saturations (above 10 percent pore volume). For very high rates of pressure drop and for high gas saturations, less than the assumed amount of gas might be trapped. Again, for better accuracy, the Wooddy-Moscrip method or a two-dimensional computer program should be used.

REFERENCES

1. Buckley, S. E., and Leverett, M. E.: "Mechanism of Fluid Displacement in Sands," *Trans. AIME*, v. 146, 1942, p 107.

2. Hicks, A. L., Fisher, W. G., and Knutson, W. G.: "Calculations of Oil Recovery by Variable-Rate Gas or Water Injection," JPRCo Technical Service Report No. 3925, December 1960.

3. Joslin, W. J.: "Applying the Frontal-Advance Equation to Vertical Segregation Reservoirs," *Jour. Pet. Tech.*, July 1959, p 169.

4. Stewart, F. M., et al.: "Pressure Maintenance by Inert Gas Injection in the High Relief Elk Basin Field," *Jour. Pet. Tech.*, v. 204, March 1955, p 49.

5. Stone, H. L., and Garder, A. O., Jr.: "Analysis of Gas-Cap or Dissolved-Gas Drive Reservoirs," *SPE Jour.*, June 1961, p 92.

6. Welge, H. J.: "Simplified Method for Computing Oil Recoveries by Gas or Water Drive," *Trans. AIME.*, v. 195, 1952, p 91.

7. Wooddy, L. D., Jr., and Moscrip, Robert, III: "Performance Calculations for Combination Drive Reservoirs," *Trans. AIME*, v. 207, 1956, p 128.